

# Antipode Preserving Cubic Maps: the Fjord Theorem

Araceli Bonifant, Xavier Buff and John Milnor

## ABSTRACT

This note will study a family of cubic rational maps which carry antipodal points of the Riemann sphere to antipodal points. It focuses particularly on the **fjords**, which are part of the central hyperbolic component but stretch out to infinity. These serve to decompose the parameter plane into subsets, each of which is characterized by a corresponding **rotation number**.

## Contents

1. INTRODUCTION . . . . .	1
2. FATOU COMPONENTS AND HYPERBOLIC COMPONENTS . . . . .	7
3. THE CENTRAL HYPERBOLIC COMPONENT $\mathcal{H}_0$ . . . . .	12
4. VISIBLE POINTS FOR MAPS IN $\mathcal{H}_0$ . . . . .	22
5. DYNAMIC ROTATION NUMBER FOR MAPS IN $\mathcal{H}_0$ . . . . .	29
6. BI-VISIBLE POINTS FOR MAPS OUTSIDE $\widehat{\mathcal{H}}_0$ . . . . .	38
7. FJORDS . . . . .	45
Appendix A. CIRCLE MAPS AND ROTATION SETS . . . . .	54
References . . . . .	61

## 1. INTRODUCTION.

By a classical theorem of Borsuk (see [3]):

*There exists a degree  $d$  map from the  $n$ -sphere to itself carrying antipodal points to antipodal points if and only if  $d$  is odd.*

For the **Riemann sphere**,  $\widehat{\mathbb{C}} = \mathbb{C} \cup \{\infty\} \cong S^2$ , the **antipodal map** is defined to be the fixed point free map  $\mathcal{A}(z) = -1/\bar{z}$ . We are interested in rational maps from the Riemann sphere to itself which carry antipodal points to antipodal points <sup>†</sup>, so that  $\mathcal{A} \circ f = f \circ \mathcal{A}$ . If all of the zeros  $q_j$  of  $f$  lie in the finite plane, then  $f$  can be written uniquely as

$$f(z) = u \prod_{j=1}^d \frac{z - q_j}{1 + \bar{q}_j z} \quad \text{with} \quad |u| = 1.$$

2000 *Mathematics Subject Classification* 37F10 (primary), 37F15, 37D05, 32A10, 32H02 (secondary).

*The first author* wishes to thank the Institute for Mathematical Sciences at Stony Brook University, where she spent her sabbatical year, and ICERM for their support to this project. *The second author* wishes to thank the Clay Mathematics Institute, ICERM, IUF and the ANR project LAMBDA, ANR-13-BS01-0002 for supporting this research. *The third author* wishes to thank ICERM for their support towards this project. *The authors* want to thank the referee for many helpful suggestions.

<sup>†</sup> The proof of Borsuk's Theorem in this special case is quite easy. A rational map of degree  $d$  has  $d + 1$  fixed points, counted with multiplicity. If these fixed points occur in antipodal pairs, then  $d + 1$  must be even.

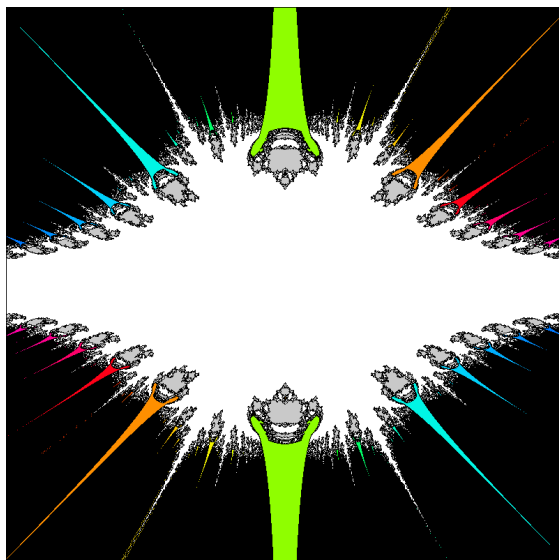


FIGURE 1. *The  $q$ -parameter plane.*

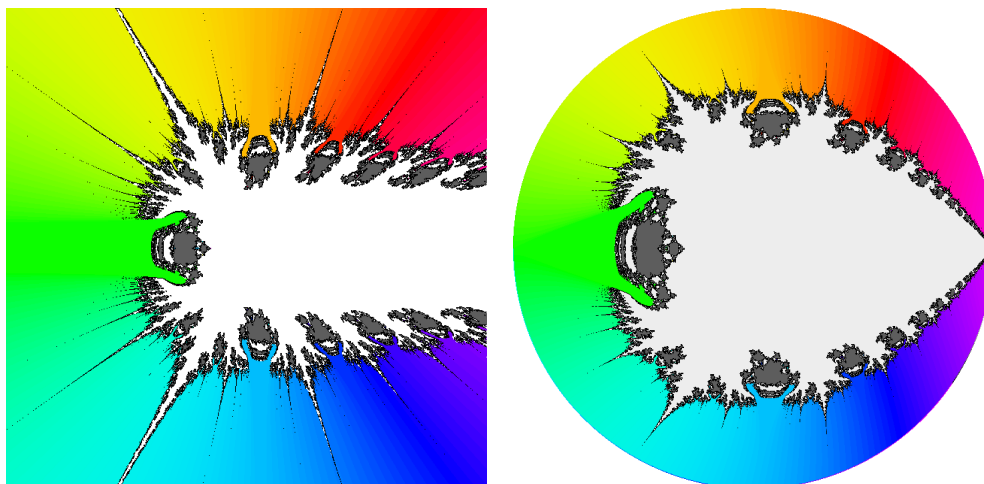


FIGURE 2. *On the left: The  $q^2$ -plane. Here the colors code the rotation number, not distinguishing between tongues and the Herman ring locus. On the right: Image of the circled  $q^2$ -plane under a homeomorphism  $\mathbb{C} \rightarrow \mathbb{D}$  which shrinks the circled plane to the unit disk.*

The simplest interesting case is in degree  $d = 3$ . To fix ideas we will discuss only the special case <sup>†</sup> where  $f$  has a critical fixed point. Putting this fixed point at the origin, we can take

---

<sup>†</sup> For a different special case, consisting of maps with only two critical points, see [13, §7] as well as [10].

$q_1 = q_2 = 0$ , and write  $q_3$  briefly as  $q$ . It will be convenient to take  $u = -1$ , so that the map takes the form

$$f(z) = f_q(z) = z^2 \frac{q - z}{1 + \bar{q}z}. \tag{1}$$

(Note that there is no loss of generality in choosing one particular value for  $u$ , since we can always change to any other value of  $u$  by rotating the  $z$ -plane appropriately.)

Figure 1 illustrates the  $q$ -parameter plane for this family of maps: (1).

- The central white region in Figure 1, resembling a porcupine, is the hyperbolic component centered at the map  $f_0(z) = -z^3$ . It consists of all  $q$  for which the Julia set is a Jordan curve separating the basins of zero and infinity. This region is simply-connected (see Theorem 3.1); but its boundary is very far from locally connected. (See [2], the sequel to this paper.)

- The colored regions in Figure 1 will be called **tongues**, in analogy with Arnold tongues. Each of these is a hyperbolic component, stretching out to infinity. Each representative map  $f_q$  for such a tongue has a self-antipodal cycle of attracting basins which are arranged in a loop separating zero from infinity. (Compare Figure 3.) Each such loop has a well defined combinatorial rotation number, as seen from the origin, necessarily rational with even denominator. These rotation numbers are indicated in Figure 1 by colors which range from red (for rotation number close to zero) to blue (for rotation number close to one).

- The black region in Figure 1 is the **Herman ring locus**. The authors will show in [2] that for the overwhelming majority of parameters  $q$  in this region, the map  $f_q$  has a Herman ring which separates the basins of zero and infinity (compare Figure 4), and that every such Herman ring has a well defined rotation number (as seen from zero), which is always a Brjuno number. If we indicate these rotation numbers also by color, then there is a smooth gradation, so that the tongues no longer stand out. (Compare Figure 2.)

- For rational rotation numbers with odd denominator, there are no such tongues or rings. Instead there are channels leading out to infinity within the central hyperbolic component. (Compare Figures 1, 2 and 5.) These will be called **fjords**, and will be a central topic of this paper.

- The gray regions and the nearby small white regions in Figures 1 and 2 represent **capture components**, such that both of the critical points in  $\mathbb{C} \setminus \{0\}$  have orbits which eventually land in the immediate basin of zero or infinity.

Note that Figure 1 is invariant under  $180^\circ$  rotation. In fact each  $f_q$  is linearly conjugate to  $f_{-q}(z) = -f_q(-z)$ . In order to eliminate this duplication, it is often convenient to use  $q^2$  as parameter. The  $q^2$ -plane of Figure 2, could be referred to as the **moduli space**, since each  $q^2 \in \mathbb{C}$  corresponds to a unique holomorphic conjugacy class of mappings of the form (1) with a marked critical fixed point at the origin. †

DEFINITION 1.1. It is often useful to add a circle of points at infinity to the complex plane. The **circled complex plane**

$$\mathbb{C} = \mathbb{C} \cup (\text{circle at infinity})$$

will mean the compactification of the complex plane which is obtained by adding one point at infinity,  $\infty_{\mathbf{t}} \in \partial\mathbb{C}$ , for each  $\mathbf{t} \in \mathbb{R}/\mathbb{Z}$ ; where a sequence of points  $w_k \in \mathbb{C}$  converges to  $\infty_{\mathbf{t}}$  if

† Note that we do not allow conjugacies which interchange the roles of zero and infinity, and hence replace  $q$  by  $\bar{q}$ . The punctured  $q^2$ -plane (with the origin removed) could itself be considered as a parameter space, for example by setting  $z = w/q$  to obtain the family of linearly conjugate maps  $F_{q^2}(w) = qf_q(w/q) = w^2(q^2 - w)/(q^2 + |q^2|w)$ , which are well defined for  $q^2 \neq 0$ .

and only if  $|w_k| \rightarrow \infty$  and  $w_k/|w_k| \rightarrow e^{2\pi i t}$ . By definition, this circled plane is homeomorphic to the closed unit disk  $\overline{\mathbb{D}}$  under a homeomorphism  $\mathbb{C} \xrightarrow{\cong} \overline{\mathbb{D}}$  of the form

$$w = re^{2\pi i t} \mapsto \eta(r)e^{2\pi i t}$$

where  $\eta : [0, \infty] \rightarrow [0, 1]$  is any convenient orientation preserving homeomorphism. (For example we could take

$$\eta(r) = r / \sqrt{1 + r^2}$$

but the precise choice of  $\eta$  will not be important.)

In particular, it is useful to compactify the  $q^2$ -plane in this way; and for illustrative purposes, it is often helpful to show the image of the circled  $q^2$ -plane under such a homeomorphism, since we can then visualize the entire circled plane in one figure. (Compare Figure 2 left and right.) The circle at infinity for the  $q^2$ -plane has an important dynamic interpretation:

**LEMMA 1.2.** *Suppose that  $q^2$  converges to the point  $\infty_{\mathbf{t}}$  on the circle at infinity. Then for any  $\varepsilon > 0$  the associated maps  $f_{\pm q}$  both converge uniformly to the rotation  $z \mapsto e^{2\pi i t} z$  throughout the annulus  $\varepsilon \leq |z| \leq 1/\varepsilon$ .*

Therefore, most of the chaotic dynamics must be concentrated within the small disk  $|z| < \varepsilon$  and its antipodal image. The proof is a straightforward exercise.  $\square$

## OUTLINE OF THE MAIN CONCEPTS AND RESULTS.

In Section 2 of the paper we discuss the various types of Fatou components for maps  $f_q$  with  $q \in \mathbb{C}$ . In particular, we show that any Fatou component which eventually maps to a Herman ring is an annulus, but that all other Fatou components are simply-connected. (See Theorem 2.1.)

We give a rough classification of hyperbolic components (either in the  $q$ -plane or in the  $q^2$ -plane), noting that every hyperbolic component is simply-connected, with a unique critically finite ‘‘center’’ point. (See Lemmas 2.4 and 2.5.)

In Section 3 we focus on the study of the central hyperbolic component  $\mathcal{H}_0$  in the  $q^2$ -plane. (The corresponding component in the  $q$ -plane will be denoted by  $\tilde{\mathcal{H}}_0$ .) We construct a canonical (but not conformal!) diffeomorphism between  $\mathcal{H}_0$  and the open unit disk (see Theorem 3.1). Using this, we can consider parameter rays (= stretching rays), which correspond to radial lines in the unit disk, each with a specified **parameter angle**  $\vartheta \in \mathbb{R}/\mathbb{Z}$ . In Theorem 3.6, we prove the following landing properties of the parameter rays  $\mathcal{R}_{\vartheta} \subset \mathcal{H}_0$ .

*If the angle  $\vartheta \in \mathbb{Q}/\mathbb{Z}$  is periodic under doubling, then the parameter ray  $\mathcal{R}_{\vartheta}$  either:*

- (a) *lands at a parabolic point on the boundary  $\partial\mathcal{H}_0$ ,*
- (b) *accumulates on a curve of parabolic boundary points, or*
- (c) *lands at a point  $\infty_{\mathbf{t}}$  on the circle at infinity, where  $\mathbf{t}$  can be described as the rotation number of  $\vartheta$  under angle doubling.*

The proof of this Theorem makes use of **dynamic internal rays**  $\mathcal{R}_{q,\theta}$  in the immediate basin of zero  $\mathcal{B}_q$  for the map  $f_q$ . These are defined using the Böttcher coordinate  $\mathfrak{b}_q$ , which

is well defined throughout some neighborhood of zero in the  $z$ -plane whenever  $q \neq 0$ . Here  $\theta$  will be called the **dynamic angle**.

In Section 4 we study, for  $q^2 \in \mathcal{H}_0$ , the set of landing points of dynamic internal rays  $\mathcal{R}_{q,\theta}$ . More precisely, if  $q^2 \in \mathcal{R}_\vartheta$  with  $\vartheta \in \mathbb{R}/\mathbb{Z}$ , then the dynamic internal ray  $\mathcal{R}_{q,\theta}$  lands if and only if the dynamic angle  $\theta$  is not an iterated preimage of the parameter angle  $\vartheta$  under doubling. In this situation, the Julia set  $\mathcal{J}(f_q)$  is a quasicircle and there is a homeomorphism  $\eta_q : \mathbb{R}/\mathbb{Z} \rightarrow \mathcal{J}(f_q)$  conjugating the tripling map to  $f_q$ :

$$\eta_q(3x) = f_q(\eta_q(x)).$$

This conjugacy is uniquely defined up to orientation, and up to the involution  $x \leftrightarrow x + 1/2$  of the circle. We specify a choice and present an algorithm which, given  $\vartheta \in \mathbb{R}/\mathbb{Z}$  and an angle  $\theta \in \mathbb{R}/\mathbb{Z}$  which is not an iterated preimage of  $\vartheta$  under doubling, returns the base three expansion of the angle  $x \in \mathbb{R}/\mathbb{Z}$  such that  $\eta_q(x)$  is the landing point of  $\mathcal{R}_{q,\theta}$ .

In Section 5 we define the **dynamic rotation number**  $\mathbf{t}$  of a map  $f_q$  with  $q^2 \in \mathcal{H}_0 \setminus \{0\}$  as follows. A point  $z \in \mathcal{J}(f_q)$  is said to be **bi-visible** if it is a landing point for both an internal ray and an external ray, in other words, if it is visible from both zero and infinity. We show that the set of bi-visible points is a rotation set for the circle map  $f_q : \mathcal{J}(f_q) \rightarrow \mathcal{J}(f_q)$ , and define  $\mathbf{t}$  to be the associated rotation number. This number  $\mathbf{t}$  depends only on the argument  $\vartheta$  of the parameter ray  $\mathcal{R}_\vartheta \subset \mathcal{H}_0$  containing  $q^2$ . The function  $\vartheta \mapsto \mathbf{t}$  is monotone and continuous of degree one. The inverse correspondence  $\mathbf{t} \mapsto \vartheta$  can be described as follows. For each  $\mathbf{t} \in \mathbb{R}/\mathbb{Z}$ , there is a unique **reduced rotation set**  $\Theta_{\mathbf{t}} \subset \mathbb{R}/\mathbb{Z}$  which is invariant under the doubling map  $\mathbf{m}_2$  and has rotation number  $\mathbf{t}$ . If  $\mathbf{t}$  is rational with denominator  $n > 1$ , then the points of  $\Theta_{\mathbf{t}}$  can be listed in numerical order within the open interval  $(0, 1)$ .

- (1) If  $\mathbf{t}$  is rational with odd denominator, then  $\vartheta$  is the unique middle element  $\theta_{(n+1)/2}$  in the rotation set  $\Theta_{\mathbf{t}}$ . This middle element  $\vartheta$  will be called the **balanced angle**.
- (2) If  $\mathbf{t}$  is rational with even denominator, there is a unique pair  $\{\theta_{n/2}, \theta_{1+n/2}\}$  in the middle. This will be called the **balanced-pair** for  $\Theta_{\mathbf{t}}$ , and the two elements of the pair will be called **almost balanced**. In this case  $\vartheta$  can be any element in the closed interval  $[\theta_{n/2}, \theta_{1+n/2}]$ .
- (3) If  $\mathbf{t}$  is irrational then  $\Theta_{\mathbf{t}}$  is topologically a Cantor set. There is a unique  $\mathbf{m}_2$ -invariant probability measure which is supported on  $\Theta_{\mathbf{t}}$ . The **balanced point**  $\vartheta$  in this case is the unique  $\vartheta$  such that both  $\Theta_{\mathbf{t}} \cap (0, \vartheta)$  and  $\Theta_{\mathbf{t}} \cap (\vartheta, 1)$  have measure  $1/2$ .

In Section 6 we study the set of points which are visible from both zero and infinity in the case that  $q^2 \notin \mathcal{H}_0$ . In Theorem 6.1, we first prove:

For any map  $f = f_q$  in our family, either

- (1) the two immediate basin closures  $\overline{\mathcal{B}}_0$  and  $\overline{\mathcal{B}}_\infty$  have a non-vacuous intersection, or else
- (2) these basin closures are separated by a Herman ring  $\mathcal{A}$ . Furthermore, this ring has topological boundary  $\partial\mathcal{A} = \mathcal{C}_0 \cup \mathcal{C}_\infty$  with  $\mathcal{C}_0 \subset \partial\mathcal{B}_0$  and  $\mathcal{C}_\infty \subset \partial\mathcal{B}_\infty$ .

This allows us to extend the concept of dynamic rotation number to maps  $f_q$  which do not represent elements of  $\mathcal{H}_0$  provided that they have locally connected Julia set. In Theorem 6.13, we also deduce the following:

If  $U$  is an attracting or parabolic basin of period two or more for a map  $f_q$ , then the boundary  $\partial U$  is a Jordan curve. The same is true for any Fatou component which eventually maps to  $U$ .

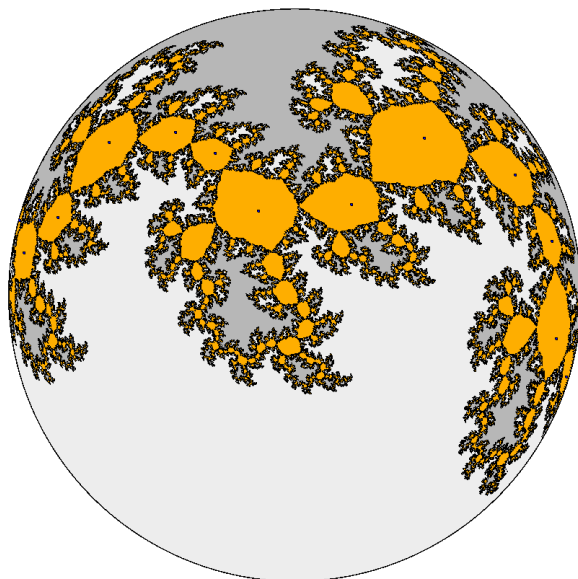


FIGURE 3. Rational rotation number with even denominator: Julia set for a point in the  $(21/26)$ -tongue. Here the Riemann sphere has been projected orthonormally onto the plane, so that only one hemisphere is visible. Zero is at the bottom and infinity at the top. Note the self-antipodal attracting orbit of period 26, which has been marked. The associated ring of attracting Fatou components separates the basins of zero and infinity. (If the sphere were transparent, then we would see the same figure on the far side, but rotated  $180^\circ$  and with light and dark gray interchanged.)

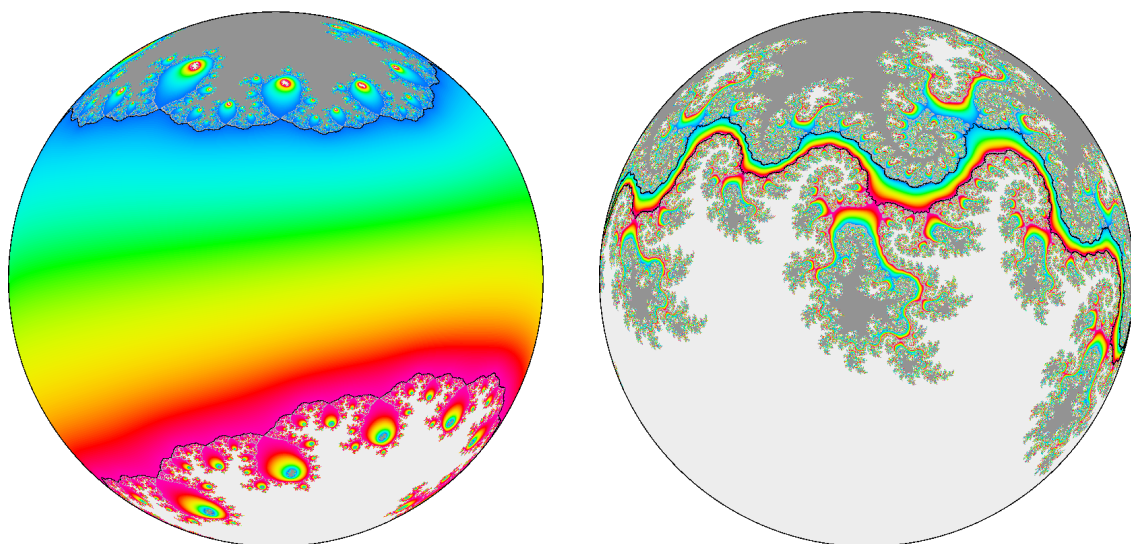


FIGURE 4. Irrational rotation number: two Herman rings on the Riemann sphere, projected orthonormally. The boundaries of the rings have been outlined. Otherwise, every point  $z$  maps to a point  $f_q(z)$  of the same color. Left example:  $q = 1 - 6i$ , modulus  $\approx 0.2081$ . Right example:  $q = 3.21 - 1.8i$ , modulus  $\approx 0.0063$ .

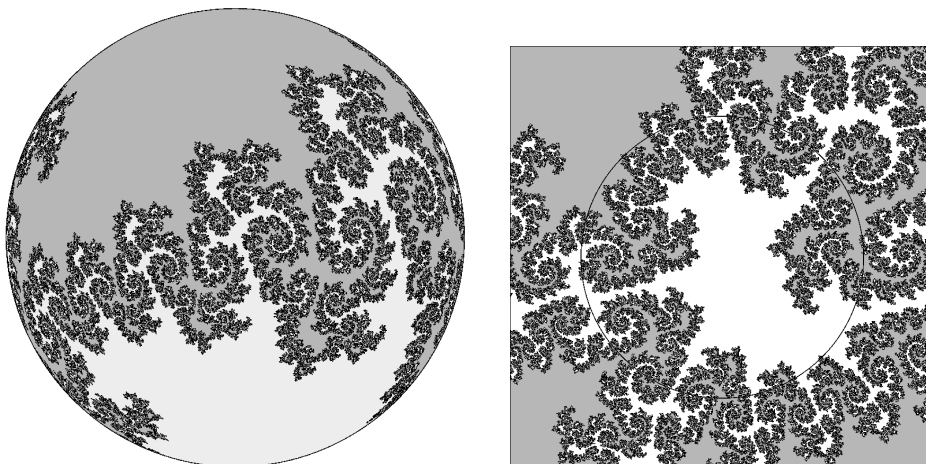


FIGURE 5. Julia set for a point in the  $(5/11)$ -fjord. This is a Jordan curve, separating the basins of zero and infinity. The left side illustrates the Riemann sphere version, and the right side shows the view in the  $z$ -plane, with the unit circle drawn in.

In Section 7, for each rational  $\mathbf{t} \in \mathbb{R}/\mathbb{Z}$  with odd denominator we prove in Theorem 7.1 the existence of an associated fjord in the main hyperbolic component  $\mathcal{H}_0$ .

*If  $\mathbf{t}$  is rational with odd denominator, and if  $\vartheta$  is the associated balanced angle, then the parameter ray  $\mathcal{R}_\vartheta$  lands at the point  $\infty_{\mathbf{t}}$  on the circle of points at infinity.*

As an application of this Fjord Theorem, we describe in Definition 7.6 the concept of **formal rotation number** for all maps  $f_q$  with  $q \neq 0$ .

We finish the paper with an Appendix in which we discuss **circle maps** and **rotation sets**. **Rotation sets** are compact subsets of the circle  $\mathbb{R}/\mathbb{Z}$  with a well defined rotation number under multiplication by some integer  $d \geq 2$ . We introduce the concept of **reduced rotation set** and describe the classification of these sets. We finish the Appendix with a short discussion of **semiconjugacies** of circle maps.

## 2. FATOU COMPONENTS AND HYPERBOLIC COMPONENTS

We first prove the following.

**THEOREM 2.1.** *Let  $U$  be a Fatou component for some map  $f = f_q$  belonging to our family (1). If some forward image  $f^{\circ k}(U)$  is a Herman ring,<sup>†</sup> then  $U$  is an annulus; but in all other cases  $U$  is simply-connected. In particular, the Julia set  $\mathcal{J}(f)$  is connected if and only if there is no Herman ring.*

The proof will make use of the following preliminary statement.

---

<sup>†</sup> A priori, there could be a cycle of Herman rings with any period. However, we will show in [2] that any Herman ring in our family is fixed, with period one.

LEMMA 2.2. *Let  $X$  and  $Y$  be connected self-antipodal subsets of the Riemann sphere. If at least one of these sets is either compact or open,<sup>‡</sup> then the intersection  $X \cap Y$  must be non-empty.*

PROOF. JORDAN CURVE CASE: Suppose that  $X$  is a Jordan curve. Then the complement  $\widehat{\mathbb{C}} \setminus X$  has two components  $U$  and  $V$ , where each closure  $\overline{U}$  or  $\overline{V}$  is a closed topological disk by the Schoenflies Theorem. These two components are necessarily interchanged by the antipodal map. For otherwise, if  $\mathcal{A}$  mapped  $U$  to itself, it would have a fixed point in  $\overline{U}$  by the Brouwer Fixed Point Theorem, which is impossible since the antipodal map has no fixed points. Now if  $X$  and  $Y$  were disjoint, since  $Y$  is connected, it would be contained in a single component  $U$  or  $V$ . Therefore  $Y$  could not be self-antipodal, contradicting our assumptions. This proves that  $X \cap Y \neq \emptyset$ .

OPEN CASE: Suppose that  $X$  is an open set. Starting at any point  $x \in X$ , we can construct an embedded path  $p: [0, 1] \rightarrow X$  with  $p(0) = x$  and  $p(1) = \mathcal{A}(x)$ . If there are no antipodal pairs within this path other than the two endpoints, then the union  $X' = p[0, 1] \cup \mathcal{A}(p[0, 1])$  will be a Jordan curve. Thus the other set  $Y$  must intersect  $X'$  by the previous Case; and hence must also intersect the larger set  $X$ . If there is some other pair of antipodal points  $p(s)$  and  $p(t)$  with  $0 < t - s < 1$ , then we can choose such a pair with  $t - s$  minimal. The corresponding construction using the path from  $p(s)$  to  $p(t)$  will then complete the argument in the Open Case.

COMPACT CASE: Suppose that  $X$  is a compact, connected and self-antipodal. Then it follows immediately from the Open Case, that no connected component of its complement can be self-antipodal. It then follows, as in the first Case that the connected self-antipodal set  $Y$  must intersect  $X$ .  $\square$

PROOF OF THEOREM 2.1. First consider the special case where  $U$  is a periodic Fatou component.

CASE 1. A ROTATION DOMAIN.

If there are no critical points in this cycle of Fatou components, then  $U$  must be either a Herman ring (necessarily an annulus), or a Siegel disk (necessarily simply connected). In either case there is nothing to prove. Thus we are reduced to the attracting and parabolic cases.

CASE 2. AN ATTRACTING DOMAIN OF PERIOD  $m \geq 2$ .

Then  $U$  contains an attracting periodic point  $z_0$  of period  $m$ . Let  $\mathcal{O}$  be the orbit of  $z_0$ , and let  $U_0$  be a small disk about  $z_0$  which is chosen so that  $f^{em}(U_0) \subset U_0$ , and so that the boundary  $\partial U_0$  does not contain any postcritical point. For each  $j \geq 0$ , let  $U_j$  be the connected component of  $f^{-j}(U_0)$  which contains a point of  $\mathcal{O}$ , thus  $f(U_j) = U_{j-1}$ . Assuming inductively that  $U_j$  is simply connected, we will prove that  $U_{j+1}$  is also simply connected. If  $U_{j+1}$  contains no critical point, then it is an unbranched covering of  $U_j$ , and hence maps diffeomorphically onto  $U_j$ . If there is only one critical point, mapping to the critical value  $v \in U_j$ , then  $U_{j+1} \setminus f^{-1}(v)$  is an unbranched covering space of  $U_j \setminus \{v\}$ , and hence is a punctured disk. It follows again that  $U_{j+1}$  is simply connected. We must show that there cannot be two critical points in  $U_{j+1}$ . Certainly it cannot contain either of the two fixed critical points, since the period is two or more. If it contained both free critical points, then it would intersect its antipodal image, and hence be self-antipodal. Similarly its image under

---

<sup>‡</sup> This condition may well be unnecessary.



$f_q$  would be self-antipodal. Therefore these two sets must intersect each other by Lemma 2.2. Thus it would again follow that the period must be one, contradicting the hypothesis.

Thus it follows inductively that each  $U_j$  is simply connected. Since the entire Fatou component  $U$  is the nested union of the  $U_{jm}$ , it is also simply connected.

CASE 3. A PARABOLIC DOMAIN OF PERIOD  $m$ .

Note first that we must have  $m \geq 2$ . In fact it follows from the holomorphic fixed point formula <sup>†</sup> that every non-linear rational map must have either a repelling fixed point (and hence an antipodal pair of repelling points in our case) or a fixed point of multiplier  $+1$ . But the latter case cannot occur. Every cubic rational map has exactly four fixed points, counted with multiplicity, where a fixed point of multiplier  $+1$  has multiplicity two or more. Every map in our family has two fixed critical points, so there cannot also be a point of multiplicity  $\geq 2$ , together with its antipode.

The argument is now almost the same as in the attracting case, except that in place of a small disk centered at the parabolic point, we take a small attracting petal which intersects all orbits in its Fatou component.

REMARK 2.3. In Cases 2 and 3, we will see in Theorem 6.13 that the boundary  $\partial U$  is always a Jordan curve.

CASE 4. AN ATTRACTING DOMAIN OF PERIOD ONE: THE BASIN OF ZERO OR INFINITY.

As noted in Case 3, the two free fixed points are necessarily repelling, so the only attracting fixed points are zero and infinity.

Let us concentrate on the basin of zero. Construct the sets  $U_j$  as in Case 2 so that  $f(U_j) = U_{j-1}$ . If there are no other critical points in this immediate basin, then it follows inductively that the  $U_j$  are all simply connected. If there is another critical point  $c$  in the immediate basin, then there will be a smallest  $j$  such that  $U_{j+1}$  contains  $c$ . Consider the Riemann-Hurwitz formula

$$\chi(U_{j+1}) = d \cdot \chi(U_j) - n,$$

where  $\chi(U_j) = 1$ ,  $d$  is the degree of the map  $U_{j+1} \rightarrow U_j$ , and  $n = 2$  is the number of critical points in  $U_{j+1}$ . If  $d = 3$ , then  $U_{j+1}$  is simply connected, and again it follows inductively that the  $U_j$  are all simply connected. However, if  $d = 2$  so that  $U_{j+1}$  is an annulus, then we would have a more complicated situation, as illustrated in Figure 6. The two disjoint closed annuli  $\bar{U}_{j+1}$  and  $\mathcal{A}(\bar{U}_{j+1})$  would separate the Riemann sphere into two simply connected regions plus one annulus. One of these simply connected regions  $E$  would have to share a boundary with  $U_{j+1}$ , and the antipodal region  $\mathcal{A}(E)$  would share a boundary with  $\mathcal{A}(U_{j+1})$ . The remaining annulus  $A$  would then share a boundary with both  $U_{j+1}$  and  $\mathcal{A}(U_{j+1})$ , and hence would be self-antipodal. We must prove that this case cannot occur.

Each of the two boundary curves of  $U_{j+1}$  (emphasized in Figure 6) must map homeomorphically onto  $\partial U_j$ . Thus one of the two boundary curves of  $A$  maps homeomorphically onto  $\partial U_j$ , and the other must map homeomorphically onto  $\mathcal{A}(\partial U_j)$ . Note that there are no critical points in  $A$ . The only possibility is that  $A$  maps homeomorphically onto the larger annulus  $A' = \widehat{\mathbb{C}} \setminus (\bar{U}_j \cup \mathcal{A}(\bar{U}_j))$ . This behavior is perfectly possible for a branched covering, but is impossible for a holomorphic map, since the modulus of  $A'$  must be strictly larger than the modulus of  $A$ . This contradiction completes the proof that each periodic Fatou component is either simply connected, or a Herman ring.

---

<sup>†</sup> See for example [14, Corollary 12.7].

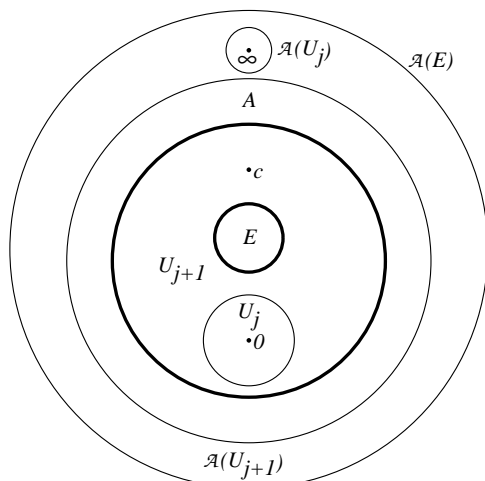


FIGURE 6. Three concentric annuli. (See Case 4.) The innermost annulus  $U_{j+1}$ , with emphasized boundary, contains the disk  $U_j$ , while the outermost annulus  $\mathcal{A}(U_{j+1})$  contains  $\mathcal{A}(U_j)$ . The annulus  $A$  lies between these two. Finally, the innermost region  $E$  and the outermost region  $\mathcal{A}(E)$  are topological disks.

#### THE PREPERIODIC CASE.

For any non-periodic Fatou component  $U$ , we know by Sullivan's nonwandering theorem that some forward image  $f^{\circ k}(U)$  is periodic. Assuming inductively that  $f(U)$  is an annulus or is simply connected, we must prove the same for  $U$ . If  $f(U)$  is simply connected, then there can be at most one critical point in  $U$ : Otherwise as in the proof of Case 2 above, if  $U$  contained both free critical points then it would intersect its antipodal image, and hence be self-antipodal; and therefore fixed. This contradicts the hypothesis that  $U$  is non-periodic. Hence as before it follows that  $U$  is simply connected. In the annulus case, the two free critical points necessarily belong to the Julia set, and hence cannot be in  $U$ . Therefore  $U$  is a finite unbranched covering space of  $f(U)$ , and hence is also an annulus. This completes the proof of Theorem 2.1.  $\square$

The corresponding result in the parameter plane is even sharper.

LEMMA 2.4. *Every hyperbolic component, either in the  $q$ -plane or in the  $q^2$ -plane, is simply connected, with a unique critically finite point (called its **center**).*

PROOF. This is a direct application of results from [16].

By Theorem 9.3 of [16], every hyperbolic component in the moduli space for rational maps of degree  $d$  with marked fixed points is a topological cell with a unique critically finite "center" point. We can also apply this result to the sub moduli space consisting of maps with one or

more marked critical fixed points [16, Remark 9.10]. The corresponding result for real forms <sup>†</sup> of complex maps is also true. (See [16, Theorem 7.13 and Remark 9.6].)

These results apply in our case, since we are working with a real form of the moduli space of cubic rational maps with two marked critical fixed points. The two remaining fixed points are then automatically marked: one in the upper half-plane and one in the lower half-plane. (Compare the discussion below.) □

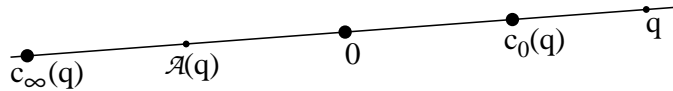


FIGURE 7.

We will need a more precise description of the four (not necessarily distinct) critical points of  $f_q$ . The critical fixed points zero and infinity are always present, and there are also two mutually antipodal **free critical points**. For  $q \neq 0$  it is not hard to compute the two free critical points as

$$c_0(q) = \left( \frac{a - 3 + \sqrt{P(a)}}{4a} \right) q, \quad \text{and} \quad c_\infty(q) = \left( \frac{a - 3 - \sqrt{P(a)}}{4a} \right) q, \quad (2)$$

where  $a = |q^2| > 0$  and  $P(a) = 9 + 10a + a^2 > 9$ . Thus  $c_0 = c_0(q)$  is a positive multiple of  $q$ , and  $c_\infty = c_\infty(q)$  is a negative multiple of  $q$ . In fact, it is not hard to verify the inequalities

$$\frac{1}{2} < \frac{a - 3 + \sqrt{P(a)}}{4a} < \frac{2}{3} \quad \text{for } a > 0,$$

and to check the asymptotic estimates

$$c_0(q) \sim \frac{2}{3} q \quad \text{as } q \rightarrow 0 \quad \text{and} \quad c_0(q) \sim \frac{1}{2} q \quad \text{as } |q| \rightarrow \infty. \quad (3)$$

In particular, whenever  $q \neq 0$ , the free critical point  $c_0(q)$  lies strictly between zero and  $q$ . It follows easily that the three finite critical points, as well as the zero  $q \in f_q^{-1}(0)$  and the pole  $\mathcal{A}(q)$ , all lie on a straight line, with  $c_0(q)$  between zero and  $q$  and with  $\mathcal{A}(q)$  between  $c_\infty(q)$  and zero, as shown in Figure 7. As  $q$  tends to infinity, note that  $c_0(q)$  also tends to infinity, but its antipode  $c_\infty(q)$  tends to zero.

Setting  $q = x + iy$ , a similar computation shows that the two **free fixed points** are given by

$$\xi_\pm(q) = i \left( y \pm \sqrt{y^2 + 1} \right) \quad \text{where} \quad y = \text{Im}(q). \quad (4)$$

Thus  $\xi_+(q)$  always lies on the positive imaginary axis, while its antipode  $\xi_-(q)$  lies on the negative imaginary axis. As noted in the proof of Theorem 2.1, both of these free fixed points must be strictly repelling. One of the two is always on the boundary of the basin of zero, and the other is always on the boundary of the basin of infinity. (More precisely, we will see in Remark 4.1 below that if  $y \neq 0$  then the landing point of the dynamic ray of angle zero in the basin of zero is that fixed point  $\xi_\pm(q)$  which is closer to the origin; while its antipode  $\xi_\mp(q)$

---

<sup>†</sup> If a family of rational maps is invariant under an antiholomorphic involution  $\mathcal{A}'$  of the Riemann sphere, then we can consider the associated **real form** of this family, consisting of those maps in the family which commute with  $\mathcal{A}'$ . (Compare [13], [16].) In practice, there are only two interesting cases: After a Möbius change of coordinates, we can always take  $\mathcal{A}'$  to be either complex conjugation (if it has fixed points), or the antipodal map (if it has none).

is the landing point of the zero ray in the basin of infinity. In the special case  $y = 0$ , both fixed points  $\pm i$  lie on both boundaries, and neither zero ray lands.)

We can now give a preliminary description of the possible hyperbolic components.

LEMMA 2.5. *Every hyperbolic component in the  $q^2$ -plane belongs to one of the following four types:*

- **The central hyperbolic component  $\mathcal{H}_0$**  (the white region in Figure 2). *This is the unique component for which the Julia set is a Jordan curve, which necessarily separates the basins of zero and infinity.* <sup>†</sup> *In this case, the critical point  $\mathbf{c}_0(q)$  necessarily lies in the basin of zero, and  $\mathbf{c}_\infty(q)$  lies in the basin of infinity. Compare Figures 5, 14 (left), and 19. The corresponding white region in the  $q$ -plane (Figure 1) is a branched 2-fold covering space, which will be denoted by  $\tilde{\mathcal{H}}_0$ .*

- **Mandelbrot Type.** *Here there are two mutually antipodal attracting orbits of period two or more, with one free critical point in the immediate basin of each one. For an example in the parameter plane with associated Julia set see Figure 10 (left and right).*

- **Tricorn Type.** *Here there is one self antipodal attracting orbit, necessarily of even period. The most conspicuous examples are the tongues which stretch out to infinity. (These will be studied in [2].) There are also small bounded tricorn. (See Figures 11 and 12.)*

- **Capture Type.** *Here the free critical points are not in the immediate basin of zero or infinity, but some forward image of each free critical point belongs in one basin or the other. (These regions are either dark grey or white in Figures 1, 2, 9, 10 (left), 11, according as the orbit of  $\mathbf{c}_0(q)$  converges to  $\infty$  or  $0$ .)*

PROOF OF LEMMA 2.5. This is mostly a straightforward exercise — Since there are only two free critical points, whose orbits are necessarily antipodal to each other, there are not many possibilities. As noted in the proof of Theorem 2.1, the two fixed points in  $\mathbb{C} \setminus \{0\}$  must be strictly repelling.

However, the uniqueness of the component  $\mathcal{H}_0$  such that the associated Julia sets are all Jordan curves requires some proof. According to Lemma 2.4, any hyperbolic component  $\mathcal{H}$  in the  $q^2$ -plane must have a unique “center point”  $q_0^2$ , such that the associated map  $f_{q_0}$  is critically finite. But it is easy to check that there is only one critically finite map in our family which has a Jordan curve Julia set, namely the map  $f_0$ . Therefore  $\mathcal{H}$  must be equal to  $\mathcal{H}_0$ .

Examples illustrating all four cases, are easily provided. (Compare the figures cited above.)

□

### 3. THE CENTRAL HYPERBOLIC COMPONENT $\mathcal{H}_0$ .

As noted in Lemma 2.5, the central hyperbolic component  $\mathcal{H}_0$  in the  $q^2$ -plane consists of all  $q^2$  such that the Julia set of  $f_q$  is a Jordan curve. The critical point  $\mathbf{c}_0(q)$  necessarily lies in the basin of zero, and  $\mathbf{c}_\infty(q)$  in the basin of infinity. We will make use of the Böttcher coordinate  $z \mapsto \mathbf{b}_q(z)$  which is defined and univalent for  $z$  in a neighborhood of zero in the dynamic plane, provided that  $q \neq 0$ , and satisfies the identity

$$\mathbf{b}_q(f_q(z)) = \mathbf{b}_q(z)^2.$$

---

<sup>†</sup> Note that any  $f_q$  having a Jordan curve Julia set is necessarily hyperbolic. For the Julia set is necessarily self-antipodal. Hence each component of its complement must contain one of the critical fixed points. (Compare the proof of Lemma 2.2.)

More precisely,  $\mathfrak{b}_q$  is well defined in an open set which has the marked critical point  $\mathfrak{c}_0(q)$  on its boundary. However, it has a well defined limiting value at this critical point.

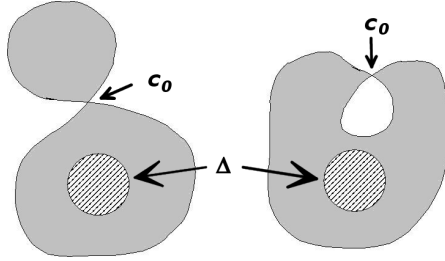


FIGURE 8. Showing the disk  $\Delta$  and two possibilities for  $f_q^{-1}(\Delta)$ .

To see this, let  $\Delta$  be the simply connected open neighborhood of zero which is bounded by the equipotential through the critical value  $f_q(\mathfrak{c}_0(q))$ . Thus the boundary of  $\Delta$  is a Jordan curve, but the preimage  $U = f_q^{-1}(\Delta)$  is bounded by two loops which meet at the free critical point. A priori, depending on the way that these loops are embedded in the plane, this preimage  $U$  (the interior of the shaded region in Figure 8) could be either connected or disconnected. But the connected case (on the right) is impossible: It would require the complement of  $\bar{U}$  to be disconnected. Furthermore, each complementary component would have to map by  $f_q$  onto the complement of  $\Delta$ , and hence contain points of the Julia set. But the Jordan curve Julia set is connected.

Thus  $U$  must have two components, and the component containing the critical fixed point must be a Jordan domain, so that each boundary point has a well defined internal angle.

**THEOREM 3.1.** *The open set  $\mathcal{H}_0$  in the  $q^2$ -plane is canonically diffeomorphic to the open unit disk  $\mathbb{D}$  by the map*

$$\mathfrak{b} : \mathcal{H}_0 \xrightarrow{\cong} \mathbb{D}$$

which satisfies  $\mathfrak{b}(0) = 0$  and carries each  $q^2 \neq 0$  to the Böttcher coordinate  $\mathfrak{b}_q(\mathfrak{c}_0(q))$  of the marked critical point.

**REMARK 3.2.** It follows that there is a canonical way of putting a conformal structure on the open set  $\mathcal{H}_0$ . However, this conformal structure becomes very wild near the boundary  $\partial\mathcal{H}_0$ . It should be emphasized that the entire  $q^2$ -plane does *not* have any natural conformal structure. (The complex numbers  $q$  and  $q^2$  are not holomorphic parameters, since the value  $f_q(z)$  does not depend holomorphically on  $q$ .)

**REMARK 3.3.** The diffeomorphism  $\mathfrak{b} : q^2 \rightarrow \mathfrak{b}_q(\mathfrak{c}_0(q))$  of Theorem 3.1 preserves angles at the origin. Equivalently, we will show that the complex derivative  $\beta = \mathfrak{b}'(0)$  at the origin is well defined, real, and strictly positive. This statement will follow from the asymptotic estimate

$$\mathfrak{b}_q(\mathfrak{c}_0(q)) \sim (2/3\sqrt{3})q^2 \quad \text{as } q \rightarrow 0. \tag{5}$$

As a first step in proving this, note the estimate  $f_q(z) \sim qz^2$  as  $z/q$  tends to zero, with  $q$  bounded. Using this, it is not hard to check that  $\mathfrak{b}_q(z) \sim qz$  under the same conditions. (Compare Remark 4.1.) In particular, it follows that  $\mathfrak{b}_q(\lambda q)/(\lambda q^2) = 1 + o(\lambda)$  as  $\lambda \rightarrow 0$  with

$q$  bounded. Similarly, with  $\lambda$  fixed and  $q \rightarrow 0$  we easily obtain

$$f_q(\lambda q) \sim \lambda^2(1 - \lambda)q^3.$$

Now suppose that  $q \rightarrow 0$  and  $\lambda \rightarrow \lambda_0$ , then

$$\mathfrak{b}_q(\lambda q) = \sqrt{\mathfrak{b}_q(f_q(\lambda q))} \sim \sqrt{\lambda_0^2(1 - \lambda_0)q^4} = q^2\lambda_0\sqrt{1 - \lambda_0}.$$

Note that we can always take the positive sign of the square root provided that  $0 < \lambda_0 < 1$ . In fact, the sign cannot change as we vary  $\lambda_0$  in this interval, and it is known to be positive in the limit as  $\lambda_0 \rightarrow 0$ . Now taking  $\lambda_0 = 2/3$  and recalling from equation (3) that  $\mathfrak{c}_0(q)$  is asymptotic to  $(2/3)q$  as  $q \rightarrow 0$  we obtain the required estimate (5).

**PROOF OF THEOREM 3.1.** The proof will depend on results from [16]. (See in particular [16, Theorem 9.3 and Remark 9.10].) In order to apply these results, we must work with polynomials or rational maps with marked fixed points.

First consider cubic polynomials of the form

$$F_a(z) = z^3 + az^2$$

with critical fixed points at zero and infinity. Let  $\tilde{\mathcal{H}}_0^{\text{poly}}$  be the principal hyperbolic component consisting of values of  $a$  such that both finite critical points of  $F_a$  lie in the immediate basin of zero. This set is simply-connected and contains no parabolic points, hence each of the two free fixed points can be defined as a holomorphic function  $\gamma_{\pm}(a)$  for  $a$  in  $\tilde{\mathcal{H}}_0^{\text{poly}}$ , with  $\gamma_{\pm}(0) = \pm 1$ . The precise formula is

$$\gamma_{\pm}(a) = \frac{-a \pm \sqrt{a^2 + 4}}{2}.$$

Now let  $\tilde{\mathcal{H}}_0^{\text{rat}}$  denote the principal hyperbolic component in the space of cubic rational maps of the form

$$f_{b,c}(z) = z^2 \frac{z + b}{cz + 1}$$

with critical fixed points at zero and infinity. This is again simply-connected. Therefore the two free fixed points can be expressed as holomorphic functions  $\xi_{\pm}(b, c)$  with  $\xi_{\pm}(0, 0) = \pm 1$ .

The basic result in [16] implies that  $\tilde{\mathcal{H}}_0^{\text{rat}}$  is naturally biholomorphic to the Cartesian product  $\tilde{\mathcal{H}}_0^{\text{poly}} \times \tilde{\mathcal{H}}_0^{\text{poly}}$ , where a given pair  $(F_{a_1}, F_{a_2}) \in \tilde{\mathcal{H}}_0^{\text{poly}} \times \tilde{\mathcal{H}}_0^{\text{poly}}$  corresponds to the map  $f_{b,c} \in \tilde{\mathcal{H}}_0^{\text{rat}}$  if and only if:

- (1) the map  $f_{b,c}$  restricted to its basin of zero is holomorphically conjugate to the map  $F_{a_1}$  restricted to its basin of zero, with the boundary fixed point  $\xi_+(b, c)$  corresponding to  $\gamma_+(a_1)$ ; and
- (2) the map  $f_{b,c}$  restricted to its basin of infinity is holomorphically conjugate to  $F_{a_2}$  restricted to its basin of zero, with the boundary fixed point  $\xi_+(b, c)$  corresponding to  $\gamma_+(a_2)$ .

Now let  $\mathcal{H}_0^{\text{poly}}$  be the moduli space obtained from  $\tilde{\mathcal{H}}_0^{\text{poly}}$  by identifying each  $F_a$  with  $F_{-a}$ . According to [15, Lemma 3.6], the correspondence which maps  $F_a$  to the Böttcher coordinate of its free critical point gives rise to a conformal isomorphism between  $\mathcal{H}_0^{\text{poly}}$  and the open unit disk.

Note that  $\tilde{\mathcal{H}}_0$ , the principal hyperbolic component in the  $q$ -plane, can be embedded real analytically as the subspace of  $\tilde{\mathcal{H}}_0^{\text{rat}}$  consisting of maps  $f_q$  which commute with the antipodal map. Since  $f_q$  restricted to the basin of infinity is anti-conformally conjugate to  $f_q$  restricted to the basin of zero, it follows easily that each  $f_q \in \tilde{\mathcal{H}}_0 \subset \tilde{\mathcal{H}}_0^{\text{rat}}$  must correspond to a pair of the form  $(F_a, F_{\pm\bar{a}}) \in \tilde{\mathcal{H}}_0^{\text{poly}} \times \tilde{\mathcal{H}}_0^{\text{poly}}$ , for some choice of sign. In fact the correct sign is  $(F_a, F_{-\bar{a}})$ .

(The other choice of sign  $(F_a, F_{\bar{a}})$  would yield maps invariant under an antiholomorphic involution with an entire circle of fixed points, conjugate to the involution  $z \leftrightarrow \bar{z}$ .)

It follows that the composition of the real analytic embedding

$$\tilde{\mathcal{H}}_0 \hookrightarrow \tilde{\mathcal{H}}_0^{\text{rat}} \cong \tilde{\mathcal{H}}_0^{\text{poly}} \times \tilde{\mathcal{H}}_0^{\text{poly}}$$

with the holomorphic projection to the first factor  $\tilde{\mathcal{H}}_0^{\text{poly}}$  is a real analytic diffeomorphism  $\tilde{\mathcal{H}}_0 \xrightarrow{\cong} \tilde{\mathcal{H}}_0^{\text{poly}}$  (but is *not* a conformal isomorphism). The corresponding assertion for  $\mathcal{H}_0 \xrightarrow{\cong} \mathcal{H}_0^{\text{poly}} \cong \mathbb{D}$  follows easily. This completes the proof of Theorem 3.1.  $\square$

**REMARK 3.4 (Mating).** (Compare [17], [20] and [12]. This remark can be skipped on a first reading.) Let  $F$  and  $G$  be (not necessarily distinct) monic cubic polynomials. Each one has a unique continuous extension to the circled plane, such that each point on the circle at infinity is mapped to itself by the angle tripling map  $\infty_\theta \mapsto \infty_{3\theta}$ . Let  $\mathbb{C}_F \uplus \mathbb{C}_G$  be the topological sphere obtained from the disjoint union  $\mathbb{C}_F \sqcup \mathbb{C}_G$  of two copies of the circled plane by gluing the two boundary circles together, identifying each point  $\infty_\theta \in \partial\mathbb{C}_F$  with the point  $\infty_{-\theta} \in \partial\mathbb{C}_G$ . Then the extension of  $F$  to  $\mathbb{C}_F$  and the extension of  $G$  to  $\mathbb{C}_G$  agree on the common boundary, yielding a continuous map  $F \uplus G$  from the sphere  $\mathbb{C}_F \uplus \mathbb{C}_G$  to itself.

Now assume that the Julia sets of  $F$  and  $G$  are locally connected. Let  $K(F) \Downarrow K(G)$  be the quotient space obtained from the disjoint union  $K(F) \sqcup K(G)$  by identifying the landing point of the  $\theta$ -ray on the Julia set  $\partial K(F)$  with the landing point of the  $-\theta$ -ray on  $\partial K(G)$  for each  $\theta$ . Equivalently,  $K(F) \Downarrow K(G)$  can be described as the quotient space of the sphere  $\mathbb{C}_F \uplus \mathbb{C}_G$  in which the closure of every dynamic ray in  $\mathbb{C}_F \setminus K(F)$  or in  $\mathbb{C}_G \setminus K(G)$  is collapsed to a point.

In many cases (but not always), this quotient space is a topological 2-sphere. In these cases, the **topological mating**  $F \Downarrow G$  is defined to be the induced continuous map from this quotient 2-sphere to itself. Furthermore, again in many cases but not always, the quotient sphere has a unique conformal structure satisfying the following three conditions:

- (1) The map  $F \Downarrow G$  is holomorphic (and hence rational) with respect to this structure.
- (2) This structure is compatible with the given conformal structures on the interiors of  $K(F)$  and  $K(G)$  whenever these interiors are non-empty.
- (3) The natural map from  $\mathbb{C}_F \uplus \mathbb{C}_G$  to  $K(F) \Downarrow K(G)$  has degree one.  $\dagger$

When these conditions are satisfied, the resulting rational map is described as the **conformal mating** of  $F$  and  $G$ .

We will show that such a mating  $F \Downarrow G$  will correspond to a map in our family, provided that  $G$  is an appropriately transformed copy of  $F$ . It will be convenient to use the notation  $z^* = -\bar{z}$  for reflection in the imaginary axis, and to define the reflected map  $F^*$  by the formula

$$F^*(z) = F(z^*)^* .$$

As an example, using the normal form  $F(z) = z^3 + az^2$ , we can write  $F^*(z) = z^3 + a^*z^2$ . Note that the Julia set  $\mathcal{J}(F^*)$  is just the reflected image  $\mathcal{J}(F)^*$ . In particular, a dynamic ray of angle  $\theta$  for  $F$  corresponds to a dynamic ray of angle  $1/2 - \theta$  for  $F^*$ .

If  $G = F^*$ , and if the conformal mating  $F \Downarrow G$  exists, then we will show that this mating commutes with an appropriately defined antipodal map, and hence corresponds to a map in our family. The proof can be summarized in the following diagram, where it is understood

---

$\dagger$  Condition (3) is needed only when  $K(F)$  and  $K(G)$  are dendrites; it follows from (1) and (2) otherwise.

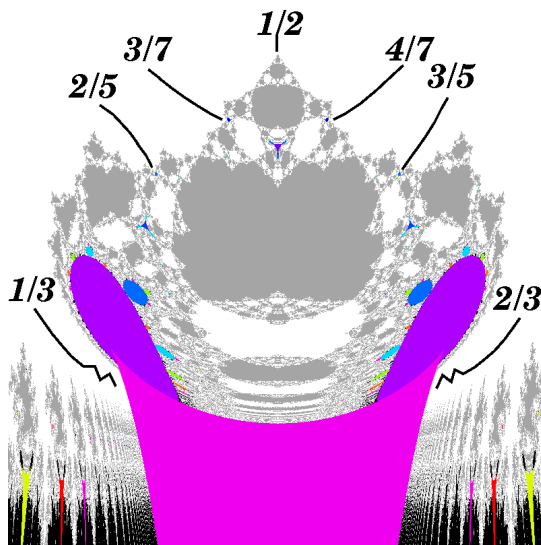


FIGURE 9. Crown at the head of the lower  $(1/2)$ -tongue in the  $q$ -plane, showing the angles of several parameter rays. ( Caution: Since the  $q$ -plane is a 2-fold branched covering of the  $q^2$ -plane, note that every parameter ray  $\mathcal{R}_\vartheta$  in the  $q^2$ -plane corresponds to two different  $\vartheta$ -rays in the  $q$ -plane, with one in the upper half-plane and one in the lower half-plane provided that  $\vartheta \neq 0$ .)

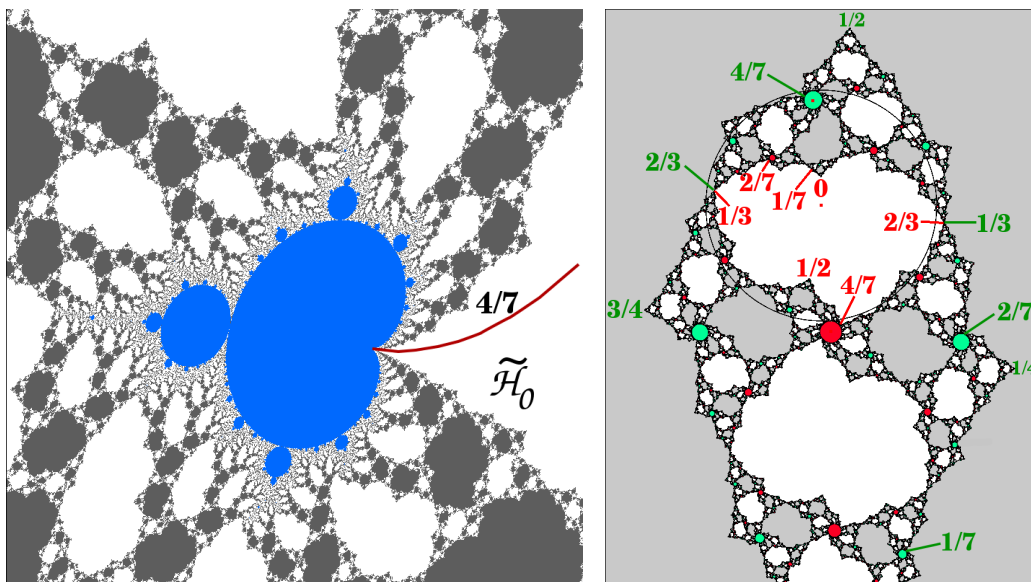


FIGURE 10. On the left: Detail to the upper right of Figure 9 centered at  $q = .1476 - 1.927 i$ , showing a small Mandelbrot set. An internal ray of angle  $4/7$  ( drawn in by hand) lands at the root point of this Mandelbrot set. Here  $\tilde{\mathcal{H}}_0$  is the white region to the right— The other white or grey regions are capture components. On the right: Julia set for the center of the small Mandelbrot set of the picture to the left with some internal and external angles labeled. ( Compare Remark 7.3.) The unit circle has been drawn to fix the scale.



that  $G = F^*$ .

$$\begin{array}{ccc}
 \mathbb{C}_F \uplus \mathbb{C}_G & \begin{array}{c} \xleftarrow{\mathcal{A}'} \\ \xrightarrow{F \uplus G} \end{array} & \mathbb{C}_F \uplus \mathbb{C}_G \\
 \downarrow & & \downarrow \\
 \mathbb{C}_F \perp\!\!\!\perp \mathbb{C}_G & \begin{array}{c} \xleftarrow{\mathcal{A}''} \\ \xrightarrow{F \perp\!\!\!\perp G} \end{array} & \mathbb{C}_F \perp\!\!\!\perp \mathbb{C}_G
 \end{array}$$

The first step is to define the appropriate ‘‘antipodal map’’  $\mathcal{A}'$  from the intermediate sphere  $\mathbb{C}_F \uplus \mathbb{C}_{F^*}$  to itself. In fact, writing the two maps as  $z \mapsto F(z)$  on  $\mathbb{C}_F$  and  $w \mapsto F^*(w)$  on  $\mathbb{C}_{F^*}$ , the required involution  $\mathcal{A}'$  sends each  $z \in \mathbb{C}_F$  to  $z^* \in \mathbb{C}_{F^*}$  and sends each  $w \in \mathbb{C}_{F^*}$  to  $w^* \in \mathbb{C}_F$ . To see that  $\mathcal{A}'$  is well defined, note that the involution  $\theta \leftrightarrow -\theta$  associated with pasting boundaries together commutes with the involution  $\theta \leftrightarrow 1/2 - \theta$  associated with the reflection  $z \mapsto z^*$  in the imaginary axis. It follows easily that two boundary points are pasted together if and only if their images under  $\mathcal{A}'$  are pasted together.

Evidently  $\mathcal{A}'$  is antiholomorphic, with no fixed points outside of the common circle at infinity. On the circle at infinity, it sends  $z = \infty_\theta$  to  $w = \infty_{1/2-\theta}$ . Since each  $z = \infty_\theta$  is identified with  $w = \infty_{-\theta}$ , this corresponds to a  $180^\circ$  rotation of the circle, with no fixed points. Thus we have proved that  $\mathcal{A}'$  is a well defined fixed point free involution of the intermediate sphere  $\mathbb{C}_F \uplus \mathbb{C}_{F^*}$ . Furthermore it is easy to check that  $\mathcal{A}'$  commutes with the map  $F \uplus F^*$ .

Next suppose that the topological mating  $F \perp\!\!\!\perp F^*$  exists. Then it is not hard to see that  $\mathcal{A}'$  gives rise to a corresponding map  $\mathcal{A}''$  of topological degree  $-1$  from the sphere  $K(F) \uplus K(F^*)$  to itself. If  $\mathcal{A}''$  had a fixed point  $\mathbf{x}$ , then there would exist a finite chain  $C$  of dynamic rays in  $\mathbb{C}_F \uplus \mathbb{C}_{F^*}$  leading from a representative point for  $\mathbf{x}$  to its antipode. This is impossible, since it would imply that the union  $C \cup \mathcal{A}''(C)$  is a closed loop separating the sphere  $\mathbb{C}_F \uplus \mathbb{C}_{F^*}$ , which would imply that the quotient  $K(F) \uplus K(F^*)$  is not a topological sphere, contrary to hypothesis.

Finally, if the conformal mating exists, we will show that the fixed point free involution  $\mathcal{A}''$  is anti-holomorphic. To see this, note that the invariant conformal structure  $\Sigma$  can be transported by  $\mathcal{A}''$  to yield a new complex structure  $\mathcal{A}''_*(\Sigma)$  which is still invariant, but has the opposite orientation. Since we have assumed that  $\Sigma$  is the only conformal structure satisfying the conditions (1), (2), (3), it follows that  $\mathcal{A}''_*(\Sigma)$  must coincide with the complex conjugate conformal structure  $\bar{\Sigma}$ . This is just another way of saying that  $\mathcal{A}''$  is antiholomorphic.

As a special case, if  $F$  belongs to the principal hyperbolic component  $\tilde{\mathcal{H}}_0^{\text{poly}}$ , then the conformal mating  $F \perp\!\!\!\perp F^*$  certainly exists. In fact, all maps  $f_q$  in  $\tilde{\mathcal{H}}_0$  can be obtained in this way as matings. (This could be used as part of an alternative proof of Theorem 3.1.) In fact Sharland [19] has shown that many maps outside of  $\tilde{\mathcal{H}}_0$  can also be described as matings. <sup>†</sup>

DEFINITION 3.5. Using the canonical dynamically defined diffeomorphism  $\mathfrak{b}$  of Theorem 3.1, each internal parameter angle  $\vartheta \in \mathbb{R}/\mathbb{Z}$  determines a **parameter ray**

$$\mathcal{R}_\vartheta = \mathfrak{b}^{-1}(\{re^{2\pi i\vartheta}; 0 < r < 1\}) \subset \mathcal{H}_0 \setminus \{0\}.$$

(These are *stretching rays* in the sense of Branner-Hubbard, see [4], [5] and [21]. In particular, any two maps along a common ray are quasiconformally conjugate to each other.)

The following result will play a key role in §7.

---

<sup>†</sup> For example, the landing points described in Theorem 3.6(a) are all matings. (Compare Figure 10 (left) in the  $q$ -plane, and (right) for an associated picture in the dynamic plane.)

**THEOREM 3.6.** *If the angle  $\vartheta \in \mathbb{Q}/\mathbb{Z}$  is periodic under doubling, then the parameter ray  $\mathcal{R}_\vartheta$  either:*

- (a) *lands at a parabolic point on the boundary  $\partial\mathcal{H}_0$ ,*
- (b) *accumulates on a curve of parabolic boundary points, or*
- (c) *lands at a point  $\infty_{\mathbf{t}}$  on the circle at infinity, where  $\mathbf{t}$  can be described as the rotation number of  $\vartheta$  under angle doubling. <sup>†</sup>*

Here Cases (a) and (c) can certainly occur. (See Figures 10 and 30 respectively.) For Case (b), numerical computations by Hiroyuki Inou strongly suggest that rays can accumulate on a curve of parabolic points without actually landing (indicated schematically in Figure 9). This will be studied further in [2]. For the analogous case of multicorns see [11].

**REMARK 3.7.** In case (b), we will show in [2] that the orbit is bounded away from the circle at infinity. If the angle  $\vartheta$  is rational but not periodic, then we will show that  $\mathcal{R}_\vartheta$  lands on a critically finite parameter value.

The proof of Theorem 3.6 will make use of the following definitions: Let  $\mathcal{B}_q$  be the immediate basin of zero for the map  $f_q$ . The case  $q^2 \notin \mathcal{H}_0$  is somewhat simpler, since the Böttcher coordinate is then well defined as a conformal isomorphism  $\mathbf{b}_q : \mathcal{B}_q \xrightarrow{\cong} \mathbb{D}$  satisfying

$$\mathbf{b}_q(f_q(z)) = (\mathbf{b}_q(z))^2.$$

Radial lines in the open unit disk  $\mathbb{D}$  then correspond to dynamic internal rays  $\mathcal{R}_{q,\theta} : [0, 1) \rightarrow \mathcal{B}_q$ , where  $\theta$  is the internal angle in  $\mathbb{D}$ . As in the polynomial case every periodic ray lands on a periodic point.

However, for the moment we are rather concerned with the more complicated case  $q^2 \in \mathcal{H}_0 \setminus \{0\}$ . In this case,  $\mathbf{b}_q$  is defined only on an open subset of  $\mathcal{B}_q$ . More precisely,  $\mathbf{b}_q$  is certainly well defined as a conformal isomorphism from a neighborhood of zero in  $\mathcal{B}_q$  to a neighborhood of zero in  $\mathbb{D}$ . Furthermore the correspondence  $z \mapsto |\mathbf{b}_q(z)|^2$  extends to a well defined smooth map from  $\mathcal{B}_q$  onto  $[0, 1)$ .

**DEFINITION 3.8.** *The dynamic internal rays are the orthogonal trajectories of the equipotential curves  $|\mathbf{b}_q(z)|^2 = \text{constant}$ .*

However, these dynamic rays are not defined everywhere in  $\mathcal{B}_q$ , since the map  $z \mapsto |\mathbf{b}_q(z)|^2$  has critical points at every critical or precritical point of  $f_q$ . Countably many of the internal rays will bifurcate off these critical or precritical points. However, every internal ray outside of this countable set is well defined as an injective map  $\mathcal{R}_{q,\theta} : [0, 1) \rightarrow \mathcal{B}_q$ , and has a well defined landing point in  $\partial\mathcal{B}_q = \mathcal{J}(f_q)$ .

The notation  $\mathcal{B}_q^{\text{vis}}$  will be used for the open subset of  $\mathcal{B}_q$  consisting of all points which are **directly visible** from the origin in the sense that there is a smooth internal ray segment from the origin which passes through the point. The topological closure  $\overline{\mathcal{B}_q^{\text{vis}}}$  will be called the set of **visible points**.

For  $q^2 \in \mathcal{H}_0 \setminus \{0\}$ , the map  $\mathbf{b}_q$  sends the set of directly visible points  $\mathcal{B}_q^{\text{vis}}$  univalently onto a proper open subset of  $\mathbb{D}$  which is obtained from the open disk by removing countably

---

<sup>†</sup> Compare the discussion of rotation numbers in the Appendix.

many radial slits near the boundary. (See Figure 13.) These correspond to the countably many internal rays from the origin in  $\mathcal{B}_q$  which bifurcate off critical or precritical points.

We will need the following:

**LEMMA 3.9.** *If  $q^2 \in \partial\mathcal{H}_0$  is a finite accumulation point for the periodic parameter ray  $\mathcal{R}_\vartheta$  of period  $n$  under doubling, then the dynamic internal ray of angle  $\vartheta$  in  $\mathcal{B}_q$  lands at a parabolic periodic point.*

**PROOF.** Let  $\{q_k^2\}$  be a sequence of points on the parameter ray  $\mathcal{R}_\vartheta \subset \mathcal{H}_0$ , converging to a limit  $q^2 \in \partial\mathcal{H}_0$  in the finite  $q^2$ -plane. Choose representatives  $q_k = \pm\sqrt{q_k^2}$ , converging to the limit  $q$ . Since  $\vartheta$  is periodic and  $q^2 \notin \mathcal{H}_0$ , the internal dynamic ray  $\mathcal{R}_{q,\vartheta}$  lands on a periodic point  $z_q = f_q^{on}(z_q)$ . If this landing point were repelling, then every nearby ray  $\mathcal{R}_{q_k,\vartheta}$  would have to land on a nearby repelling point of  $f_{q_k}$ . (See [8, Lemma B1].) But this is impossible, since each  $\mathcal{R}_{q_k,\vartheta}$  must bifurcate. Thus  $z_q$  must be a parabolic point.  $\square$

**PROOF OF THEOREM 3.6.** Since the ray  $\mathcal{R}_{q,\vartheta}$  landing on  $z_q$  has period  $n$ , we say that this point  $z_q$  has **ray period**  $n$ . Equivalently, each connected component of the immediate parabolic basin of  $z_q$  has exact period  $n$ . If the period of  $z_q$  under  $f_q$  is  $p$ , note that the multiplier of  $f_q^{op}$  at  $z_q$  must be a primitive  $(n/p)$ -th root of unity. (Compare [8, Lemmas 2.2, 2.4].) The set of all parabolic points of ray period  $n$  forms a real algebraic subset of the  $q^2$ -plane. Hence each connected component is either a one-dimensional real algebraic curve or an isolated point. Since the set of all accumulation points of the parameter ray  $\mathcal{R}_\vartheta$  is necessarily connected, the only possibilities are that it lands at a parabolic point or accumulates on a connected subset of a curve of parabolic points. (We will show in [2] that the set of accumulation points is always bounded away from the circle at infinity.)

Now suppose that the sequence  $\{q_k^2\}$  converges to a point on the circle at infinity. It will be convenient to introduce a new coordinate  $u = z/q$  in place of  $z$  for the dynamic plane. The map  $f_q$  will then be replaced by the map

$$u \mapsto \frac{f_q(uq)}{q} = \frac{q^2 u^2 (1 - u)}{1 + |q^2|u}.$$

Dividing numerator and denominator by  $|q^2|u$ , and setting  $\lambda = q^2/|q^2|$  and  $b = 1/|q^2|$ , this takes the form

$$u \mapsto g_{\lambda,b}(u) = \frac{\lambda u(1 - u)}{1 + b/u},$$

with  $|\lambda| = 1$  and  $b > 0$ . The virtue of this new form is that the sequence of maps  $g_{\lambda_k,b_k}$  associated with  $\{q_k^2\}$  converges to a well defined limit  $P_\lambda(u) = \lambda u(1 - u)$  as  $b \rightarrow 0$ , or in other words as  $|q^2| \rightarrow \infty$ . (Compare Figure 14.) Furthermore, the convergence is locally uniform for  $u \in \mathbb{C} \setminus \{0\}$ . Note that  $u = 0$  is a fixed point of multiplier  $\lambda$  for  $P_\lambda$ . A quadratic polynomial can have at most one non-repelling periodic orbit. (This is an easy case of the Fatou-Shishikura inequality.) Hence it follows that all other periodic orbits of  $P_\lambda$  are strictly repelling.

Since  $\vartheta$  is a periodic angle, the external ray of angle  $\vartheta$  for the polynomial  $P_\lambda$  must land at some periodic point. In fact, we claim that it must land at the origin. For otherwise it would land at a repelling point. We can then obtain a contradiction, just as in the preceding case. Since the maps  $g_{\lambda_k,b_k}$  converge to  $P_\lambda$  locally uniformly on  $\widehat{\mathbb{C}} \setminus \{0\}$  the corresponding Böttcher coordinates in the basin of infinity also converge locally uniformly, and hence the associated external rays converge. Hence it would follow that the rays of angle  $\vartheta$  from infinity for the maps  $g_{\lambda_k,b_k}$  would also land on a repelling point for large  $k$ . (See [8, Lemma B1].) But this is impossible since, as in the previous case, these rays must bifurcate.

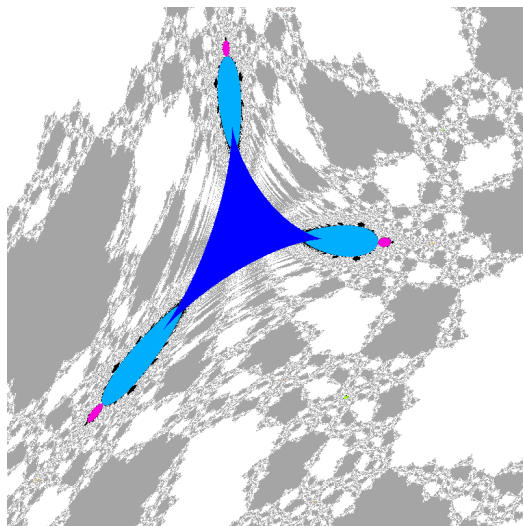


FIGURE 11. Magnified picture of a tiny speck in the upper right of Figure 9, showing a period six tricorn centered at  $q \approx 0.394 - 2.24i$ . The white and grey regions are capture components. (For a corresponding Julia set, see Figure 12.)

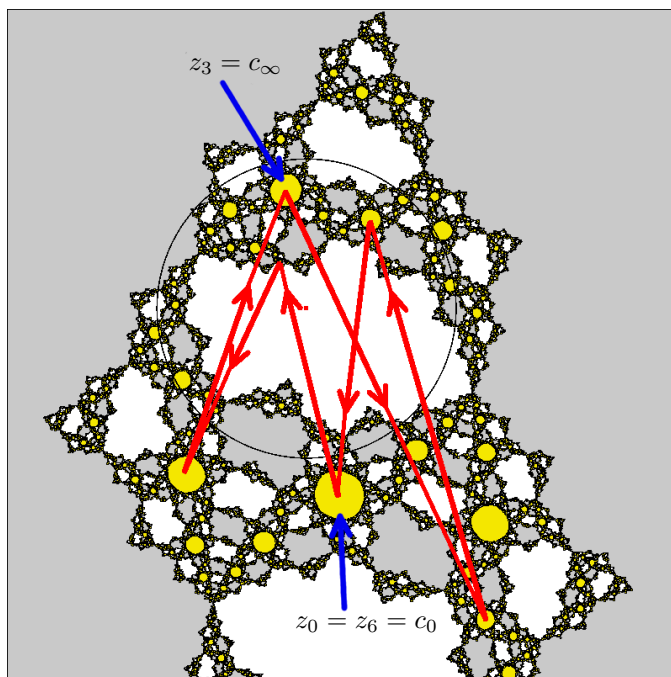


FIGURE 12. Julia set corresponding to the small tricorn of Figure 11.

This proves that the external ray of angle  $\vartheta$  for the quadratic map  $P_\lambda$  lands at zero. Since  $|\lambda| = 1$ , the Snail Lemma <sup>†</sup> then implies that the map  $P_\lambda$  is parabolic, or in other

---

<sup>†</sup> See for example [14].

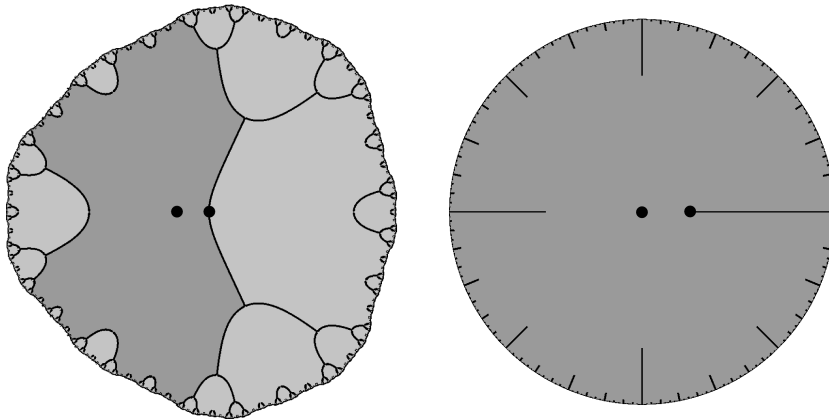


FIGURE 13. On the left: the basin  $\mathcal{B}_q$ . In this example,  $q > 0$  so that the critical point  $\mathbf{c}_0(q)$  is on the positive real axis. Points which are visible from the origin are shown in dark gray, and the two critical points in  $\mathcal{B}_q$  are shown as black dots, with zero to the left. On the right: a corresponding picture in the disk of Böttcher coordinates. Note that the light grey regions on the left correspond only to slits on the right.

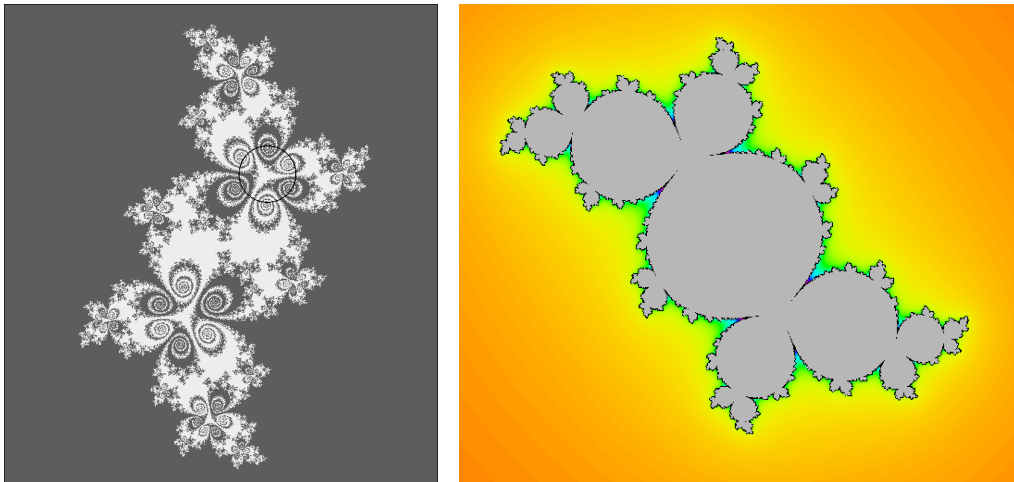


FIGURE 14. On the left: Julia set for a map  $f_q$  on the  $2/7$  ray. The limit of this Julia set as we tend to infinity along the  $2/7$  ray, suitably rescaled and rotated, would be the Julia set for the quadratic map  $w \mapsto e^{2\pi it}w(1-w)$ , as shown on the right. Here  $t = 1/3$  is the rotation number of  $2/7$  under angle doubling. In this infinite limit, the unit circle (drawn in as a small circle near the top of the figure on the left) shrinks to the parabolic fixed point.

words that  $\lambda$  has the form  $e^{2\pi i\mathbf{t}}$  for some rational  $\mathbf{t}$ . It follows that the angle  $\vartheta$  has a well defined rotation number, equal to  $\mathbf{t}$ , under angle doubling. Now recalling that  $\lambda_k \rightarrow \lambda$  where  $\lambda_k = q_k^2/|q_k^2|$ , it follows that  $q_k^2$  must converge to the point  $\infty_{\mathbf{t}}$  as  $k \rightarrow \infty$ . If the  $\vartheta$ -ray has no accumulation points in the finite plane, then it follows that this ray actually lands at the point  $\infty_{\mathbf{t}}$ . This completes the proof of Theorem 3.6.  $\square$

4. VISIBLE POINTS FOR MAPS IN  $\mathcal{H}_0$ .

If  $q^2 \in \mathcal{H}_0$ , then,  $f_q$  is in the same hyperbolic component as  $f_0(z) = -z^3$ . It follows that  $f_q$  on its Julia set is topologically conjugate to  $f_0$  on its Julia set (the unit circle). As a consequence, if we specify one of the two fixed points  $\xi_{\pm}(q)$  on the Julia set, then there is a canonical orientation preserving homeomorphism  $\eta_q : \mathbb{R}/\mathbb{Z} \rightarrow \mathcal{J}(f_q)$  which conjugates the tripling map  $\mathbf{m}_3 : x \mapsto 3x$  to  $f_q$ , so that

$$\eta_q(3x) = f_q(\eta_q(x)) ,$$

and so that  $\eta_q(0)$  is the specified fixed point  $\xi_{\pm}(q)$ . (The other fixed point is then  $\eta_q(1/2) = \xi_{\mp}(q)$ .) Here it is understood that the Julia set is given its usual orientation, as seen from the origin. We will call  $\eta_q$  a **canonical coordinate** on the Jordan curve Julia set.

Now suppose that  $q^2$  belongs to the ray  $\mathcal{R}_{\vartheta}$ , and let

$$\mathbf{cpc}(\vartheta) = \{ \theta \in \mathbb{R}/\mathbb{Z} ; \exists m \geq 0 \text{ with } 2^m \theta = \vartheta \}$$

be the countable dense set consisting of all “critical or precritical” angles, that is those angles which eventually map to  $\vartheta$  under doubling. Thus, if  $\theta \notin \mathbf{cpc}(\vartheta)$ , the dynamic ray  $\mathcal{R}_{q,\theta}$  is smooth and lands at some point  $\zeta_q(\theta) \in \mathcal{J}(f_q)$ . On the other hand, if  $\theta \in \mathbf{cpc}(\vartheta)$ , then the dynamic ray  $\mathcal{R}_{q,\theta}$  bifurcates and we define

$$\zeta_q^{\pm}(\theta) = \lim \zeta_q(\theta \pm \varepsilon) \quad \text{as } \varepsilon \searrow 0 \quad \text{with } \theta \pm \varepsilon \notin \mathbf{cpc}(\vartheta).$$

The limit exists since  $\mathcal{J}(f_q)$  is a Jordan curve and  $\zeta_q$  preserves the cyclic ordering. <sup>†</sup>

Recall that there are two possible choices for the canonical Julia coordinate  $\eta_q$ . We will choose  $\eta_q : \mathbb{R}/\mathbb{Z} \rightarrow \mathcal{J}(f_q)$  so that

$$\eta_q(0) = \zeta_q(0) \text{ when } \vartheta \neq 0 \quad \text{and} \quad \eta_q(0) = \zeta_q^-(0) \text{ when } \vartheta = 0.$$

Thus, in the generic case when  $\vartheta \neq 0$ ,  $\eta_q(0)$  is the landing point of the zero dynamic ray.

REMARK 4.1. The landing point of the zero dynamic ray can be described more precisely as follows. First note the asymptotic estimate  $f_q(z) = qz^2 + O(z^3)$ , as  $z \rightarrow 0$  with  $q$  uniformly bounded. Since the Böttcher coordinate  $z \mapsto \mathbf{b}_q(z)$  is uniquely defined and locally univalent at the origin for  $q \neq 0$ , we also have an estimate of the form  $\mathbf{b}_q(z) = \alpha_q z + O(z^2)$ , as  $z \rightarrow 0$  with  $q$  bounded, where the derivative  $\alpha_q = \mathbf{b}'_q(0)$  is non-zero for  $q \neq 0$ . The identity  $\mathbf{b}_q \circ f_q(z) = \mathbf{b}_q(z)^2$  then implies that  $\alpha_q q = \alpha_q^2$ , hence  $\alpha_q = q$ . This implies the asymptotic estimate

$$\mathbf{b}_q(z) \sim qz \quad \text{as } z \rightarrow 0$$

(as noted in Remark 3.3). Therefore the angle of a ray measured in  $\mathbf{b}_q$ -coordinates at the origin is equal to the angle as measured in the  $z$ -plane plus the argument of  $q$ . In particular, the zero ray  $\mathcal{R}_{q,0}$  has initial vector pointing towards the point  $\bar{q}$  in the  $z$ -plane. For  $q$  real, this ray lies on the real axis, and crashes into the critical point  $\mathbf{c}_0(q)$  (Figure 13). However, for all  $q \notin \mathbb{R}$  this ray must land at that fixed point  $\xi_{\pm}(q)$  which lies on the boundary of the basin of zero. (Compare Equation (4) in Section 2.) For example, if  $q$  lies on the positive imaginary axis, then the zero ray is contained in the negative imaginary axis, and hence must land on  $\xi_{-}(q)$ . It follows by continuity that the landing point is  $\xi_{-}(q)$  whenever  $q$  lies in the upper half-plane, and similarly the landing point is  $\xi_{+}(q)$  when  $q$  lies in the lower half-plane.

---

<sup>†</sup> By definition, a bijection  $\zeta : X \rightarrow X'$  between finite subsets of a topological circle **preserves cyclic order** if it extends to an orientation preserving homeomorphism of the circle. In the case of an infinite subset  $X$ , the corresponding condition must be satisfied for every finite subset of  $X$ .

REMARK 4.2. For each fixed  $\theta$ , as  $q^2$  varies along some stretching ray  $\mathcal{R}_\vartheta$ , the angle  $\eta_q^{-1}(\zeta_q(\theta))$  does not change (and thus depends only on  $\vartheta$  and  $\theta$ ). To see this, note that  $\eta_q$  depends continuously on  $q$  for  $q \notin \mathbb{R}$ . In addition,  $\theta$  is periodic of period  $p$  for the doubling map  $\mathbf{m}_2 : \theta \mapsto 2\theta$  if and only if  $\zeta_q(\theta)$  is periodic of period  $p$  for  $f_q$ , hence if and only if  $\eta_q^{-1}(\zeta_q(\theta))$  is periodic of period  $p$  for  $\mathbf{m}_3$ . The result follows since the set of periodic points of  $\mathbf{m}_3$  and the set of non-periodic points are both totally disconnected.

Now let  $\mathcal{V}_q \subset \mathcal{J}(f_q)$  be the closure of the set of landing points of smooth internal rays. (This is also the set of visible points in  $\mathcal{J}(f_q)$ .) Let

$$V_\vartheta = \eta_q^{-1}(\mathcal{V}_q) \subset \mathbb{R}/\mathbb{Z}$$

be the set of all Julia coordinates which correspond to visible points. Our goal is to describe  $V_\vartheta$  in terms of  $\vartheta$ , and in terms of the monotone but discontinuous function

$$\theta \mapsto \varphi_\vartheta(\theta) = \eta_q^{-1} \circ \zeta_q(\theta), \quad \text{where } q^2 \in \mathcal{R}_\vartheta \text{ with } q \neq 0.$$

However, this function is not defined at the countably many points  $\theta \in \mathbf{cpc}(\vartheta)$  where it has a jump discontinuity. To obtain a monotone function which is well defined everywhere, we can either pass to the right hand limit

$$b(\theta) = \varphi_\vartheta^+(\theta) = \eta_q^{-1} \circ \zeta_q^+(\theta)$$

which is continuous from the right, or the corresponding left hand limit  $a(\theta) = \varphi_\vartheta^-(\theta) \leq \varphi_\vartheta^+(\theta)$  which is continuous from the left. A precise computation of these functions  $\varphi_\vartheta^\pm(\theta)$  will be given in Theorem 4.8.

Any connected component of  $(\mathbb{R}/\mathbb{Z}) \setminus V_\vartheta$  will be called a **gap** in  $V_\vartheta$ . Recall that  $\mathbf{cpc}(\vartheta)$  is the countable set consisting of all  $\theta$  such that  $2^m \theta = \vartheta \in \mathbb{R}/\mathbb{Z}$  for at least one  $m \geq 0$ . If  $\theta \in \mathbf{cpc}(\vartheta)$  with  $\theta \neq 0$ , then, as illustrated in Figure 15, the left and right limits  $\varphi_\vartheta^\pm(\theta)$  are the boundary points of a gap  $(a(\theta), b(\theta))$ , consisting of points which are not visible from the origin.

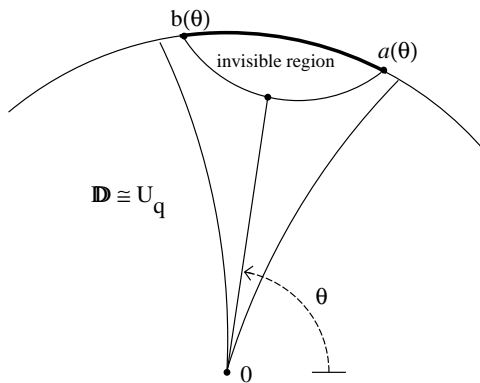


FIGURE 15. Schematic picture after mapping the basin  $\mathcal{B}_q$  homeomorphically onto the unit disk, showing three internal rays. Here the middle internal ray of angle  $\theta$  bifurcates from a critical or precritical point. The corresponding left and right limit landing points span a gap  $G_\vartheta(\theta) = (a(\theta), b(\theta)) := (\varphi_\vartheta^-(\theta), \varphi_\vartheta^+(\theta))$ .

On the other hand, if  $\theta = 0$  and hence  $\vartheta = 2^m \theta = 0$ , we are in the situation illustrated in Figure 13. Our conventions are such that the bottom fixed point  $\xi_+$  in this figure has

Julia coordinate  $x = 0$ , while the top fixed point has Julia coordinate  $x = 1/2$ . Therefore, the associated gap is the interval  $(0, 1/2)$ .

DEFINITION 4.3. For each non-zero  $\theta \in \mathbf{cpc}(\vartheta)$ , let  $G_\vartheta(\theta)$  be the open interval

$$G_\vartheta(\theta) = (\varphi_\vartheta^-(\theta), \varphi_\vartheta^+(\theta)).$$

However, in the special case  $\dagger$   $\theta = 0$  (and hence  $\vartheta = 0$ ), let  $G_0(0) = (0, 1/2)$ .

LEMMA 4.4. *The gaps in  $V_\vartheta$  are precisely these open intervals  $G_\vartheta(\theta)$ , where  $\theta$  varies over the set  $\mathbf{cpc}(\vartheta)$ . The image by  $\mathbf{m}_3$  of a gap of length less  $\ell < 1/3$  is a gap of length  $3\ell$ . The **critical gap**  $G_\vartheta = G_\vartheta(\vartheta)$  is the unique gap of length  $\ell \geq 1/3$  in  $V_\vartheta$ , and always satisfies  $1/3 \leq \ell(G_\vartheta) < 2/3$ . It follows that the length of an arbitrary gap  $G_\vartheta(\theta)$  is equal to the length of the critical gap divided by  $3^m$ , where  $m$  is the smallest integer with  $2^m\theta = \vartheta$ .*

PROOF. If an internal ray  $\mathcal{R}_{q,\theta}$  lands at  $\zeta_q(\theta)$ , then the image ray  $\mathcal{R}_{q,2\theta}$  lands at  $\zeta_q(2\theta) = f_q \circ \zeta_q(\theta)$ . It follows that the set of landing points of smooth rays is invariant by  $f_q$ , and so the set  $V_\vartheta$  satisfies  $\mathbf{m}_3(V_\vartheta) \subset V_\vartheta$ .

Let  $G = (a, b)$  be any gap. If the length of  $G$  is less than  $1/3$ , then  $\mathbf{m}_3$  is injective on  $\overline{G}$ . Since  $a$  and  $b$  are in  $V_\vartheta$  and since  $V_\vartheta$  is invariant by  $\mathbf{m}_3$ , we see that the two ends of  $\mathbf{m}_3(G)$  are in  $V_\vartheta$ . To prove that  $\mathbf{m}_3(G)$  is a gap, it is therefore enough to prove that  $\mathbf{m}_3(G) \cap V_\vartheta = \emptyset$ .

First,  $\eta_q(a)$  and  $\eta_q(b)$  can be approximated by landing points of smooth rays. So, there is a (possibly constant) non-decreasing sequence of angles  $\theta_n^-$  and a non-increasing sequence of angles  $\theta_n^+$  in the complement of  $\mathbf{cpc}(\vartheta)$  such that the sequence  $\{\zeta_q(\theta_n^-)\}$  converges to  $\eta_q(a)$  as  $n \rightarrow \infty$ , and  $\{\zeta_q(\theta_n^+)\}$  converges to  $\eta_q(b)$ . Then, the sequence of angles  $a_n = \varphi_\vartheta(\theta_n^-) \in V_\vartheta$  is non-decreasing and converges to  $a$ , and the sequence of angles  $b_n = \varphi_\vartheta(\theta_n^+) \in V_\vartheta$  is non-increasing and converges to  $b$ .

Now, choose  $n$  large enough such that the length of the interval  $I_n = (a_n, b_n)$  is less than  $1/3$  and let  $\Delta$  be the triangular region bounded by the rays  $\mathcal{R}_{q,\theta_n^\pm}$ , together with  $\eta_q(I_n)$ . (See Figure 15; but note that we have not yet proved that there is a central bifurcating ray.) Then  $f_q$  maps  $\Delta$  homeomorphically onto the triangular region  $\Delta'$  which is bounded by the internal rays of angle  $\mathcal{R}_{q,2\theta_n^\pm}$  together with  $\eta_q(\mathbf{m}_3(I_n)) = f_q(\eta_q(I_n))$ . In fact  $f_q$  clearly maps the boundary  $\partial\Delta$  homeomorphically onto  $\partial\Delta'$ . Since  $f_q$  is an open mapping, it must map the interior into the interior, necessarily with degree one.

We can now prove that  $\mathbf{m}_3(G) \cap V_\vartheta = \emptyset$ . Indeed, if this were not the case, then  $\Delta'$  would contain a smooth ray landing on  $\eta_q(\mathbf{m}_3(G)) = f_q(\eta_q(G))$ . Since  $f_q : \Delta \rightarrow \Delta'$  is a homeomorphism,  $\Delta$  would contain a smooth ray landing on  $\eta_q(G)$ , which is impossible since  $G \cap V_\vartheta = \emptyset$ . This completes the proof that the image under  $\mathbf{m}_3$  of a gap of length  $\ell < 1/3$  is a gap of length  $3\ell$ .

We can iterate the argument until the length of the gap  $\mathbf{m}_3^m(G)$  is  $3^m\ell \geq 1/3$ . So, there is at least one gap  $G_\star$  of length  $\ell_\star \geq 1/3$ . If  $\ell_\star \geq 2/3$ , or if there were two gaps of length  $\geq 1/3$ , then almost every point  $x$  in  $\mathbb{R}/\mathbb{Z}$  would have two preimages in this gap or gaps. (The only exceptions would be the preimages of the endpoints when the lengths add up to exactly  $2/3$ .) This is impossible, since almost every point in  $\mathcal{J}(f_q)$  which is the landing point of a smooth internal ray  $\mathcal{R}_{q,\theta}$  has two preimages which are landing points of the smooth internal

$\dagger$  The case  $\vartheta = \theta = 0$  requires extra care because the landing point of the zero internal ray jumps discontinuously as  $\vartheta$  crosses zero, or in other words as the parameter  $q$  crosses the real axis.



rays  $\mathcal{R}_{q,\theta/2}$  and  $\mathcal{R}_{q,\theta/2+1/2}$ . (In this case, the only exception is the ray  $\mathcal{R}_{q,2\theta}$  which passes through the critical value.)

Thus there is exactly one gap  $G_\star$  of length  $\ell_\star \geq 1/3$ ; we have  $\ell_\star < 2/3$  and the gaps are precisely the iterated preimages of  $G_\star$ . Furthermore, the orbit of each such iterated preimage remains in  $(\mathbb{R}/\mathbb{Z}) \setminus G_\star$  until it lands on  $G_\star$ . To complete the proof of Lemma 4.4, we must show that this longest gap  $G_\star$  is precisely the critical gap  $G_\theta = G_\theta(\theta)$ . In the case  $\theta = 0$ , the critical gap  $G_0 = (0, 1/2)$  certainly has length greater than  $1/3$ . In the case  $\theta \neq 0$ , we proceed by contradiction. If the length of the interval  $(\varphi_\theta^-(\theta), \varphi_\theta^+(\theta))$  were less than  $1/3$ , then as above, we could build a triangular region  $\Delta$  containing the bifurcating ray  $\mathcal{R}_{q,\theta}$  and map it homeomorphically by  $f_q$  to a triangular region  $\Delta'$ . This would contradict the fact that the critical point  $\mathbf{c}_0(q)$  is on the bifurcating ray  $\mathcal{R}_{q,\theta}$ , therefore in  $\Delta$ . This completes the proof of Lemma 4.4.  $\square$

LEMMA 4.5. *If  $\theta$  is not periodic for  $\mathbf{m}_2$ , then the length of the critical gap  $G_\theta$  is  $1/3$ . If  $\theta$  is periodic of period  $p$  for  $\mathbf{m}_2$ , then the length of  $G_\theta$  is  $\frac{3^{p-1}}{3^p - 1} \in (1/3, 1/2]$ .*

PROOF. Let  $\ell$  be the length of the critical gap  $G_\theta$ . According to Lemma 4.4,  $1/3 \leq \ell < 2/3$ . If  $\theta$  is not periodic for  $\mathbf{m}_2$ , then  $2\theta$  is not an iterated preimage of  $\theta$  under doubling, hence the internal ray  $\mathcal{R}_{q,2\theta}$  must land at some point  $z \in \mathcal{J}(f_q)$ . This point has three preimages  $z_0, z_1$  and  $z_2$  in  $\mathcal{J}(f_q)$ . The ray  $\mathcal{R}_{q,\theta+1/2}$  lands at one of those preimages, say  $z_0$ , and the ends of the gap  $G_\theta$  are  $\eta_q^{-1}(z_1)$  and  $\eta_q^{-1}(z_2)$ . In particular,  $\mathbf{m}_3$  maps the two ends of  $G_\theta$  to a common point, so that  $\ell = 1/3$ .

Now suppose that  $\theta$  is periodic of period  $p$  for  $\mathbf{m}_2$ . Then the internal ray  $\mathcal{R}_{q,2\theta}$  bifurcates and there is a gap  $G_\theta(2\theta)$ . The successive images of this gap under tripling must remain disjoint until the image covers the critical gap. Since the endpoints of  $G_\theta$  are periodic of period  $p$ , this is only possible if the image of the gap  $G_\theta$  by  $\mathbf{m}_3$  covers the gap  $G_\theta(2\theta)$  twice and the rest of the circle once. In particular, the length of  $G_\theta(2\theta)$  must be  $3\ell - 1$ . In addition,  $\mathbf{m}_3^{op-1}(G_\theta(2\theta)) = G_\theta$ , which implies that

$$3^{p-1} \cdot (3\ell - 1) = \ell, \quad \text{hence} \quad \ell = \frac{3^{p-1}}{3^p - 1} \quad \text{as required.}$$

$\square$

We have just seen that the gaps are precisely the iterated preimages of  $G_\theta$  and that the orbit of each such iterated preimage remains in  $(\mathbb{R}/\mathbb{Z}) \setminus G_\theta$  until it lands on  $G_\theta$ . It follows that  $V_\theta$  is the Cantor set consisting of all angles whose orbit under  $\mathbf{m}_3$  avoids  $G_\theta$ .

REMARK 4.6. In all cases, the sum of the lengths of all of the gaps is given by

$$\sum_{\theta} \ell(G_\theta(\theta)) = 1. \tag{6}$$

so that the complementary set  $V_\theta$  is a set of measure zero. One way of proving this is to choose an open interval  $I \subset G_\theta$  of length exactly  $1/3$ . Then it is not hard to show that the iterated preimages of  $I$  are pairwise disjoint, with total length  $\sum_{m \geq 0} 2^m/3^{m+1} = 1$  (provided that we exclude those preimages which are contained in  $I$ ). Since these preimages are all contained in the union of gaps, the conclusion follows. (For a related discussion, see Proposition 4.11 below.) Alternatively, Equation (6) can be proved by a fairly straightforward computation, using Lemmas 4.4 and 4.5.

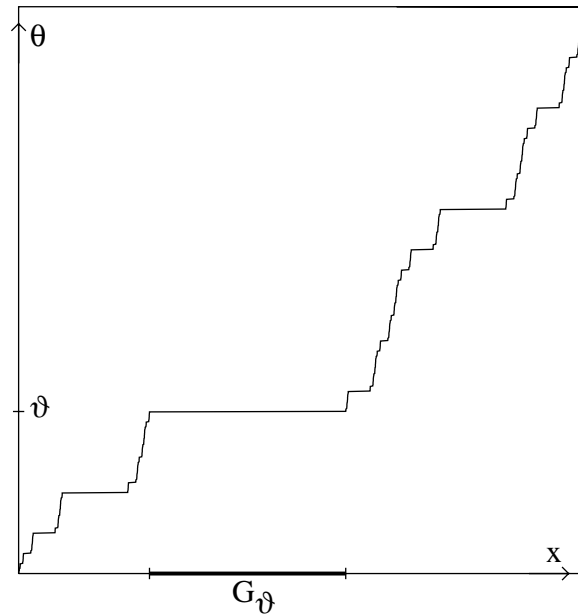


FIGURE 16. Graph of the left inverse  $\psi_\vartheta$  of the map  $\varphi_\vartheta^\pm$  for the case  $\vartheta = 2/7$ . ( Compare Remark 4.7.) This inverse is continuous and monotone, mapping each gap  $G_\theta$  to the corresponding  $\theta$ . In particular, the critical gap  $G_\vartheta = [6/26, 15/26]$  maps to  $\vartheta$ . Outside of the gaps,  $\psi_\vartheta$  conjugates  $\mathbf{m}_3$  to  $\mathbf{m}_2$  ( In this example, the endpoints of  $G_\vartheta$  have period 3 under tripling, so that  $\vartheta = \psi_\vartheta(G_\vartheta)$  has period 3 under doubling.)

REMARK 4.7. The maps  $\varphi_\vartheta^+$  and  $\varphi_\vartheta^-$  have a common left inverse  $\psi_\vartheta : \mathbb{R}/\mathbb{Z} \rightarrow \mathbb{R}/\mathbb{Z}$  defined by

$$\begin{cases} \psi_\vartheta(x) = \theta & \text{if } x = \varphi_\vartheta^\pm(\theta) \text{ and} \\ \psi_\vartheta(x) = \theta & \text{if } x \in \overline{G_\theta} . \end{cases}$$

(Compare Figure 16.) This map  $\psi_\vartheta$  is continuous and monotone, is constant on the closure of each gap, and satisfies

$$\psi_\vartheta \circ \mathbf{m}_3 = \mathbf{m}_2 \circ \psi_\vartheta \quad \text{on } V_\vartheta.$$

(It is a left inverse to  $\varphi_\vartheta$  in the sense that  $\psi_\vartheta \circ \varphi_\vartheta^\pm$  is the identity map of  $\mathbb{R}/\mathbb{Z}$ .)

A precise algorithm for computing the left and right limit maps  $\varphi_\vartheta^\pm$  is given as follows.

THEOREM 4.8. Given  $\vartheta \in [0, 1)$ , set  $\theta_{\min} = \min(\vartheta, 1/2)$  and  $\theta_{\max} = \max(\vartheta, 1/2)$ , so that  $0 \leq \theta_{\min} \leq \theta_{\max} < 1$ .

- For any  $\theta \in [0, 1)$ , the right hand limit function is given by

$$\varphi_\vartheta^+(\theta) = \frac{x_0}{3} + \frac{x_1}{9} + \frac{x_2}{27} + \dots, \tag{7}$$

where  $x_m$  takes the value 0, 1, or 2 according as the angle  $2^m\theta$  belongs to the interval  $[0, \theta_{\min})$ ,  $[\theta_{\min}, \theta_{\max})$  or  $[\theta_{\max}, 1)$  modulo  $\mathbb{Z}$ .

- Similarly, for  $\theta \in (0, 1]$  the left hand limit is given by

$$\varphi_\vartheta^-(\theta) = \frac{x'_0}{3} + \frac{x'_1}{9} + \frac{x'_2}{27} + \dots, \tag{8}$$

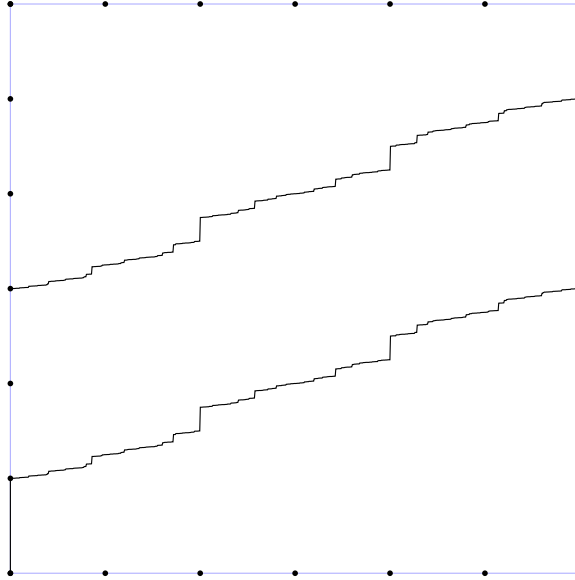


FIGURE 17. Graph of the functions  $a(\vartheta) < b(\vartheta)$  on the unit interval. (Compare Remark 4.9.) Note that the critical gap length satisfies  $b(\vartheta) - a(\vartheta) \geq 1/3$ , with strict inequality only when  $\vartheta$  is periodic under doubling. (This corresponds to places where there are jump discontinuities in both graphs.) The axes have been marked in units of  $1/6$ .

where  $x'_m$  takes the value 0, 1, or 2 according as the angle  $2^m\theta$  belongs to the interval  $(0, \theta_{\min}]$ ,  $(\theta_{\min}, \theta_{\max}]$  or  $(\theta_{\max}, 1]$  modulo  $\mathbb{Z}$ .

Here the functions  $\varphi^\pm$  have a jump discontinuity at every point  $\theta \in \text{cpc}(\vartheta)$ , but at all  $\theta \notin \text{cpc}(\vartheta)$  these left and right limits are equal so that  $\varphi$  is defined and continuous.

REMARK 4.9. For  $\vartheta \neq 0$  the left hand endpoint  $a(\vartheta) = \varphi_\vartheta^-(\vartheta)$  of  $G_\vartheta$  is continuous from the left as a function of  $\vartheta$ . Similarly, the right hand endpoint  $b(\vartheta) = \varphi_\vartheta^+(\vartheta)$  is continuous from the right. Both  $a(\vartheta)$  and  $b(\vartheta)$  are monotone as functions of  $\vartheta$ . (Compare Figure 17.) Evidently the function  $\varphi_\vartheta$  is discontinuous at  $\theta \in (0, 1)$  if and only if the left and right limits  $\varphi_\vartheta^\pm(\theta)$  are different. This certainly happens whenever  $\theta \in \text{cpc}(\vartheta)$ . It might seem that the expressions for  $\varphi_\vartheta^+$  and  $\varphi_\vartheta^-$  should also be different whenever  $2^m\theta = 1/2$  for some  $m$ , and hence  $2^n\theta = 0$  for all  $n > m$ . However, a brief computation shows that the discontinuity in  $x_m/3^{m+1}$  is precisely canceled out by the discontinuity in  $\sum_{n>m} x_n/3^{n+1}$ .

PROOF OF THEOREM 4.8. First suppose that  $\vartheta \neq 0$ , so that exactly one of the two fixed points of  $\mathbf{m}_3$  is visible. (Compare Remark 4.1.) This visible fixed point is the landing point of the ray  $\mathcal{R}_{q,0}$  and we normalized  $\eta_q$  so that this fixed point is  $\eta_q(0)$ . The other fixed point,  $\eta_q(1/2)$  is not visible since the map  $\mathbf{m}_2$  has only one fixed point.

The internal ray of angle  $1/2$  maps to the zero ray under  $f_q$ , hence it must land at an immediate preimage of the fixed point with Julia coordinate  $x = 0$ . In other words, it must land at either the  $1/3$  point or the  $2/3$  point along the Julia set. To fix our ideas, let us suppose that it lands at  $x = 2/3$ , as shown in Figure 18. (The proof when it lands at  $x = 1/3$  would be completely analogous.) Since the critical gap  $G_\vartheta$  has length at least  $1/3$ , and is contained in

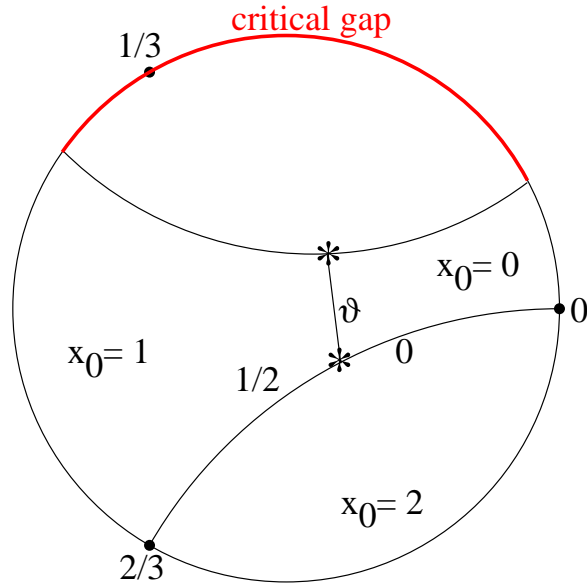


FIGURE 18. A schematic figure for the proof of Equation (7) in the case where the internal  $1/2$ -ray lands at the  $2/3$  point on the Julia set. Here the two stars represent critical points: zero below and  $\mathbf{c}_0(q)$  above. The three angles around the outer circle represent Julia coordinates  $x$ , while the three angles around the lower star represent internal angles  $\theta$ .

the interval between  $0$  and  $2/3$ , it follows immediately that the point  $x = 1/3$  must lie within the closure  $\overline{G_\vartheta}$ . For an internal ray of angle  $\theta \notin \text{cpc}(\vartheta)$  with  $0 \leq \theta < \vartheta$ , the landing point in the Julia set must evidently have angle  $0 < x = \varphi(\theta) < 1/3$ . Similarly, if  $\vartheta \leq \theta < 1/2$  then  $1/3 \leq x < 2/3$ , and if  $1/2 \leq \theta < 1$  then  $2/3 \leq x < 1$ . Thus we have determined the initial  $x_0$  in the base three expansion  $x = \sum x_m/3^{m+1}$ . The higher coefficients  $x_m$  are then determined by applying the same argument to  $3^m\theta$ . Thus we have proved Equation (7), and the proof of Equation (8) is analogous. This proves Theorem 4.8 in the case  $\vartheta \neq 0$ .

The proof when  $\vartheta = 0$  is only slightly harder. In this case, the zero ray bifurcates, and the critical gap is the open interval  $(0, 1/2)$ , bounded by the two fixed points under tripling. (See Figure 13-left, where the endpoints  $x = 0$  and  $x = 1/2$  of the critical gap are near the bottom and top.) In this case, the set  $\mathbf{V}_0$  of visible Julia coordinates is the classical Cantor middle third set within the interval  $[1/2, 1]$ . That is we must first remove the middle third  $(2/3, 5/6)$  which is an immediate preimage of  $(0, 1/2)$  under tripling. Then we must remove the middle third of each of the remaining intervals  $[1/2, 2/3]$  and  $[5/6, 1]$ , and so on.

The zero and  $1/2$  internal rays in Figure 13-left bifurcate from the real axis. Evidently any internal ray of angle  $\theta \in (0, 1/2)$  can only land at a point in the upper left quadrant, with Julia coordinate  $x \in (1/2, 3/4)$ , if it lands at all. But since the middle third interval  $(2/3, 5/6)$  is excluded, this means that  $x \in (1/2, 2/3) \subset (1/3, 2/3)$ . Similarly, if  $\theta \in (1/2, 1)$ , then  $x \in (5/6, 1) \subset (2/3, 1)$ . Thus the initial coefficient  $x_0$  of the base 3 expansion of  $x$  is  $1$  or  $2$  according as  $\theta$  belongs to  $(0, 1/2)$  or  $(1/2, 1)$ . But this is just the value prescribed by the algorithm (7) or (8) in this case, since we have  $\theta_{\min} = 0$  and  $\theta_{\max} = 1/2$  when  $\vartheta = 0$ . The higher coefficients  $x_m$  are determined in the same way, using the internal angle  $2^m\theta$  and the Julia coordinate  $3^m x$ . This proves Theorem 4.8 for the case  $\vartheta = 0$  with  $\theta \notin \text{cpc}(0)$ ; and the left and right limit cases follow easily.  $\square$

DEFINITION 4.10. If  $I \subset \mathbb{R}/\mathbb{Z}$  is any open set, we denote by  $X_d(I)$  the compact set consisting of points in  $\mathbb{R}/\mathbb{Z}$  whose orbit under multiplication by  $d$  avoids  $I$ .

PROPOSITION 4.11. Let  $I$  be an open interval of length  $1/3$  which is either equal to  $G_\vartheta$  or compactly contained in  $G_\vartheta$ . Then the set  $V_\vartheta$  is equal to the set  $X_3(I)$ .

Thus, if the angle  $\vartheta$  is not periodic under doubling, so that the critical gap  $G_\vartheta$  has length  $1/3$ , then the set  $V_\vartheta$  is equal to  $X_3(I)$ , taking  $I$  to be the critical gap  $G_\vartheta$ . In the periodic case, where  $G_\vartheta$  has length  $3^{p-1}/(3^p - 1) > 1/3$ , we can take  $I$  to be any open interval of length  $1/3$  which is compactly contained in the critical gap.

PROOF OF PROPOSITION 4.11. It is enough to observe that the orbit of any point that enters  $G_\vartheta$  eventually enters  $I$ . If  $I = G_\vartheta$ , there is nothing to prove. So, assume  $I$  is compactly contained in  $G_\vartheta$ . Let  $H$  be either one of the two components of  $G_\vartheta \setminus I$ . Then,

$$\text{Length}(H) < \text{Length}(G_\vartheta) - \text{Length}(I) = \frac{3^{p-1}}{3^p - 1} - \frac{1}{3} = \frac{1}{3(3^p - 1)}$$

and therefore

$$(3^p - 1)\text{Length}(H) < \frac{1}{3} = \text{Length}(I).$$

It follows that

$$\text{Length}(\mathbf{m}_3^{\circ p}(H)) = 3^p \text{Length}(H) < \text{Length}(H) + \text{Length}(I).$$

Since the boundary points of  $G_\vartheta$  are periodic of period  $p$ , this implies that

$$\mathbf{m}_3^{\circ p}(H) \subset H \cup I.$$

Since  $\mathbf{m}_3^{\circ p}$  multiplies distance by  $3^p$ , the orbit of any point in  $H$  under  $\mathbf{m}_3^{\circ p}$  eventually enters  $I$ , as required.  $\square$

## 5. DYNAMIC ROTATION NUMBER FOR MAPS IN $\mathcal{H}_0$

We now explain how to assign a **dynamic rotation number** to every parameter  $q^2$  on the parameter ray  $\mathcal{R}_\vartheta$ .

As previously, we denote by  $\mathcal{V}_q$  the set of points  $z \in \mathcal{J}(f_q)$  which are visible from the origin. In the previous section, we saw that  $\mathcal{V}_q = \eta_q(V_\vartheta)$  where  $V_\vartheta$  is the set of angles whose orbit under  $\mathbf{m}_3$  never enters the critical gap  $G_\vartheta$ . The set of points  $z \in \mathcal{J}(f_q)$  which are visible from infinity is the antipodal set

$$\mathcal{A}(\mathcal{V}_q) = \eta_q(1/2 + V_\vartheta).$$

So, the set of **bi-visible points**, that is those which are simultaneously visible from zero and infinity, is simply

$$\eta_q(X_\vartheta) \quad \text{with} \quad X_\vartheta = V_\vartheta \cap (1/2 + V_\vartheta).$$

Note that  $X_\vartheta$  is the set of angles whose orbit under  $\mathbf{m}_3$  avoids both  $G_\vartheta$  and  $1/2 + G_\vartheta$ .

LEMMA 5.1. For any  $\vartheta \in \mathbb{R}/\mathbb{Z}$ , this set  $X_\vartheta$  of bi-visible Julia coordinates is a rotation set, with a well defined rotation number in  $\mathbb{R}/\mathbb{Z}$ .

PROOF. For definitions, and the proof that every rotation set has a rotation number, see the Appendix. Since the length of  $G_\vartheta$  is at most  $3^0/(3^1 - 1) = 1/2$ , the intervals  $G_\vartheta$  and  $1/2 + G_\vartheta$  are disjoint. Let  $I_1 \subset G_\vartheta$  be an open interval of length  $1/3$ , either equal to  $G_\vartheta$ , or compactly contained in  $G_\vartheta$ . Set  $I_2 = 1/2 + I_1$  and  $I = I_1 \cup I_2$ . It follows easily from the proof of Proposition 4.11 that  $X_\vartheta$  is equal to the set  $X_3(I)$  of points whose orbit under tripling never enters  $I$ . The Lemma now follows immediately from the following statement, which is proved as Lemma A.7 in the Appendix:

If  $I_1, I_2, \dots, I_{d-1}$  are disjoint open intervals in  $\mathbb{R}/\mathbb{Z}$ , each of length exactly  $1/d$ , then the compact set  $X(I_1 \cup \dots \cup I_{d-1})$ , consisting of points of  $\mathbb{R}/\mathbb{Z}$  whose orbit under  $\mathbf{m}_d$  never hits any of these sets, is a rotation set. □

REMARK 5.2. If we only assume that  $I_1 \subset G_\vartheta$  without assuming that it is compactly contained, and set  $I = I_1 \cup (1/2 + I_1)$ , then the set  $X_3(I)$  is still a rotation set containing  $X_\vartheta$ , but it may also contain extra points with no dynamical meaning. However, the rotation number of  $X_3(I)$  is still equal to the rotation number of  $X_\vartheta$ .

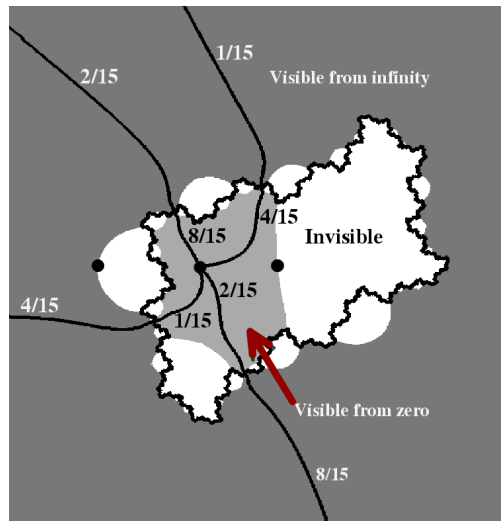


FIGURE 19. The Julia set of a map  $f_q$  with dynamic rotation number  $1/4$ . There are four points visible from both zero and infinity. The white points are not visible from either zero or infinity. The angles of the rays from infinity, counterclockwise starting from the top, are  $1/15, 2/15, 4/15$  and  $8/15$ , while the corresponding rays from zero have angles  $4/15, 8/15, 1/15$  and  $2/15$ . The heavy dots represent the finite critical points.

DEFINITION 5.3 (Dynamic Rotation Number). For any parameter  $q^2 \in \mathcal{R}_\vartheta$ , the rotation number  $\mathbf{t} = \rho(\vartheta)$  associated with the set

$$X_\vartheta = V_\vartheta \cap (1/2 + V_\vartheta) \subset \mathbb{R}/\mathbb{Z},$$

representing points in the Julia set which are bi-visible, will be called the **dynamic rotation number** <sup>†</sup> of the map  $f_q$  or of the point  $q^2$  in moduli space.

---

<sup>†</sup> This definition will be extended to many points outside of  $\mathcal{H}_0$  in Section 6. (See also Definition 7.6.)

The monotone degree one map  $\psi_{\vartheta} : \mathbb{R}/\mathbb{Z} \rightarrow \mathbb{R}/\mathbb{Z}$  defined in Remark 4.7 is a semiconjugacy between

$$\mathbf{m}_3 : V_{\vartheta} \rightarrow V_{\vartheta} \quad \text{and} \quad \mathbf{m}_2 : \mathbb{R}/\mathbb{Z} \rightarrow \mathbb{R}/\mathbb{Z}.$$

Restricting  $\psi_{\vartheta}$  to the  $\mathbf{m}_3$ -rotation set  $X_{\vartheta} \subset V_{\vartheta}$ , the image  $\psi_{\vartheta}(X_{\vartheta})$  is an  $\mathbf{m}_2$ -rotation set, with rotation number equal to  $\mathbf{t} = \rho(\vartheta)$ . In fact, this rotation set is reduced. (See Definition A.11 in the Appendix.) According to Goldberg (see Theorem A.15), there is a unique such rotation set  $\Theta_{\mathbf{t}}$ . If  $q^2 \in \mathcal{R}_{\vartheta}$ , then  $\Theta_{\mathbf{t}}$  is the set of internal angles of bi-visible points.

The entire configuration consisting of the rays from zero and infinity with angles in  $\Theta_{\mathbf{t}}$ , together with their common landing points in the Julia set, has a well defined rotation number  $\mathbf{t}$  under the map  $f_q$ . For example, in Figure 19 the light grey region is the union of interior rays, while the dark grey region is the union of rays from infinity. These two regions have four common boundary points, labeled by the points of  $X_{\vartheta}$ . The entire configuration of four rays from zero and four rays from infinity maps onto itself under  $f_q$  with combinatorial rotation number  $\mathbf{t}$  equal to  $1/4$ .

LEMMA 5.4. *The dynamic rotation number  $\mathbf{t}$  is continuous and monotone (but not strictly monotone) as a function  $\rho(\vartheta)$  of the critical angle  $\vartheta$ . Furthermore, as  $\vartheta$  increases from zero to one, the dynamic rotation number also increases from zero to one. (Thus  $\rho$  is a monotone degree one circle map.)*

PROOF. Setting  $G_{\vartheta} = (a(\vartheta), b(\vartheta))$ , and setting  $I_{\vartheta} = (a(\vartheta), a(\vartheta) + 1/3) \subset G_{\vartheta}$ , we have  $\rho(\vartheta) = \text{rot}(X_2(I_{\vartheta}))$  where  $X_2(I_{\vartheta})$  is the set of points whose orbit never enters  $I_{\vartheta}$  under iteration of  $\mathbf{m}_2$ . Hence continuity from the left follows from Remark 4.9. Continuity from the right and monotonicity follow by a similar argument.  $\square$

We will describe the function  $\vartheta \mapsto \mathbf{t} = \rho(\vartheta)$  conceptually in Theorem 5.7, and give an explicit computational description in Theorem 5.10. (For a graph of this function see Figure 20.) We first need a preliminary discussion.

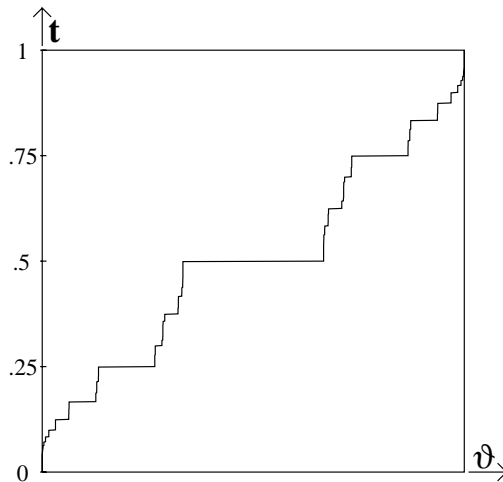


FIGURE 20. Graph of the dynamic rotation number  $\mathbf{t}$  as a function of the critical angle  $\vartheta$ .

**PROPOSITION 5.5.** *If  $\mathbf{t} = \rho(\vartheta)$  is rational, then the set  $X_{\vartheta}$  is a union of at most two periodic orbits under  $\mathbf{m}_3$ . More precisely,  $X_{\vartheta}$  is a single periodic orbit if the denominator of  $\mathbf{t}$  is even, but is the union of two disjoint periodic orbits if the denominator is odd.*

As examples, in Figure 22 and 14, we have  $\vartheta = 2/7$  with rotation number  $\mathbf{t} = 1/3$  under  $\mathbf{m}_2$ ; and in fact  $X_{\vartheta}$  is the union of two cycles, both with rotation number  $1/3$ . On the other hand, in Figures 19 and 21, we have  $\mathbf{t} = 1/4$ , and the set  $X_{\vartheta}$  is a single cycle of rotation number  $1/4$ . (In this example,  $\vartheta$  can be any angle between  $2/15$  and  $4/15$ . Compare Figure 20.)

**PROOF OF PROPOSITION 5.5.** According to Lemma A.12 in the Appendix, every point in the rotation set  $X_{\vartheta}$  is eventually periodic under  $\mathbf{m}_3$ . Therefore if there is any non-periodic element  $x \in X_{\vartheta}$ , there must be one for which the immediate forward image  $\mathbf{m}_3(x)$  is periodic. Note that  $\mathbf{m}_3(x)$  has three immediate preimages under  $\mathbf{m}_3$ , namely  $x$  itself and the two points  $x \pm 1/3$ . We claim that at most one of these three points can be in  $X_{\vartheta}$ , and hence represent a visible point of the Julia set. In fact there is an interval of length greater than  $1/3$  in  $\mathbb{R}/\mathbb{Z}$  representing points invisible from the origin, and a disjoint interval of the same length representing points invisible from infinity. Each of the intervals must contain at least one of the points  $x$  and  $x \pm 1/3$ . Therefore at most one of these three points can be in  $X_{\vartheta}$ , and hence be bi-visible. Since one of these three points must be in our periodic cycle, and hence in  $X_{\vartheta}$ , it follows that our non-periodic point  $x$  cannot be in  $X_{\vartheta}$ .

Thus  $X_{\vartheta}$  is a finite union of periodic orbits. The further argument will depend of results of Lisa Goldberg, as described in Theorem A.15 in the Appendix. In the  $\mathbf{m}_3$  case, she shows that a period  $n$  cyclic rotation set  $X$  is completely specified by its rotation number  $\mathbf{t}$ , together with the number  $n_0$  of points of  $X$  which lie in the interval  $[0, 1/2)$ . Here  $n_0$  can be any integer between zero and  $n$ . Two such cyclic rotation sets are called **compatible**, if their union is a rotation set, or equivalently if and only if each gap in one contains exactly one point of the other. In the  $\mathbf{m}_3$  case it is easy to see that compatibility is only possible if the difference  $|n'_0 - n_0|$  between the respective numbers of points in  $[0, 1/2)$  is exactly one. (In fact Goldberg shows that this is an *if and only if* condition.)

Note that the antipodal map corresponds to the involution  $x \leftrightarrow x + 1/2$  which interchanges the subintervals  $[0, 1/2)$  and  $[1/2, 1)$  and replaces  $n_0$  by  $n - n_0$ .

**Odd Case.** If the period  $n$  is odd, then a single cycle with  $n$  elements clearly cannot be self-antipodal. In this case there must be two cycles in  $X_{\vartheta}$ . Furthermore, the numbers  $n_0 \in [0, n]$  associated with these two cycles must be  $(n - 1)/2$  and  $(n + 1)/2$ , and there cannot be a third compatible cycle.

**Even Case.** If  $n$  is even, there cannot be two antipodal cycles, since the difference between  $n_0$  and  $n - n_0$  is always even. Hence there can only be a single self-antipodal cycle with  $n_0 = n/2$ . This completes the proof of Proposition 5.5.  $\square$

**DEFINITION 5.6 (Balance).** For each  $\mathbf{t} \in \mathbb{R}/\mathbb{Z}$ , let  $\Theta_{\mathbf{t}}$  be the unique reduced rotation set with rotation number  $\mathbf{t}$  under the doubling map  $\mathbf{m}_2$  (see Remark A.14 in the Appendix). If  $\mathbf{t}$  is rational with denominator  $n > 1$ , then the points of  $\Theta_{\mathbf{t}}$  can be listed in numerical order within the open interval  $(0, 1)$  as  $\theta_1 < \theta_2 < \dots < \theta_n$ . If  $n$  is odd, then there is a unique middle element  $\theta_{(n+1)/2}$  in this list. By definition, this middle element will be called the **balanced** angle in this rotation set. For the special case  $n = 1$ , the unique element  $0 \in \Theta_0$  will be called the balanced element.



On the other hand, if  $n$  is even, then there is no middle element. However, there is a unique pair  $\{\theta_{n/2}, \theta_{1+n/2}\}$  in the middle. By definition, this will be called the **balanced-pair** for this rotation set, and the two elements of the pair will be called **almost balanced**.

Finally, if  $t$  is irrational, then  $\Theta_t$  is topologically a Cantor set. There is a unique  $\mathbf{m}_2$ -invariant probability measure which is supported on  $\Theta_t$ . (This follows easily from Remark A.3 in the Appendix. Intuitively, the measure of any open interval in  $\mathbb{R}/\mathbb{Z}$  is the proportion of elements of an arbitrary orbit in  $\Theta_t$  which lie in the interval.) By definition, the **balanced point** in this case is the unique  $\theta$  such that both  $\Theta_t \cap (0, \theta)$  and  $\Theta_t \cap (\theta, 1)$  have measure  $1/2$ . To show that  $\theta$  is uniquely defined, we must show that that  $\theta$  cannot fall in a gap of  $\Theta_t$ . As in Remark A.3, there is a semiconjugacy  $\psi : \Theta_t \rightarrow \mathbb{R}/\mathbb{Z}$  between  $\mathbf{m}_2$  on  $\Theta_t$  and rotation by  $\mathbf{t}$  on the circle. The endpoints of each gap map to a single point under  $\psi$ , and all of these images lie in a single orbit under rotation by  $\mathbf{t}$ . Since  $\mathbf{t}$  is irrational, the interval between any two points of this image orbit must be irrational. Since zero must lie in a gap, it follows that the interval between zero and any other gap cannot have invariant measure exactly  $1/2$ . Therefore, the balanced angle  $\theta$  is unique.

Here is a conceptual description of the many valued function  $\mathbf{t} \mapsto \vartheta$ .

**THEOREM 5.7.** *If  $\mathbf{t}$  is either irrational, or rational with odd denominator, then  $\vartheta$  is equal to the unique balanced angle in the rotation set  $\Theta_t$ . However, if  $\mathbf{t}$  is rational with even denominator, then there is an entire closed interval of corresponding  $\vartheta$ -values. This interval is bounded by the unique balanced-pair in  $\Theta_t$ .*

We first prove one special case of this theorem.

**LEMMA 5.8.** *Suppose that the dynamic rotation number is  $\mathbf{t} = m/n = m/(2k + 1)$ , rational with odd denominator. Then the corresponding critical angle  $\vartheta$  is uniquely determined and is characterized by the following two properties (as in Definition 5.6):*

- *The critical angle  $\vartheta$  is periodic under doubling with rotation number  $\mathbf{t}$ .*
- *The critical angle  $\vartheta$  is balanced. If  $k > 0$  this means that exactly  $k$  of the points of the orbit  $\{2^\ell \vartheta\}$  belong to the open interval  $(0, \vartheta) \bmod 1$ , and  $k$  belong to the interval  $(\vartheta, 1) \bmod 1$ .*

Figure 22 provides an example to illustrate this lemma. Here  $\vartheta = 2/7$ , and the rotation number is  $\mathbf{t} = 1/3$ . Exactly one point of the orbit of  $\vartheta$  under doubling belongs to the open interval  $(0, \vartheta)$ , and exactly one point belongs to  $(\vartheta, 1)$ . The critical gap  $G_\vartheta$  for points visible from the origin is the arc from  $19/26 \equiv -7/26$  to  $2/26$ , of length  $9/26$ . Similarly the critical gap  $1/2 + G_\vartheta$  for points visible from infinity is the interval  $(6/26, 15/26)$  also of length  $9/26$ .

**PROOF OF LEMMA 5.8.** According to [7], there is only one  $\mathbf{m}_2$ -periodic orbit with rotation number  $\mathbf{t}$ , and clearly such a periodic orbit is balanced with respect to exactly one of its points. (Compare Remark A.13 in the Appendix and Definition 5.6.)

To show that  $\vartheta$  has these two properties, consider the associated  $\mathbf{m}_3$ -rotation set  $X_\vartheta$ . Since  $X_\vartheta$  is self-antipodal with odd period, it must consist of two mutually antipodal periodic orbits. As illustrated in Figure 22, we can map  $X_\vartheta$  to the unit circle in such a way that  $\mathbf{m}_3$  corresponds to the rotation  $z \mapsto e^{2\pi i \mathbf{t}} z$ . If the rotation number is non-zero, so that  $k \geq 1$ , then

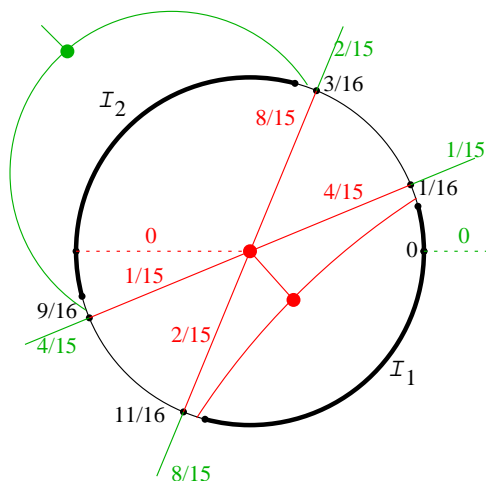


FIGURE 21. Schematic picture representing the Julia set by the unit circle for a map with rotation number  $1/4$ . Here  $I_2$  can be any open interval  $(x, x + 1/3)$  with  $3/16 \leq x < x + 1/3 \leq 9/16$ , and  $I_1 = I_2 + 1/2$ . The interior angles (in red) and the exterior angles (in green) double under the map, while the angles around the Julia set (in black) multiply by 3. Heavy dots indicate critical points.

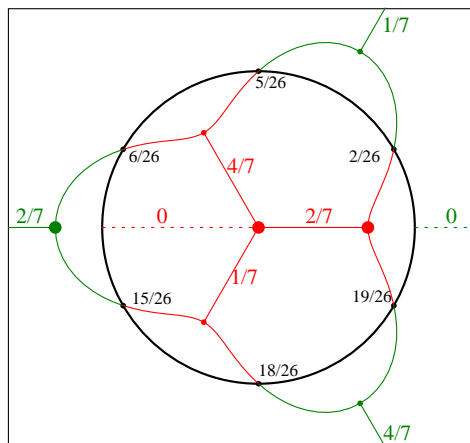


FIGURE 22. The circle in this cartoon represents the Julia set (which is actually a quasicircle) for a map belonging to the  $2/7$  ray in  $\mathcal{H}_0$ . The heavy dots represent the three finite critical points. As in Figure 21, the interior angles (red) and exterior angles (green) are periodic under doubling, while the angles around the Julia set are periodic under tripling. (The figure is topologically correct, but all angles are distorted.)

each of the two periodic orbits must map to the vertices of a regular  $(2k + 1)$ -gon. Clearly as we traverse the unit circle, we meet the points of these two orbits alternately. As in Figure 22, one of the two fixed points  $0$  and  $1/2$  of  $\mathbf{m}_3$  must lie in the interval  $G_{\vartheta}$ , and the other must lie in  $1/2 + G_{\vartheta}$ . It follows that  $2k + 1$  of the points of  $X_{\vartheta}$  lie in the interval  $(0, 1/2)$ , and the other  $2k + 1$  must lie in  $(1/2, 1)$ . Since each point of the orbit of  $\vartheta$  corresponds to two

points of  $X_{\vartheta}$ , it follows that  $k$  of the points of the orbit of  $\vartheta$  must lie in the open interval  $(0, \vartheta)$  and  $k$  must lie in  $(\vartheta, 1)$ , as required.

The case of rotation number  $\mathbf{t} = 0$  is somewhat different. (Compare the proof of Theorem 4.8.) In this case, with  $\vartheta = 0$ , the rotation set  $X_{\vartheta}$  for  $\mathbf{m}_3$  consists of the two fixed points 0 and  $1/2$ . The corresponding rotation set  $\Theta_{\mathbf{t}}$  for  $\mathbf{m}_2$  consists of the single fixed point zero, which is balanced by definition.  $\square$

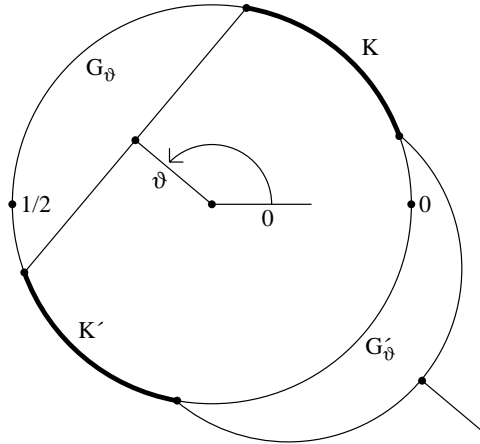


FIGURE 23. Schematic diagram for any example with rotation number  $\mathbf{t} \neq 0$  (with the Julia set represented as a perfect circle).

**PROOF OF THEOREM 5.7.** The general idea of the argument can be described as follows. (Compare Figure 23.) Since the case  $\mathbf{t} = 0$  was dealt with in Lemma 5.8, we may assume that  $\mathbf{t} \neq 0$ . Let  $G_{\vartheta}$  be the critical gap of angle  $\vartheta$  for rays from zero, and let  $G'_{\vartheta} = 1/2 + G_{\vartheta}$  be the corresponding gap for rays from infinity. Then the complement  $\mathbb{R}/\mathbb{Z} \setminus (G_{\vartheta} \cup G'_{\vartheta})$  consists of two closed intervals. One component  $K$  is contained in the open interval  $(0, 1/2)$  and the other,  $K' = 1/2 + K$ , is contained in  $(1/2, 1)$ . Thus any self-antipodal set which is disjoint from  $G_{\vartheta} \cup G'_{\vartheta}$  must have half of its points in  $K$  and the other half in  $K'$ . Assuming that  $0 \in G'_{\vartheta}$  as in Figure 23, it follows that all points of  $K$  correspond to internal angles in the interval  $(0, \vartheta)$ , while all points of  $K'$  correspond to internal angles in the interval  $(\vartheta, 1)$ . (Here we are assuming that  $0 \in G'_{\vartheta}$  and hence  $1/2 \in G_{\vartheta}$ . The proof is similar if  $0 \in G_{\vartheta}$ .) In each case, this observation will lead to the appropriate concept of balance:

**Case 1: Odd Denominator.** If the rotation number  $\mathbf{t}$  has odd denominator, then the required statement is proved in Lemma 5.8. In this case, the critical angle  $\vartheta$  also belongs to the rotation set  $\Theta_{\mathbf{t}}$ . The dynamic ray of angle  $\vartheta$  always bifurcates infinitely often (compare Figure 13).

**Case 2. Irrational  $\mathbf{t}$ .** It follows from Remark A.3 in the Appendix, that the set  $X_{\vartheta}$  carries a unique probability measure  $\mu$  invariant by  $\mathbf{m}_3$ . The push-forward of  $\mu$  under  $\psi_{\vartheta}$  is necessarily equal to the unique probability measure  $\nu$  carried on  $\Theta_{\mathbf{t}}$  and invariant by  $\mathbf{m}_2$ . By symmetry,  $\mu(K) = \mu(K') = 1/2$ . Therefore,

$$\nu[0, \vartheta] = \nu[\vartheta, 1] = 1/2.$$

By definition, this means that the angle  $\vartheta$  is balanced. In particular, as noted in Definition 5.6, it follows that  $\vartheta \in \Theta_{\mathbf{t}}$ .

**Case 3. Even Denominator  $n$ .**

**Case 3A. with  $\vartheta \notin \Theta_{\mathbf{t}}$ .** (This is the generic case, as illustrated in Figure 19.) By symmetry, the number of points of  $X_{\vartheta}$  in  $K$  is equal to the number of points of  $X_{\vartheta}$  in  $K'$ . Therefore the number of points in  $\Theta_{\mathbf{t}}$  in  $(0, \vartheta)$  is equal to the number of points of  $\Theta_{\mathbf{t}}$  in  $(\vartheta, 1)$ . (In other words, the set  $X_{\vartheta}$  is “balanced” with respect to  $\vartheta$  in the sense that half of its elements belong to the interval  $(0, \vartheta)$  and half belong to  $(\vartheta, 1)$ .) If  $\{\vartheta^-, \vartheta^+\} \subset \Theta_{\mathbf{t}}$  is the unique **balanced pair** for this rotation number, in the sense of Definition 5.6, this means that  $\vartheta^- < \vartheta < \vartheta^+$ . As an example, for rotation number  $1/4$  with  $\Theta_{\mathbf{t}} = \{1/15, 2/15, 4/15, 8/15\}$ , the balanced pair consists of  $2/15$  and  $4/15$ . Thus in this case the orbit is balanced with respect to  $\vartheta$  if and only if  $2/15 < \vartheta < 4/15$ .

**Case 3B. with  $\vartheta \in \Theta_{\mathbf{t}}$ .** Then  $X_{\vartheta}$  is a single self-antipodal orbit by Proposition 5.5. Furthermore  $n/2$  of these points must lie in  $(0, 1/2)$  and  $n/2$  in  $(1/2, 1)$ . (Compare Figure 23.) The image of this orbit in  $\Theta_{\mathbf{t}}$  can not be quite balanced with respect to  $\vartheta$  since  $\vartheta$  itself does not lie in either one of the two open intervals  $(0, \vartheta)$  and  $(\vartheta, 1)$ . Hence only one of these intervals can contain  $n/2$  points and the other must contain only  $n/2 - 1$  points. Therefore  $\vartheta$  belongs to the balanced pair for  $\Theta_{\mathbf{t}}$ . (Examples of such balanced pairs are  $\{1/3, 2/3\}$  with rotation number  $\mathbf{t} = 1/2$ , and  $\{2/15, 4/15\}$  with rotation number  $\mathbf{t} = 1/4$ .)

Since we have dealt with all possible cases, this completes the proof of Theorem 5.7. □

**LEMMA 5.9.** *Let  $\{\vartheta, \vartheta'\}$  be a balanced pair with rotation number  $\mathbf{t} = m/n = m/(2h)$ , expressed as a fraction in lowest terms. Then the difference  $|\vartheta' - \vartheta|$  is equal to  $2^{h-1}/(2^{2h} - 1)$ .*

**PROOF.** List the gaps in the rotation set containing  $\vartheta$  and  $\vartheta'$  in dynamic order as  $G_1, G_2, \dots, G_{2h}$ , where each  $G_j$  has length  $2^{j-1}/(2^{2h} - 1)$ . (Compare Remark A.13 in the Appendix.) For the balanced gap, we must prove that  $j$  is equal to the half-period  $h = n/2$ , so that the length is  $2^{h-1}/(2^{2h} - 1)$ . To see this, note that the cyclic order of the gaps  $G_j$  around the circle corresponds to the cyclic order of the residue classes  $mj$  modulo  $2h$ . The longest gap  $G_{2h}$  must contain the angle zero, so the balanced gap (half way around the circle) must correspond to the residue class with  $mj \equiv h \pmod{2h}$ . Since  $m$  and  $2h$  are relatively prime, it follows easily that  $j = h$ , as required. □

Rather than direct computation of the correspondence  $\rho : \vartheta \mapsto \mathbf{t}$ , it is more convenient to work with the inverse correspondence

$$\mathbf{t} \mapsto \vartheta = \rho^{-1}(\mathbf{t}) ,$$

which is a many-valued function with jump discontinuities. In order to obtain a single valued inverse function we need to work with the right hand limit

$$\rho^{-1}(\mathbf{t}^+) = \lim_{\epsilon \searrow 0} \rho^{-1}(\mathbf{t} + \epsilon) .$$

**THEOREM 5.10.** *This right hand limit is well defined, continuous from the right, and strictly monotone. It is discontinuous at  $\mathbf{t}$  if and only if  $\mathbf{t}$  is rational with even denominator, and can*

be computed as <sup>†</sup>

$$\rho^{-1}(\mathbf{t}^+) = \sum_{\ell \geq 0} \frac{\mathbf{floor}(1/2 + \ell \mathbf{t})}{2^{\ell+1}}. \tag{9}$$

PROOF. It will be convenient to write the right side of Equation (9) as  $\sum_{\ell} \eta_{\ell}(\mathbf{t})$  where

$$\eta_{\ell}(\mathbf{t}) = \mathbf{floor}(1/2 + \ell \mathbf{t})/2^{\ell+1} \quad \text{for } \ell \geq 0.$$

For each  $\ell \geq 0$ , note that the correspondence  $\mathbf{t} \mapsto \eta_{\ell}(\mathbf{t})$  is a step function with  $\eta_{\ell}(0) = 0$  and  $\eta_{\ell}(1) = \ell/2^{\ell+1}$ . Evidently this step function has precisely  $\ell$  discontinuities.

The discontinuity of any monotone function  $f$  at a point  $x$  can be measured by the difference

$$\mathbf{jump}_x(f) = \lim_{\epsilon \searrow 0} f(x + \epsilon) - \lim_{\epsilon \searrow 0} f(x - \epsilon).$$

Using this notation, we have

$$\mathbf{jump}_{\mathbf{t}}(\eta_{\ell}) = 1/2^{\ell+1} \quad \text{whenever } 1/2 + \mathbf{t} \ell \text{ is an integer,}$$

but  $\mathbf{jump}_{\mathbf{t}}(\eta_{\ell}) = 0$  otherwise. The function  $\mathbf{t} \mapsto \sum_{\ell} \eta_{\ell}(\mathbf{t})$  converges uniformly, taking the value zero at  $\mathbf{t} = 0$  and the value one <sup>†</sup> at  $\mathbf{t} = 1$ :

$$\sum_{\ell \geq 0} \eta_{\ell}(1) = \sum_{\ell \geq 0} \ell/2^{\ell+1} = 1.$$

Similarly, the analogous series using limits from the left rather than limits from the right converges uniformly. It follows that the discontinuity of  $\sum_{\ell} \eta_{\ell}$  at any point  $\mathbf{t}$  is given by

$$\mathbf{jump}_{\mathbf{t}}\left(\sum_{\ell \geq 0} \eta_{\ell}\right) = \sum_{\ell \geq 0} \mathbf{jump}_{\mathbf{t}}(\eta_{\ell}). \tag{10}$$

Thus the function  $\mathbf{t} \mapsto \sum_{\ell} \eta_{\ell}(\mathbf{t})$  is continuous except at fractions  $\mathbf{t} = m/2h$  with even denominator. It is strictly monotone since the fractions  $m/2h$  are everywhere dense. Furthermore the sum of the jumps of  $\sum_{\ell} \eta_{\ell}$  over all points  $\mathbf{t} = m/2h$  is precisely equal to  $+1$ . The value of the sum (10) at a fraction  $\mathbf{t} = m/2h$  in lowest terms can be computed as the sum of  $1/2^{\ell+1}$  over all  $\ell \geq 0$  such that

$$1/2 + \ell \mathbf{t} = \frac{h + \ell m}{2h} \in \mathbb{Z},$$

or in other words, the sum over all  $\ell$  with  $\ell m \equiv h \pmod{2h}$ . Since  $m$  and  $2h$  are relatively prime, this is equivalent to the requirement that  $\ell \equiv h \pmod{2h}$ , so that  $\ell$  can take the values  $h, 3h, 5h, \dots$ . Thus the discontinuity of  $\sum_{\ell} \eta_{\ell}$  at  $m/2h$  is

$$\mathbf{jump}_{m/2h}\left(\sum_{\ell} \eta_{\ell}\right) = \frac{1}{2} \left( \frac{1}{2^h} + \frac{1}{2^{3h}} + \frac{1}{2^{5h}} + \dots \right) = \frac{2^{h-1}}{2^{2h} - 1}. \tag{11}$$

In particular, it follows that the sum of the expression (11) over all  $m/2h$  in the unit interval is precisely equal to one.

Comparing Lemma 5.9, we see that the function  $\mathbf{t} \mapsto \sum_{\ell} \eta_{\ell}(\mathbf{t})$  has the same jumps at the same places as the required function  $\mathbf{t} \mapsto \rho^{-1}(\mathbf{t}^+)$ . Since the sum of these jumps is  $+1$ , and since both functions are continuous from the right, mapping zero to zero and one to one, it

<sup>†</sup> By definition,  $\mathbf{floor}(x)$ , sometimes called the “integer part” of the real number  $x$ , is the largest integer with  $\mathbf{floor}(x) \leq x$ .

<sup>†</sup> The required identity  $1/4 + 2/8 + 3/16 + 4/32 + \dots = 1$  can be verified by differentiating the equation  $1 + x + x^2 + \dots = 1/(1 - x)$ , then evaluating at  $x = 1/2$ , and dividing by 4.

follows that the two functions are identically equal. In fact the value of either function at a point  $\mathbf{t}_0$  is the sum of the jumps at the points  $\mathbf{t} \in (0, \mathbf{t}_0]$ .  $\square$

6. BI-VISIBLE POINTS FOR MAPS OUTSIDE  $\widetilde{\mathcal{H}}_0$ .

Next let us extend the study of bi-visible points to maps  $f_q$  which do not belong to  $\widetilde{\mathcal{H}}_0$ , or in other words  $q^2 \notin \mathcal{H}_0$ . Fixing some  $f_q$ , let  $\mathcal{B}_0$  and  $\mathcal{B}_\infty$  be the immediate basins of zero and infinity.

**THEOREM 6.1.** *For any map  $f = f_q$  in our family, either*

- (1) *the two basin closures  $\overline{\mathcal{B}}_0$  and  $\overline{\mathcal{B}}_\infty$  have a non-vacuous intersection, or else*
- (2) *these basin closures are separated by a Herman ring  $\mathcal{A}$ . Furthermore, this ring has topological boundary  $\partial\mathcal{A} = \mathcal{C}_0 \cup \mathcal{C}_\infty$  with  $\mathcal{C}_0 \subset \partial\mathcal{B}_0$  and  $\mathcal{C}_\infty \subset \partial\mathcal{B}_\infty$ .*

**PROOF.** Assume  $\overline{\mathcal{B}}_0 \cap \overline{\mathcal{B}}_\infty = \emptyset$ . Since  $\widehat{\mathbb{C}}$  is connected, there must be at least one component  $A$  of  $\widehat{\mathbb{C}} \setminus (\overline{\mathcal{B}}_0 \cup \overline{\mathcal{B}}_\infty)$  whose closure intersects both  $\overline{\mathcal{B}}_0$  and  $\overline{\mathcal{B}}_\infty$ . We will show that this set  $A$  is necessarily an annulus. If  $A$  were simply connected, then the boundary  $\partial A$  would be a connected subset of  $\overline{\mathcal{B}}_0 \cup \overline{\mathcal{B}}_\infty$  which intersects both of these sets, which is impossible. The complement of  $A$  cannot have more than two components, since each complementary component must contain either  $\mathcal{B}_0$  or  $\mathcal{B}_\infty$ . This proves that  $A$  is an annulus, with boundary components  $C_0 \subset \overline{\mathcal{B}}_0$  and  $C_\infty \subset \overline{\mathcal{B}}_\infty$ . Evidently  $A$  is unique, and hence is self-antipodal.

Note that  $f(A) \supset A$ . This follows easily from the fact that  $f$  is an open map with  $f(C_0) \subset \partial\mathcal{B}_0$  and  $f(C_\infty) \subset \partial\mathcal{B}_\infty$ .

In fact, we will prove that  $A$  is a fixed Herman ring for  $f$ . The map  $f$  that carries  $f^{-1}(A)$  onto  $A$  is a proper map of degree 3. The argument will be divided into three cases according as  $f^{-1}(A)$  has 1, 2 or 3 connected components.

**Three Components (the good case).** In this case, one of the three components, say  $A'$ , must be preserved by the antipodal map (because  $A$  is preserved by the antipodal map). Then  $f : A' \rightarrow A$  has degree 1 and is therefore an isomorphism. In particular, the modulus of  $A'$  is equal to the modulus of  $A$ . Since the annuli  $A$  and  $A'$  are both self-antipodal, they must intersect by Lemma 2.2. In fact  $A'$  must actually be contained in  $A$ . Otherwise  $A'$  would have to intersect the boundary  $\partial A$ , which is impossible since it would imply that  $f(A') = A$  intersects  $f(\partial A) \subset (\overline{\mathcal{B}}_0 \cup \overline{\mathcal{B}}_\infty)$ . Furthermore  $A'$  must wind once around  $A$ , since otherwise it could not be self-antipodal. Therefore, since  $\text{mod } A = \text{mod } A'$  it follows from a standard extremal length argument that  $A' = A$ . Thus the annulus  $A$  is invariant by  $f$ , which shows that it is a fixed Herman ring for  $f$ .

**Two Components.** In this case, one of the two components would map to  $A$  with degree 1 and the other would map with degree 2. Each must be preserved by the antipodal map, which is impossible since any two self-antipodal annuli must intersect.

**One Component.** To prove that  $f^{-1}(A)$  cannot be connected, we will use a length-area argument that was suggested to us by Misha Lyubich.

In order to apply this length-area argument, we will need to consider conformal metrics and the associated area elements. Setting  $z = x + iy$ , it will be convenient to use the notation  $\mu = g(z)|dz|^2$  with  $g(z) > 0$  for a conformal metric, and the notation  $|\mu| = g(z)dx \wedge dy$  for the associated area element. If  $z \mapsto w = f(z)$  is a holomorphic map, then the push-forward of

the measure  $|\mu| = g(z)dx \wedge dy$  is defined to be the measure

$$f_*|\mu| = \sum_{\{z; f(z)=w\}} \frac{g(z)}{|f'(z)|^2} du \wedge dv,$$

where  $w = u + iv$ . Thus, for compatibility, we must define the **push-forward** of the metric  $\mu = g(z)|dz|^2$  to be the possibly singular <sup>†</sup> metric

$$f_*\mu = \sum_{\{z; f(z)=w\}} \frac{g(z)}{|f'(z)|^2} |dw|^2,$$

We will need the following Lemma.

LEMMA 6.2. *Let  $A$  and  $A'$  be two annuli in  $\widehat{\mathbb{C}}$ ,  $U \subset A'$  an open subset, and  $f : U \rightarrow A$  a proper holomorphic map. Suppose that a generic curve joining the two boundary components of  $A$  has a preimage by  $f$  which joins the boundary components of  $A'$ . Then the moduli satisfy*

$$\text{mod } A' \leq \text{mod } A$$

with equality if and only if  $U = A'$  and  $f : A' \rightarrow A$  is an isomorphism.

Here a curve will be described as “generic” if it does not pass through any critical value. We must also take care with the word “joining”, since the boundary of  $A$  is not necessarily locally connected. The requirement is simply that the curve is properly embedded in  $A$ , and that its closure joins the boundary components of  $A$ .

PROOF. Let  $\mu = g(z)|dz|^2$  be an extremal (flat) metric on  $A'$ . Note that

$$\text{Area}_{f_*\mu}(A) = \text{Area}_\mu U \leq \text{Area}_\mu A'. \quad (12)$$

(Here  $f_*\mu$  stands for the push-forward of  $\mu$  restricted to  $U$ .) Let  $\gamma$  be a generic curve joining the two boundary components of  $A$ , let  $\gamma'$  be a preimage of  $\gamma$  by  $f$  which connects the two boundary components of  $A'$ , and let  $\gamma'_0 \subset \gamma'$  be a minimal segment of this curve which joins the two boundaries. Then

$$\begin{aligned} \text{Length}_{f_*\mu} \gamma &= \int_{w \in \gamma} \sqrt{\sum_{f(z)=w} \frac{g(z)}{|f'(z)|^2}} |dw| \\ &\geq \int_{z \in \gamma'_0} \sqrt{|g(z)|} |dz| = \text{Length}_\mu \gamma'_0 \geq \sqrt{\text{Area}_\mu A' \cdot \text{mod } A'}, \end{aligned} \quad (13)$$

where the last inequality holds since  $\mu$  is extremal. Squaring the inequality (13) and using (12), we obtain

$$\frac{(\text{Length}_{f_*\mu} \gamma)^2}{\text{Area}_{f_*\mu} A} \geq \frac{(\text{Length}_\mu \gamma'_0)^2}{\text{Area}_\mu A'} \geq \text{mod } A'. \quad (14)$$

---

<sup>†</sup> This pushed-forward metric has poles at critical values, and discontinuities along the image of the boundary. However, for the length-area argument, it only needs to be measurable with finite area. (See [1].)

Now let  $\nu$  vary over all conformal metrics on  $A$ . By the definition of extremal length,

$$\begin{aligned} \text{mod}A &= \sup_{\nu} \inf_{\gamma} \left\{ \frac{(\text{Length}_{\nu}(\gamma))^2}{\text{Area}_{\nu}A} \right\} \\ &\geq \inf_{\gamma} \left\{ \frac{(\text{Length}_{f_*\mu}\gamma)^2}{\text{Area}_{f_*\mu}A} \right\} \\ &\geq \text{mod}(A'). \end{aligned}$$

Now assume that  $\text{mod}(A) = \text{mod}(A')$ , then  $f_*\mu$  is an extremal metric on  $A$ . This implies that there are many curves  $\gamma$  of minimal length, so we can choose a generic one. Inequality (13) then becomes an equality, so that  $\gamma'_0$  is the only component of  $f^{-1}(\gamma)$  which crosses  $U$ . As a consequence,  $f : U \rightarrow A$  has degree 1 and hence is a conformal isomorphism. The hypothesis of the Lemma now implies that a generic curve joining the two boundaries of  $U$  also joins the two boundaries of  $A'$ . Evidently it follows that  $U = A'$ , and hence that  $f : A' \rightarrow A$  is an isomorphism.  $\square$

We will apply this lemma to the annulus  $A$  of Theorem 6.1, taking  $A = A'$  and  $U = f^{-1}(A)$ . (Recall that we are in the case in which  $f^{-1}(A)$  is connected.) Note that  $f^{-1}(A) \subset A$ . In fact  $f^{-1}(A)$  must intersect  $A$  since both are self-antipodal; but  $f^{-1}(A)$  cannot intersect the boundary of  $A$  since the existence of any intersection would imply that  $A = f(f^{-1}(A))$  intersects  $f(\partial A) \subset (\overline{\mathcal{B}}_0 \cup \overline{\mathcal{B}}_{\infty})$ .

LEMMA 6.3. *A generic curve joining the two boundary components of  $A$  has a preimage by  $f$  which also joins the two boundary components of  $A$ .*

(Again a “generic” curve means one that does not pass through a critical value, so that each of its three preimages is a continuous lifting of the curve. Note that any preimage automatically lies in  $f^{-1}(A) = U \subset A$ .)

PROOF. We may assume that  $\mathcal{B}_0$  contains only one critical point, since the case where it contains two critical points is well understood. (Compare § 3.) Thus a generic point of  $\mathcal{B}_0$  has two preimages in  $\overline{\mathcal{B}}_0$  and a third preimage in a disjoint copy  $\mathcal{B}'_0$ . Similarly a generic point in the closure  $\overline{\mathcal{B}}_0$  has two preimages in  $\overline{\mathcal{B}}_0$  and one preimage in  $\overline{\mathcal{B}'_0}$ . There is a similar discussion for the antipodal set  $\mathcal{B}_{\infty}$ .

A generic path  $\gamma$  through  $A$  from some point of  $\mathcal{B}_0$  to some point of  $\mathcal{B}_{\infty}$  has three preimages. Two of the three start at points of  $\overline{\mathcal{B}}_0$  and the third starts at a point of  $\overline{\mathcal{B}'_0}$ . Similarly, two of the three preimages end at points of  $\overline{\mathcal{B}}_{\infty}$ , and one ends at a point of  $\overline{\mathcal{B}'_{\infty}}$ . It follows easily that at least one of the three preimages must cross from  $\overline{\mathcal{B}}_0$  to  $\overline{\mathcal{B}}_{\infty}$ , necessarily passing through  $A$ .

This completes the proof of Lemma 6.3, and also of Theorem 6.1.  $\square$

$\square$

DEFINITION 6.4. A point in the Julia set for the map  $f_q \notin \widetilde{\mathcal{H}}_0$  will be called **bi-visible** if it is the landing point of both an internal ray from zero and an external ray from infinity.

COROLLARY 6.5. *If the Julia set of  $f_q \notin \widetilde{\mathcal{H}}_0$  is connected and locally connected, then there are bi-visible points.*



PROOF. Since  $f_q \notin \widetilde{\mathcal{H}}_0$  the free critical point  $\mathbf{c}_0 = \mathbf{c}_0(q)$  does not belong to the basin of zero:  $\mathbf{c}_0 \notin \mathcal{B}_0$ . Hence the Böttcher coordinate defines a diffeomorphism from  $\mathcal{B}_0$  onto  $\mathbb{D}$ . Following Carathéodory, local connectivity implies that the inverse diffeomorphism extends to a continuous map from  $\mathbb{D}$  onto  $\widetilde{\mathcal{B}}_0$ . In particular, it follows that every point of  $\partial\mathcal{B}_0$  is the landing point of a ray from zero. Since  $\mathcal{J}(f_q)$  is connected, there can be no Herman rings, and the conclusion follows easily from Theorem 6.1.  $\square$

REMARK 6.6. Even when the Julia set is not locally connected there may be examples with bi-visible points.

We will show that any  $f_q \notin \widetilde{\mathcal{H}}_0$  with a bi-visible point has a well defined rotation number. We want to thank Saeed Zakeri for his substantial help with the proofs of Theorems 6.8 and 6.12.

DEFINITION 6.7. A **meridian** for the map  $f_q$  is a path from zero to infinity in the dynamic plane which can be described as the union of an internal ray from zero and an external ray from infinity, together with their common landing point. Note that the image of a meridian under the antipodal map is again a meridian. The union of two antipodal meridians is a Jordan curve  $\mathcal{C}$  which separates the sphere into two mutually antipodal simply-connected regions.

#### THE PERIODIC CASE.

THEOREM 6.8. *If the map  $f_q$  with  $q^2 \notin \mathcal{H}_0$  has a periodic bi-visible point, then the set of all bi-visible points for  $f_q$  forms a single self-antipodal periodic orbit of even period  $n = 2h$ . Furthermore, each point  $b_j$  in this orbit is contained in a unique meridian  $M_j$ . If we number these  $M_j$  in positive cyclic order as seen from the origin, with  $j \in \mathbb{Z}/(2h)$ , then there is an  $r$  relatively prime to  $2h$  so that  $f_q(M_j) = M_{j+r}$  for all  $j$ , hence there is a well defined rotation number  $r/(2h)$ .*

To begin the proof, note that any meridian for a bi-visible point  $b$  of period  $n$  must also have period  $n$ . In fact the iterate  $f_q^{on}$  is bijective in a neighborhood of  $b$ , so it must preserve the cyclic order of the finitely many internal and external rays landing on  $b$ . Since internal rays must map to internal rays, it follows that every such ray must be  $f_q^{on}$ -invariant.

Let  $B$  be a finite set of periodic bi-visible points for the map  $f_q$ . Without loss of generality we may assume that  $f_q(B) = B = \mathcal{A}(B)$ . We can construct an associated set of disjoint meridians by choosing one representative point for each periodic cycle in  $B$ , and choosing internal rays from zero to these representative points. Taking the images of these rays under both the antipodal map and the iterates of  $f_q$ , we easily obtain the required collection of meridians; which are disjoint since no two rays can intersect.

Number the resulting meridians in positive cyclic order as seen from the origin as  $M_j$  with  $j \in \mathbb{Z}/(2h)$ . It then follows that  $\mathcal{A}(M_j) = M_{j+h}$ . The region between  $M_j$  and  $M_{j+1}$  in cyclic order will be called the **sector**  $S_j$ . We will assume that the numbering has been chosen so that the zero internal ray lies in  $S_0$ , while the zero external ray lies in  $S_h$ .

LEMMA 6.9. *With the  $M_j$  constructed as above, there is a well defined  $r \neq 0$  in  $\mathbb{Z}/(2h)$  such that  $f_q(M_j) = M_{j+r}$  for every  $j$ .*

Thus we can say that  $\{M_j\}$  has **rotation number**  $r/(2h)$ . (In particular, this implies that all of the points in  $B$  have the same period.) It follows that *all* periodic bi-visible points have the same period and rotation number. For if  $B'$  is any other finite set of periodic bi-visible points, then  $B \cup B'$  is also such a set.

The proof of Lemma 6.9 will be based on a further Lemma. If  $M_j$  has internal angle  $\theta_j \in \mathbb{Q}/\mathbb{Z}$ , then the **angular width**  $w_j$  of  $S_j$  at the origin is defined by the conditions that

$$w_j \equiv \theta_{j+1} - \theta_j \pmod{\mathbb{Z}}, \quad \text{with } 0 < w_j < 1.$$

Each sector  $S_j$  has an angular width  $w_j > 0$  measured at the origin, and another angular width  $w'_j > 0$  measured at infinity, with

$$\sum_j w_j = \sum_j w'_j = 1, \quad w'_j = w_{j+h}.$$

LEMMA 6.10. *The angular width of the sector  $S_0$  containing the zero internal ray necessarily satisfies  $w_0 \geq 1/2$ ; and similarly  $w'_h \geq 1/2$ .*

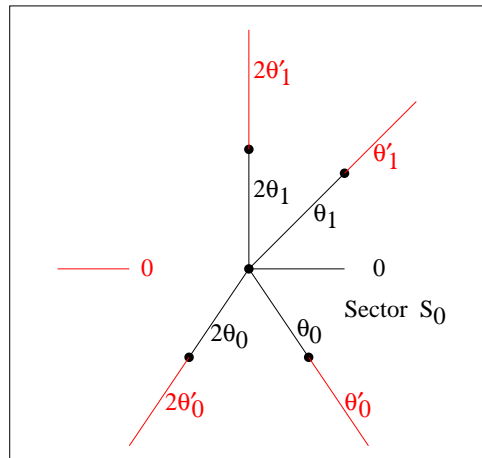


FIGURE 24. *Illustration for the proof that  $S_0$  has angular width at least  $1/2$ .*

If  $\phi' \neq \phi''$  in  $\mathbb{R}/\mathbb{Z}$ , the notation  $[\phi', \phi'']$  will be used for the closure of the open interval consisting of all angles  $\phi$  such that  $\phi', \phi, \phi''$  are in positive cyclic order.

PROOF OF LEMMA 6.10. Suppose to the contrary that  $w_0 < 1/2$ , as in Figure 24. Then the interval  $[\theta_0, \theta_1]$  of length  $w_0$  must map bijectively to the interval  $[2\theta_0, 2\theta_1]$  of length  $2w_0$ . Furthermore,  $[2\theta_0, 2\theta_1]$  clearly contains  $[\theta_0, \theta_1]$ , since the fixed point zero under doubling belongs to  $[\theta_0, \theta_1]$ .

Now consider the corresponding angles  $2\theta'_0, \theta'_0, \theta'_1, 2\theta'_1$  at infinity, which must lie in positive cyclic order around  $\mathbb{R}/\mathbb{Z}$ . In particular, if  $\delta_0$  is the angular separation between  $2\theta'_0$  and  $\theta'_0$ , and  $\delta_1$  is the angular separation between  $\theta'_1$  and  $2\theta'_1$ , then  $\delta_0 + w'_0 + \delta_1 < 1$ . Furthermore we must have

$$\theta'_0 + \delta_0 = 0 = \theta'_1 - \delta_1 \quad \text{in } \mathbb{R}/\mathbb{Z},$$

and therefore  $w'_0 = \delta_0 + \delta_1$ , so that zero lies between  $\theta'_0$  and  $\theta'_1$  in cyclic order. It follows that the zero ray from infinity must lie in the sector  $S_0$ . But this is impossible, since we know that this zero ray lies in the antipodal sector  $S_h$ . This contradiction completes the proof of Lemma 6.10.  $\square$

PROOF OF LEMMA 6.9. Since the set of angles  $\{\theta_j\}$  has a gap of length  $w_0 \geq 1/2$ , it follows from Lemma A.10 in the Appendix that  $\{\theta_j\}$  is a rotation set.  $\square$

REMARK 6.11. It follows from Lemma 6.9 that  $f_q$  cannot have any strictly preperiodic bi-visible point. In fact the existence of a preperiodic point certainly implies the existence of periodic points, so that Lemma 6.9 applies. But if the immediate preimage of a point in a quadratic rotation set is not in the rotation set, then it must lie in the major gap around zero. Thus any corresponding preperiodic meridian would have to have its internal ray in  $S_0$  and its external ray in  $S_h$ , which is impossible.

PROOF OF THEOREM 6.8. We will first show that the set  $B$  above must be a single self-antipodal periodic orbit. If  $B$  contained two disjoint periodic orbits, then the internal angles for each one would form a quadratic rotation set. But according to Goldberg there is only one quadratic rotation set for each rotation number. (Compare Remark A.13 in the Appendix.)

Next we must show that there is only one choice of meridians. Suppose there were two different internal rays landing on a given bi-visible point. Constructing meridians as above, the two different choices would necessarily give rise to two different rotation numbers, again using the uniqueness of quadratic rotation sets with given rotation number. But now suppose we modify the construction, using one choice for the internal rays, but the antipode of the other choice for the external rays. This would yield a choice of meridians with one rotation number measured at zero and a different rotation number measured at infinity. Since rays cannot cross each other, this is topologically impossible.

This almost completes the proof of Theorem 6.8. It only remains to show that there cannot be another bi-visible point which is neither periodic nor preperiodic. However, it will follow immediately from Theorem 6.12 below that this possibility cannot occur.

#### THE NON-PERIODIC CASE.

THEOREM 6.12. *If  $f_q$  has a bi-visible point with infinite orbit under  $f_q$ , then  $f_q$  has a well defined irrational rotation number. Furthermore any other bi-visible point will give rise to the same irrational rotation number.*

PROOF. Choose a meridian  $M_0$ , and for each  $k > 0$  consider the set of meridians  $M_j = f_q^{\circ j}(M_0)$  with  $0 \leq j < k$ , together with their antipodes  $\mathcal{A}(M_j)$ . (This is different from the numbering of meridians used above. Note that an infinite forward orbit must clearly be disjoint from the antipodal forward orbit.) Since rays landing on different points cannot cross each other, these  $2k$  meridians must be pairwise disjoint (except at zero and infinity). Thus they divide the Riemann sphere into  $2k$  sectors. As in the proof of Lemma 6.10, we can check that the internal angular width of the sectors containing the zero internal ray must be  $\geq 1/2$ . Since this is true for all  $k$ , it follows that there is a well defined rotation number, and as in the proof of Theorem 6.8 we can check that this rotation number does not depend on the choice of initial meridian.

Now suppose that there is a different bi-visible point whose forward images are disjoint from all of the  $M_j$ . Choosing corresponding meridians  $\widehat{M}_i$ , the union of the  $\widehat{M}_i$  is clearly disjoint

from the union of the  $M_j$ , so  $\{M_j\} \cup \{\widehat{M}_i\}$  would have a well defined irrational rotation number. Therefore  $\{M_j\}$  and  $\{\widehat{M}_i\}$  must have the same rotation number. This completes the proof of Theorems 6.8 and 6.12.  $\square$

Here is another important application of the concept of meridian.

**THEOREM 6.13.** *If  $U$  is an attracting or parabolic basin of period two or more for a map  $f_q$ , then the boundary  $\partial U$  is a Jordan curve. The same is true for any Fatou component which eventually maps to  $U$ .*

**PROOF.** The first step is to note the the Julia set  $\mathcal{J}(f_q)$  is connected and locally connected. In fact, since  $f_q$  has an attracting or parabolic point of period two or more, it follows that every critical orbit converges to an attracting or parabolic point. In particular, there can be no Herman rings, so the Julia set is connected by Theorem 2.1. It then follows by Tan Lei and Yin Yongcheng [22] that the Julia set is also locally connected. Thus by Corollary 6.5 there is a bi-visible point. Hence we can choose a pair of antipodal meridians, forming a Jordan curve  $\mathcal{C}$ .

Evidently  $U$  is a bounded subset of the finite plane  $\mathbb{C}$ . Hence the complement  $\mathbb{C} \setminus \overline{U}$  of the closure has a unique unbounded component  $V$ . Let  $U'$  be the complement  $\mathbb{C} \setminus \overline{V}$ . We will first show that  $U'$  has Jordan curve boundary. This set  $U'$  is connected since  $U$  is connected, and is simply-connected since its complement is connected. Choosing a base point in  $U'$ , the hyperbolic geodesics from the base point will sweep out  $U'$ , yielding a Riemann homeomorphism from the standard open disk  $\mathbb{D}$  onto  $U'$ . Since the Julia set is locally connected, this extends to a continuous mapping  $\overline{\mathbb{D}} \rightarrow \overline{U'}$  by Carathéodory. If two such geodesics landed at a single point of  $\overline{U'}$ , then their union would map onto a Jordan curve in  $\overline{U'}$  which would form the boundary of an open set  $U''$ , which is necessarily contained in  $U'$  by the way that  $U'$  was constructed. But then any intermediate geodesic would be trapped within  $U''$ , and hence could only land at the same boundary point. Since this is impossible by the Riesz brothers' theorem, <sup>†</sup> it follows that the pair  $(\overline{U'}, \partial U')$  must be homeomorphic to  $(\overline{\mathbb{D}}, \partial \mathbb{D})$ .

Thus, to complete the proof, we need only show that  $U = U'$ . But otherwise we could choose some connected component  $Y$  of  $U' \setminus U$ . (Compare Figure 25. Such a set  $Y$  would be closed as a subset of  $U'$ , but its closure  $\overline{Y}$  would necessarily contain one or more points of  $\partial U'$ .)

Note then that no iterated forward image of the boundary  $\partial Y$  can cross the self-antipodal Jordan curve  $\mathcal{C}$  which was described in the first paragraph of the proof. In fact any neighborhood of a point of  $\partial Y$  must contain points of  $U$ . Thus if  $f_q^{\circ j}(\partial Y)$  contained points on both sides of  $\mathcal{C}$ , then the connected open set  $f_q^{\circ j}(U)$  would also. But any connected open set crossing  $\mathcal{C}$  must clearly intersect either the basin of zero or the basin of infinity, which is impossible for forward images of the bounded periodic component  $U$ .

Note that the union  $Y \cup U$  is an open subset of  $U'$ . In fact any point  $y \in Y$  has a neighborhood which is contained in  $Y \cup U$ . For otherwise every neighborhood would have to intersect one or more other components  $Y' \neq Y$ . Any single  $Y' \neq Y$  is a closed subset of  $U'$ , disjoint from  $Y$ , and hence can be avoided by a small enough neighborhood of  $y$ . But if there were a sequence of points belong to different components and converging to  $y$ , then it would contradict local connectivity of the Julia set.

---

<sup>†</sup> For the classical results used here, see for example [14, Theorems 17.14 and A.3].

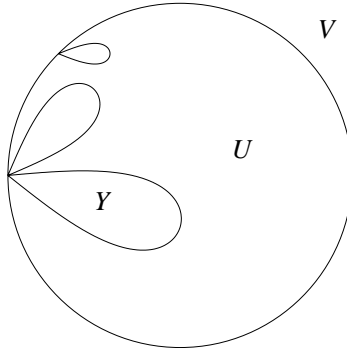


FIGURE 25. Schematic picture for the proof of Theorem 6.13. Here  $U'$  is represented by the open unit disk, and a typical component of  $U' \setminus U$  is labeled  $Y$ .

We will show that some forward image of the interior  $\overset{\circ}{Y}$  must contain the point at infinity, and hence must contain some neighborhood of infinity. For otherwise, since  $\partial Y \subset \partial U$  certainly has bounded orbit, it would follow from the maximum principle that  $Y$  also has bounded orbit. This would imply that the open set  $Y \cup U$  is contained in the Fatou set. On the other hand,  $Y$  must contain points of  $\partial U$ , which are necessarily in the Julia set, yielding a contradiction.

Similarly the forward orbit of  $\overset{\circ}{Y}$  must contain zero. There are now two possibilities. First suppose that some forward image  $f_q^{\circ j}(Y)$  contains just one of the two points zero and infinity. Then it follows that the boundary  $\partial f_q^{\circ j}(Y) \subset f_q^{\circ j}(\partial Y)$  must cross  $\mathcal{C}$ , yielding a contradiction.

Otherwise, since an orbit can hit zero or infinity only by first hitting the preimage  $q$  or  $\mathcal{A}(q)$ , it follows that there must be some  $j \geq 0$  such that  $f_q^{\circ j}(Y)$  contains both of  $q$  and  $\mathcal{A}(q)$ , but neither of zero and infinity. But this is impossible. Since  $f_q^{\circ j}(\partial Y)$  cannot cross  $\mathcal{C}$ , it must lie on one side of  $\mathcal{C}$ . Suppose for example that it lies on the side containing  $q$ . Then it cannot separate  $\mathcal{A}(q)$  from zero and infinity. Since  $f_q^{\circ j}(Y)$  does not contain zero or infinity by hypothesis, it cannot contain  $\mathcal{A}(q)$ . This contradiction proves that  $U' = U$ , and thus completes the proof of Theorem 6.13.  $\square$

## 7. FJORDS

Let  $\mathbf{t} \in \mathbb{R}/\mathbb{Z}$  be rational with odd denominator. It will be convenient to use the notation  $\vartheta = \vartheta_{\mathbf{t}} \in \mathbb{R}/\mathbb{Z}$  for the unique angle which satisfies the equation  $\rho(\vartheta) = \mathbf{t}$ . In other words,  $\vartheta$  is the unique angle which is balanced, with rotation number  $\mathbf{t}$  under doubling, as computed in Theorem 5.10. (Compare Lemma 5.8.) This section will sharpen Theorem 3.6 by proving the following result.

**THEOREM 7.1 (The Fjord Theorem).** *With  $\mathbf{t}$  and  $\vartheta = \vartheta_{\mathbf{t}}$  as above, the internal ray in  $\mathcal{H}_0$  of angle  $\vartheta$  lands at the point  $\infty_{\mathbf{t}}$  on the circle of points at infinity.*

(We will see in Corollary 7.7 that every other internal ray is bounded away from this point.) Intuitively, we should think of the  $\vartheta_{\mathbf{t}}$  ray as passing to infinity **through the  $\mathbf{t}$ -fjord**. (Compare Figure 30.)

In order to prove this result, it is enough by Theorem 3.6 to show that the parameter ray  $\mathcal{R}_{\vartheta}$  has no finite accumulation point on  $\partial \mathcal{H}_0$  (that is, no accumulation point outside of the

circle at infinity). In fact, we will show that the existence of a finite accumulation point would lead to a contradiction.

For the first part of the argument, let  $\vartheta$  be any periodic angle such that the parameter ray  $\mathcal{R}_\vartheta$  has a finite accumulation point  $q^2$ . Choose a sequence of points  $q_k$  converging to  $q$ , such that each  $q_k^2$  belongs to this parameter ray. Then for each  $q_k$ , the internal dynamic ray  $\mathcal{R}_{q_k, \vartheta}$  bifurcates at the critical point  $c_0(q_k)$ . However, there are well defined left and right limit rays which extend all the way to the Julia set  $\mathcal{J}(f_{q_k})$ . Intuitively, these can be described as the Hausdorff limits

$$\mathcal{R}_{q_k, \vartheta^\pm} = \lim_{\varepsilon \searrow 0} \mathcal{R}_{q_k, \vartheta \pm \varepsilon}$$

as  $\vartheta \pm \varepsilon$  tends to  $\vartheta$  from the left or right. More directly, the limit ray  $\mathcal{R}_{q_k, \vartheta^+}$  can be constructed by starting out along  $\mathcal{R}_{q_k, \vartheta}$  and then taking the left hand branch at every bifurcation point, and  $\mathcal{R}_{q_k, \vartheta^-}$  can be obtained similarly by taking every right hand branch. (Compare Figure 13.) It is not hard to see that the landing points  $\zeta_{q_k}^\pm(\vartheta)$  of these left and right limit rays are well defined repelling periodic points, with period equal to the period of  $\vartheta$ . In the terminology of Remark 4.9 these periodic landing points form the endpoints of the “critical gap” in the corresponding rotation set. Their coordinates around the Julia set  $\mathcal{J}(f_{q_k}) \cong \mathbb{R}/\mathbb{Z}$  can be computed from Theorem 4.8.

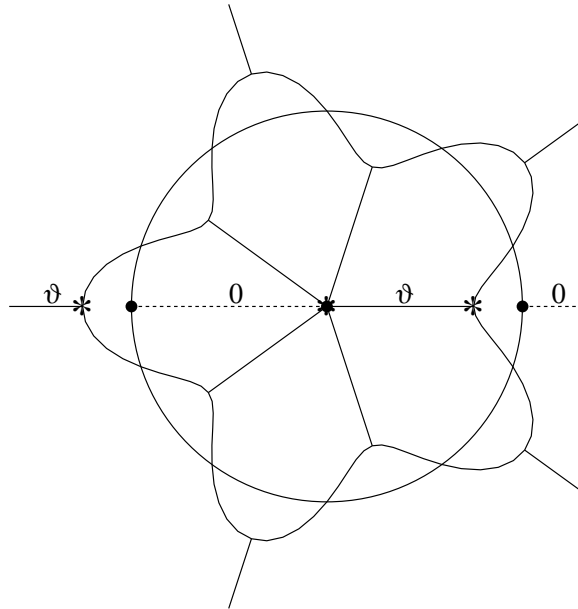


FIGURE 26. Schematic picture for the dynamics of  $f_{q_k}$  when  $q_k^2$  is on the  $\vartheta$  parameter ray for some balanced angle  $\vartheta$ . Here the basin of zero is represented by the open unit disk. The three finite fixed points are represented by heavy dots, and the three finite critical points are represented by stars. (The zero point is both fixed and critical.) For the illustrated case with period 5, the angle  $\vartheta$  can be either  $\pm 4/31$  with rotation number  $\pm 1/5$ , or  $\pm 10/31$  with rotation number  $\pm 2/5$ .

PROPOSITION 7.2. As above, consider a sequence of points  $q_k$  converging to a finite limit  $q$ , where each  $q_k^2$  belongs to the  $\vartheta$  parameter ray, and where  $q^2$  belongs to the boundary  $\partial\mathcal{H}_0$ . But now assume that the period of  $\vartheta$  is odd (or more generally assume that the

associated parabolic orbit for  $f_q$  is not self-antipodal). Then the corresponding left and right limit landing points  $\zeta_{q_k}^\pm(\vartheta) \in \mathcal{J}(f_{q_k})$  must both converge towards the landing point for the dynamic ray  $\mathcal{R}_{q,\vartheta}$ , which is a parabolic periodic point in  $\mathcal{J}(f_q)$  by Lemma 3.9.

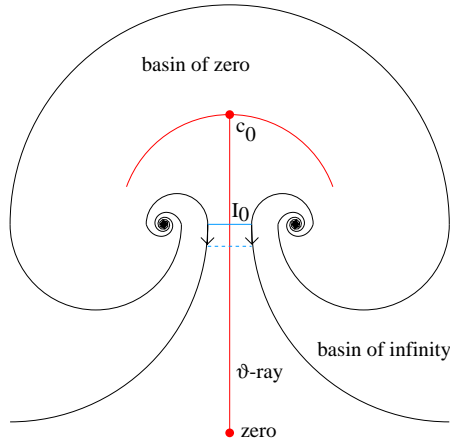


FIGURE 27. Schematic picture for part of the Julia set  $\mathcal{J}(f_{q_k})$ , which is a Jordan curve. As the gap  $I_0$  shrinks to a point, we will show that the two repelling points which are the landing points of the left and right limit rays must converge to this same point.

PROOF OF THEOREM 7.1, ASSUMING PROPOSITION 7.2. Since the angle  $\vartheta = \vartheta_t$  is balanced, exactly  $h$  angles in its orbit under doubling lie in the open interval  $(0, \vartheta)$ , and  $h$  lie in  $(\vartheta, 1)$ . Each of these gives rise to both a left and a right limit ray, which land at two distinct points of period  $n$  in the Julia set. (Compare Figure 22 which illustrates the case  $h = 1, n = 3$ , as well as Figure 26 which illustrates the case  $h = 2, n = 5$ .) Half of the  $4h$  resulting periodic points all lie in one connected interval between the two fixed points on the Julia set, and the other half will lie in the complementary interval. There are also two limit rays associated with the angle  $\vartheta$ . One of these will lie in one interval between the Julia fixed points, and the other will lie in the complementary interval. This shows that the rotation set under tripling, consisting of all of these left and right limit points, is “balanced”, with exactly  $2h + 1$  points in the interval  $(0, 1/2) \subset \mathbb{R}/\mathbb{Z} \cong \mathcal{J}(f_q)$ , and exactly  $2h + 1$  in the interval  $(1/2, 1)$ .

The same description holds for the antipodal rays from infinity; so the set of all left and right limit rays from infinity is also balanced. But according to Goldberg, a rotation set consisting of periodic orbits under tripling is uniquely determined by its rotation number together with the number of points in  $(0, 1/2)$  and the number of points in  $(1/2, 1)$ . (Compare Remark A.14 in the Appendix.) This proves that the left and right limit rays from zero and infinity land on precisely the same  $4h + 2 = 2n$  points. If we number these  $2n$  points of period  $n$  in cyclic order around the circle, then half of the pairs of consecutive points around the circle will be left and right limit points for a ray from zero, and the complementary half will be left and right limits for rays from infinity.

Now according to Proposition 7.2, as  $q_k^2$  tends to a finite limit on  $\partial\mathcal{H}_0$ , each pair of left and right limit rays must converge to a common limit. (Compare Figure 27.) But this means that the entire  $2n$  point rotation set must collapse to a single point. This is clearly impossible,

since the rotation set is made up of  $n$  pairs of antipodal points. This contradiction proves that the ray  $\mathcal{R}_\vartheta$  has no finite limit. Hence by Theorem 3.6 it must land at the point  $\infty_t$ . This completes the proof of Theorem 7.1, modulo Proposition 7.2.  $\square$

**REMARK 7.3.** The requirement that  $\vartheta$  must be balanced is essential here. As an example of the situation when the angle  $\vartheta$  has no rotation number or is unbalanced, see Figure 10 (right). In this example, the internal dynamic rays with angle  $1/7, 2/7, 4/7$  land at the root points of a cycle of attracting basins, and the corresponding external rays land at an antipodal cycle of attracting basins. These are unrelated to the two points visible from zero and infinity along the  $1/3$  and  $2/3$  rays.

**PROOF OF PROPOSITION 7.2.** As  $q_k$  converges to  $q$ , where each  $q_k^2$  belongs to the  $\vartheta$  parameter ray and  $q^2$  belongs to  $\partial\mathcal{H}_0$ , we must show that the landing point  $\zeta_{q_k}^+(\vartheta)$  of the right hand dynamic limit ray  $\mathcal{R}_{q_k, \vartheta^+}$  converges to the landing point  $z_0$  of  $\mathcal{R}_{q, \vartheta}$ , which is a well defined parabolic point by Lemma 3.9. The corresponding statement for left limit rays will follow similarly.

**First Step (Only one boundary fixed point).** Let  $B$  be the immediate parabolic basin containing the marked critical point  $\mathbf{c}_0$  for the limit map  $f_q$ , and let  $F_q = f_q^{\circ n}$  be the  $n$ -fold iterate, where  $n$  is the period of  $\vartheta$ . First note that there is only one fixed point for  $F_q$  in the boundary  $\partial B$ . Indeed, this boundary is a Jordan curve by Theorem 6.13. Since  $n$  is odd, the cycle of basins containing  $B$  cannot be self-antipodal, hence  $\mathbf{c}_0$  must be the only critical point of  $F_q$  in  $B$ . It follows easily that the map  $F_q$  restricted to  $\partial B$  is topologically conjugate to angle doubling, with only one fixed point.

**Second Step (Slanted rays).** For  $q_k^2$  on the  $\vartheta$  parameter ray, it will be convenient to work with *slanted rays* in  $\mathcal{B}_{q_k}^{\text{vis}}$ , that is, smooth curves which make a constant angle with the equipotentials, or with the dynamic rays. (Here we are following the approach of Petersen and Ryd [18].) Let  $\mathbb{H}$  be the upper half-plane. Using the universal covering map

$$\exp : \mathbb{H} \rightarrow \mathbb{D} \setminus \{0\}, \quad \exp(w) = e^{2\pi iw},$$

and embedding  $\mathcal{B}_{q_k}^{\text{vis}}$  into  $\mathbb{D}$  by the Böttcher coordinate  $\mathbf{b}_{q_k}$ , as in Figure 13, the dynamic rays in  $\mathcal{B}_{q_k}^{\text{vis}}$  correspond to vertical lines in  $\mathbb{H}$ , and the slanted rays correspond to lines of constant slope  $dv/du$ , where  $w = u + iv$ . (See Figure 28.)

Let  $\widehat{\vartheta}$  be a representative in  $\mathbb{R}$  for  $\vartheta \in \mathbb{R}/\mathbb{Z}$ . Fixing some arbitrary slope  $\mathbf{s}_0 > 0$  and some sign  $\pm$ , let  $\mathbf{S}^\pm$  be the sector consisting of all  $u + iv$  in  $\mathbb{H}$  with

$$\pm(u - \widehat{\vartheta}) > 0 \quad \text{and} \quad \frac{v}{|u - \widehat{\vartheta}|} > \mathbf{s}_0.$$

If  $q_k^2$  is close enough to  $q^2$  along the  $\vartheta$  parameter ray, then we will prove that the composition  $w \mapsto \mathbf{b}_{q_k}^{-1}(\exp(w)) \in \mathcal{B}_{q_k}^{\text{vis}}$  is well defined throughout  $\mathbf{S}^\pm$ , yielding a holomorphic map

$$\mathbf{b}_{q_k}^{-1} \circ \exp : \mathbf{S}^\pm \rightarrow \mathcal{B}_{q_k}^{\text{vis}}. \tag{15}$$

To see this, we must show that the sectors  $\mathbf{S}^\pm \subset \mathbb{H}$  are disjoint from all of the vertical line segments in  $\mathbb{H}$ , which correspond to critical or precritical points in  $\mathcal{B}_{q_k}$ . If  $\mathbf{b}_{q_k}(\mathbf{c}_0) = \exp(\widehat{\vartheta} + i\mathfrak{h})$ , note that the critical slit has height  $\mathfrak{h}$ , which tends to zero as  $q_k$  tend to the limit  $q$ . For a precritical point  $z$  with  $f_{q_k}^{\circ j}(z) = \mathbf{c}_0$ , the corresponding slit height is  $\mathfrak{h}/2^j$ .

First consider the  $n$  vertical slits corresponding to points on the critical orbit, together with all of their integer translates. If the  $\mathbf{S}^\pm$  are disjoint from these, then we claim that they are disjoint from all of the precritical slits. For any precritical point  $f_{q_k}^{\circ p}(z) = \mathbf{c}_0$ , we can set



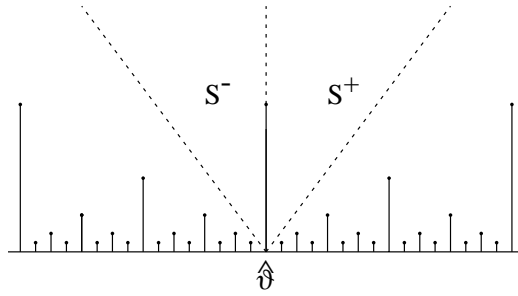


FIGURE 28. Two slanted rays in the upper half-plane. Here the vertical dotted line represents the  $\vartheta$  dynamic ray, and the solid interval below it represents the corresponding invisible part of  $\mathcal{B}_{q_k}$ .

$p = i + jn$  with  $0 \leq i < n$  and  $j \geq 0$ . Then the image  $f_{q_k}^{\circ jn}(z)$  will represent a point on the vertical segment corresponding to the postcritical angle  $2^i \hat{\vartheta}$ , or to some integer translate of this. Using the fact that  $f_{q_k}^{\circ n}$  corresponds to multiplication by  $2^n$  modulo one, with  $\hat{\vartheta}$  as a fixed point, we see that the endpoint of the  $z$  slit must belong to the straight line segment joining the point  $\hat{\vartheta} \in \partial\mathbb{H}$  to the endpoint of the  $2^i \hat{\vartheta}$  slit, or to some integer translate of it. Thus we need impose only  $n$  inequalities on the slope  $s_0$ . Furthermore, for fixed  $s_0 > 0$  all of these inequalities will be satisfied for  $q_k$  sufficiently close to  $q$ .

**Third Step (Landing).** To study the landing of slanted rays, the following estimate will be used. Given a bounded simply-connected open set  $U \subset \mathbb{C}$ , let  $d_U(z_0, z_1)$  be the hyperbolic distance between any two points of  $U$ , and let  $r(z_0)$  be the Euclidean distance of  $z_0$  from  $\partial U$ . Then

$$|z_1 - z_0| \leq r(z_0) \left( e^{2d_U(z_0, z_1)} - 1 \right). \tag{16}$$

In particular, for any fixed  $h_0$ , as  $z$  converges to a boundary point of  $U$ , the entire neighborhood  $\{z'; d_U(z, z') < h_0\}$  will converge to this boundary point. To prove the inequality (16), note that the hyperbolic metric has the form  $\rho(z)|dz|$  where  $2\rho(z)r(z) > 1$ . (See for example [14, Corollary A.8].) If  $a$  is the hyperbolic arc length parameter along a hyperbolic geodesic, so that  $da = \rho(z)|dz|$ , note that

$$\log \frac{r(z_1)}{r(z_0)} = \int_{z_0}^{z_1} \frac{dr}{r} \leq \int_{z_0}^{z_1} \frac{|dz|}{r} < 2 \int_{z_0}^{z_1} \rho(z)|dz| = 2d_U(z_0, z_1),$$

and hence  $r(z_1) \leq r(z_0)e^{2d_U(z_0, z_1)}$ , or more generally

$$r(z) \leq r(z_0)e^{2(a(z)-a(z_0))}.$$

It follows that

$$|z_1 - z_0| \leq \int_{z_0}^{z_1} |dz| = \int_{z_0}^{z_1} \frac{da}{\rho(z)} < 2 \int_{z_0}^{z_1} r(z_0)e^{2(a(z)-a(z_0))} da.$$

Since the indefinite integral of  $2e^{2a} da$  is  $e^{2a}$ , the required formula (16) follows easily.

**LEMMA 7.4.** Any left or right slanted ray  $\mathcal{S}_{q_k}^\pm$  for  $f_{q_k}$  lying within the corresponding sector  $\mathbf{S}^\pm$  necessarily lands at a fixed point for  $F_{q_k}$ , provided that  $k$  is sufficiently large. Furthermore, this landing point is always equal to the landing point  $\zeta_{q_k}^\pm(\vartheta)$  of the corresponding left or right limit ray.

PROOF. Note that the map  $F_{q_k} = f_{q_k}^{\circ n}$  corresponds to the hyperbolic isometry  $w \mapsto 2^n w$  from  $\mathbf{S}^\pm$  onto itself, mapping each slanted ray  $v/u = \text{constant}$  in the sector  $\mathbf{S}^\pm$  to itself. Furthermore, the hyperbolic distance between  $w$  and  $2^n w$  is a constant, independent of  $w$ . Since the map from  $\mathbf{S}^\pm$  to the basin of zero  $\mathcal{B}_{q_k}$  reduces hyperbolic distance, it follows that  $d_{\mathcal{B}_{q_k}}(z, F_{q_k}(z))$  is uniformly bounded as  $z$  varies. Hence as  $z$  tends to the boundary of  $\mathcal{B}_{q_k}$  the Euclidean distance  $|F_{q_k}(z) - z|$  tends to zero. It follows that any accumulation point of a slanted ray on the boundary  $\partial\mathcal{B}_{q_k}$  must be a fixed point of  $F_{q_k}$ . Since there are only finitely many fixed points, it follows that the slanted ray must actually land.

We must also show that the landing point of the left or right slanted ray is identical to the landing point of the left or right limit ray. Consider for example the right hand slanted ray in Figure 28. Since it crosses every vertical ray to the right of  $\vartheta$ , its landing point cannot be to the right of the landing point of the limit vertical ray. On the other hand, since the slanted ray is to the right of the limit ray, its landing point can't be to the left of the limit landing point. This proves the Lemma.  $\square$

**Fourth Step (Limit rays and the Julia set).** Now consider a sequence of points  $q_k$  on the  $\vartheta$  parameter ray converging to the landing point  $q$ , and choose some fixed slope  $s_0 > 0$ . After passing to a subsequence, we can assume that the landing points of the associated left or right slanted rays  $\mathcal{S}_{q_k}^\pm$  converge to some fixed point of  $F_q$ . Also, since the non-empty compact subsets of  $\widehat{\mathbb{C}}$  form a compact metric space in the Hausdorff topology, we can assume that this sequence of slanted rays  $\mathcal{S}_{q_k}^\pm$  has a Hausdorff limit, which will be denoted by  $\widehat{\mathcal{S}}^\pm$ . We will prove the following statement.

*Any intersection point of  $\widehat{\mathcal{S}}^\pm$  with the Julia set  $\mathcal{J}(F_q)$  is a fixed point of  $F_q$ .*

To see this, choose any  $\varepsilon > 0$ . Note first that any intersection point  $z_0$  of  $\widehat{\mathcal{S}}^\pm$  and  $\mathcal{J}(F_q)$  can be  $\varepsilon$ -approximated by a periodic point  $z_1$  in  $\mathcal{J}(F_q)$ . We can then choose  $k$  large enough so that the corresponding periodic point  $z_2 \in \mathcal{J}(F_{q_k})$  is  $\varepsilon$ -close to  $z_1$ . On the other hand, we can also choose  $k$  large enough so that the ray  $\mathcal{S}_{q_k}^\pm$  is  $\varepsilon$ -close to  $\widehat{\mathcal{S}}^\pm$ . In particular, this implies that there exists a point  $z_3 \in \mathcal{S}_{q_k}^\pm$  which is  $\varepsilon$ -close to  $z_0$ .

Then  $z_3$  is  $3\varepsilon$ -close to a point  $z_2 \in \mathcal{J}(F_{q_k})$ , so it follows from Inequality (16) that the distance  $|F_{q_k}(z_3) - z_3|$  tends to zero as  $\varepsilon \rightarrow 0$ . Since  $z_3$  is arbitrarily close to  $z_0$  and  $F_{q_k}$  is uniformly arbitrarily close to  $F_q$ , it follows by continuity that  $F_q(z_0) = z_0$ , as asserted.

**Fifth Step (No escape).** First suppose that there is only one  $\dagger$  parabolic basin  $B$  with root point  $\widehat{z}$  at the landing point of the dynamic ray  $\mathcal{R}_{q,\vartheta}$ . In this case the proof proceeds as follows. Note that the intersection of the Hausdorff limit with the basin of zero is just the slanted ray  $\mathcal{S}_q^\pm$ . In fact we will prove that

$$\widehat{\mathcal{S}}^\pm \subset B \cup \{\widehat{z}\} \cup \mathcal{S}_q^\pm. \tag{17}$$

Intuitively this means that once  $\widehat{\mathcal{S}}^\pm$  hits the root point  $\widehat{z} \in \partial B$ , it can never again leave  $B \cup \{\widehat{z}\}$ .

It will be convenient to assign to each point  $z$  in any left or right slanted ray  $\mathcal{S}_{q_k}^\pm$  for  $F_{q_k}$  the parameter  $\tau = -\log_{3^n} G_k(z)$ , where  $G_k(z) > 0$  is the Green's function with  $G_k(F_{q_k}(z)) = 3nG_k(z)$ . This yields a parametrization  $\sigma_k : \mathbb{R} \rightarrow \mathbb{C}$  of the slanted ray  $\mathcal{S}_{q_k}^\pm$  which satisfies

$$F_{q_k}(\sigma_k(\tau)) = \sigma_k(\tau - 1). \tag{18}$$

---

$\dagger$  Conjecturally this is always the case. There are certainly maps  $f_q$  with more than one basin incident to each parabolic point: The root point of any satellite of any copy of the Mandelbrot set in parameter space provides an example. However, the corresponding parabolic orbits do not seem to be visible from either zero or infinity.

Intuitively we will think of  $\tau$  as the “time”, as we follow the ray from  $z = 0$  (with  $\tau = -\infty$ ) towards the Julia set (with  $\tau \rightarrow +\infty$ ). According to Equation (18), the ray can pass through a given point  $z$  at time  $\tau$  only if it has already passed through  $F_{q_k}(z)$  at time  $\tau - 1$ .

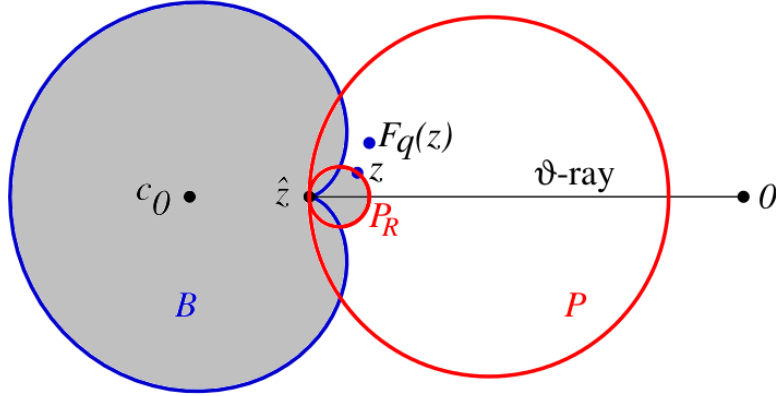


FIGURE 29. A parabolic basin  $B$  and repelling petals  $P_R \subset P$  for  $F_q$ . The shadowed region represents the open set  $P_R \cup B \cup \{\hat{z}\}$  which is a trapping region for the slanted rays  $\mathcal{S}_{q_k}^\pm$  with  $k$  large. Once such a ray has spent one time unit within this region, it can never again cross its boundary.

Let  $P$  be a repelling petal for  $F_q$ , and let  $\Phi: P \rightarrow \mathbb{C}$  be a repelling Fatou coordinate for  $F_q$ , chosen so that  $\Phi(F_q(z)) = \Phi(z) + 1$ . Without loss of generality, assume  $\Phi(P)$  contains the left half-plane  $\{\operatorname{Re} \Phi(z) < 0\}$ . For  $R > 0$ , consider the smaller petal  $P_R := \{z \in P; \operatorname{Re} \Phi(z) < -R\}$ . Note that  $P_R \cup B \cup \{\hat{z}\}$  is a neighborhood of  $\hat{z}$ . (Compare Figure 29.)

Suppose that we follow a slanted ray  $\mathcal{S}_{q_k}^\pm$  as  $\tau$  increases. If  $k$  is large enough, then it will uniformly approximate the slanted ray  $\mathcal{S}_q^\pm$  throughout any fixed time interval  $\tau \leq \text{constant}$ . Since  $\mathcal{S}_q^\pm$  lands at  $\hat{z}$  through the repelling petal  $P_R$ , it follows that  $\mathcal{S}_{q_k}^\pm$  must stay in  $P_R$  for at least one unit of time,  $\tau_0 \leq \tau \leq \tau_0 + 1$ , provided that  $k$  is large enough. We then claim that  $\sigma_k(\tau) \in P_R \cup B \cup \{\hat{z}\}$  for all  $\tau \geq \tau_0$ .

Indeed, if this were not the case, then there would be a smallest time  $\tau_k \geq \tau_0$  such that  $z_k := \sigma_k(\tau_k)$  is in the boundary of  $P_R \cup B \cup \{\hat{z}\}$ . Note that  $\tau_k \geq \tau_0 + 1$ , and therefore  $\tau_0 \leq \tau_k - 1 < \tau_k$ , which implies that

$$F_{q_k}(z_k) = \sigma_k(\tau_k - 1) \in P_R \cup B \cup \{\hat{z}\}. \quad (19)$$

Passing to an infinite subsequence if necessary, we may assume that  $z_k$  converges to a point  $z$  in the boundary of  $P_R \cup B \cup \{\hat{z}\}$  as  $k \rightarrow \infty$ . (Remember that  $\hat{z}$  is an interior point of the shaded region). According to the first step,  $\hat{z}$  is the only fixed point of  $F_q$  in the boundary of  $B$ . Therefore, according to the fourth step, the intersection of  $\mathcal{S}^\pm$  with the boundary of  $B$  is reduced to  $\hat{z}$ . It follows that  $z$  belongs to  $\partial P_R \setminus \overline{B}$ . Hence, as illustrated in Figure 29, the image  $F_q(z)$  must belong to  $P \setminus (\overline{P_R} \cup \overline{B})$ . But this is impossible since  $F_q(z)$  is the limit of points  $F_{q_k}(z_k)$  which, according to Equation (19), belong to  $P_R \cup B \cup \{\hat{z}\}$ .

This contradiction proves that the limit ray  $\overline{\mathcal{S}^\pm}$  cannot escape from  $P_R \cup B \cup \{\hat{z}\}$ . Since by taking  $R$  large enough we are free to choose an arbitrarily small  $P_R$ , the limit ray  $\overline{\mathcal{S}^\pm}$  cannot escape from  $B \cup \{\hat{z}\}$ . This completes the proof of Proposition 7.2 in the case that there is only one basin  $B$  incident to  $\hat{z}$ . If there are several incident basins  $B_1, \dots, B_k$ , then a similar argument would show that the limit ray cannot escape from  $\overline{B_1} \cup \dots \cup \overline{B_k}$ , and

the conclusion would again follow. This completes the proof of Proposition 7.2, and hence of Theorem 7.1.  $\square$

FORMAL ROTATION NUMBER: THE PARAMETER SPACE DEFINITION.

As a Corollary to Theorem 7.1, we can describe a concept of rotation number which makes sense for *all* maps  $f_q$  with  $q \neq 0$ . (Compare the dynamic rotation number which is defined for points in  $\mathcal{H}_0$  in Definition 5.3, and for many points outside of  $\mathcal{H}_0$  in Section 6.)

Let  $I \subset \mathbb{R}/\mathbb{Z}$  be a closed interval such that the endpoints  $t_1$  and  $t_2$  are rational numbers with odd denominator, and let  $\mathcal{W}(I) \subset \mathbb{C}$  be the compact triangular region bounded by the unique rays which join  $\infty_{t_1}$  and  $\infty_{t_2}$  to the origin, together with the arc at infinity consisting of all points  $\infty_t$  with  $t \in I$ . (Compare Figure 30.)

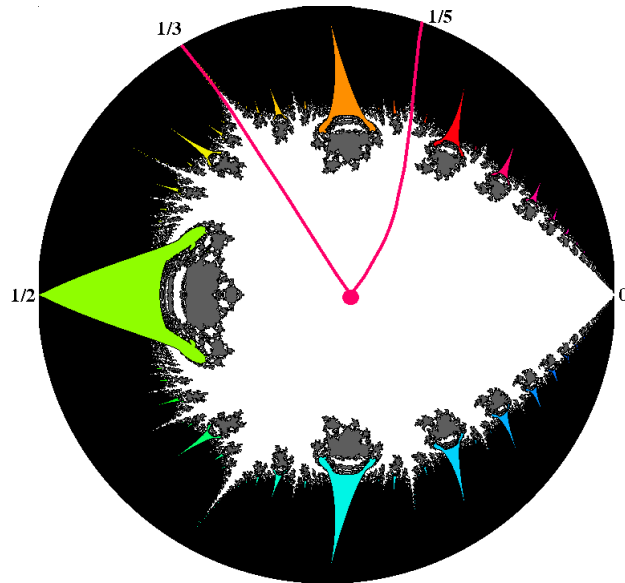


FIGURE 30. Unit disk model for the circled  $q^2$ -plane, with two rays from the origin to the circle at infinity sketched in.

For any angle  $t \in \mathbb{R}/\mathbb{Z}$ , let  $\mathcal{W}_t$  be the intersection of the compact sets  $\mathcal{W}(I)$  as  $I$  varies over all closed intervals in  $\mathbb{R}/\mathbb{Z}$  which contain  $t$  and have odd-denominator rational endpoints.

LEMMA 7.5. *Each  $\mathcal{W}_t$  is a compact connected set which intersects the circle at infinity only at the point  $\infty_t$ . These sets  $\mathcal{W}_t$  intersect at the origin, but otherwise are pairwise disjoint. In particular, the intersections  $\mathcal{W}_t \cap (\mathbb{C} \setminus \mathcal{H}_0)$  are pairwise disjoint compact connected sets. (Here it is essential that we include points at infinity.)*

PROOF. The argument is straightforward, making use of the fact that  $\mathcal{H}_0$  is the union of an increasing sequence of open sets bounded by equipotentials.  $\square$

DEFINITION 7.6. Points in  $\mathcal{W}_t \setminus \{0\}$  have **formal rotation number** equal to  $t$ . It is sometimes convenient to refer to these as points in the  **$t$ -wake**.

It is not difficult to check that this is compatible with Definition 5.3 in the special case of points which belong to  $\mathcal{H}_0$ . This formal rotation number is continuous as a map from  $\mathbb{C} \setminus \{0\}$  to  $\mathbb{R}/\mathbb{Z}$  (or equivalently as a retraction from  $\mathbb{C} \setminus \{0\}$  onto the circle at infinity which is naturally isomorphic to  $\mathbb{R}/\mathbb{Z}$ ). In fact, if we take any open interval in  $\mathbb{R}/\mathbb{Z}$  bounded by two rational points with odd denominator, then the preimage in  $\mathbb{C} \setminus \{0\}$  is an open set bounded by two parameter rays.

One immediate consequence of Lemma 7.5 is the following.

**COROLLARY 7.7.** *For  $\mathbf{t}$  rational with odd denominator, the ray  $\mathcal{R}_{\vartheta_{\mathbf{t}}}$  of Theorem 7.1 is the only internal ray in  $\mathcal{H}_0$  which accumulates on the point  $\infty_{\mathbf{t}}$ .*

In fact, for any  $\mathbf{t}' \neq \mathbf{t}$  the ray  $\mathcal{R}_{\vartheta_{\mathbf{t}'}}$  is contained in a compact set  $\mathcal{W}_{\mathbf{t}'}$  which does not contain  $\infty_{\mathbf{t}}$ .  $\square$

**REMARK 7.8 (Accessibility and Fjords).** A topological boundary point

$$q_0^2 \in \partial\mathcal{H}_0 \subset \mathbb{C}$$

is said to be **accessible** from  $\mathcal{H}_0$  if there is a continuous path  $\mathbf{p} : [0, 1] \rightarrow \mathbb{C}$  such that  $\mathbf{p}$  maps the half-open interval  $(0, 1]$  into  $\mathcal{H}_0$ , and such that  $\mathbf{p}(0) = q_0^2$ . Define a **channel** to  $q_0^2$  within  $\mathcal{H}_0$  to be a function  $\mathbf{c}$  which assigns to each open neighborhood  $U$  of  $q_0^2$  in  $\mathbb{C}$  a connected component  $\mathbf{c}(U)$  of the intersection  $U \cap \mathcal{H}_0$  satisfying the condition that

$$U \supset U' \implies \mathbf{c}(U) \supset \mathbf{c}(U').$$

(If  $U_1 \supset U_2 \supset \dots$  is a basic set of neighborhoods shrinking down to  $q_0^2$ , then clearly the channel  $\mathbf{c}$  is uniquely determined by the sequence  $\mathbf{c}(U_1) \supset \mathbf{c}(U_2) \supset \dots$ . Here, we can choose the  $U_j$  to be simply connected, so that the  $\mathbf{c}(U_j)$  will also be simply connected.)

By definition, the access path  $\mathbf{p}$  lands on  $q_0^2$  **through** the channel  $\mathbf{c}$  if for every neighborhood  $U$  there is an  $\varepsilon > 0$  so that  $\mathbf{p}(\tau) \in \mathbf{c}(U)$  for  $\tau < \varepsilon$ . It is not hard to see that every access path determines a unique channel, and that for every channel  $\mathbf{c}$  there exists one and only one homotopy class of access paths which land at  $q_0^2$  through  $\mathbf{c}$ .

The word **fjord** will be reserved for a channel to a point on the circle at infinity which is determined by an internal ray which lands at that point.

**REMARK 7.9 (Are there Irrational Fjords?).** It seems likely, that there are uncountably many irrational rotation numbers  $\mathbf{t} \in \mathbb{R}/\mathbb{Z}$  such that the ray  $\mathcal{R}_{\vartheta_{\mathbf{t}}} \subset \mathcal{H}_0$  lands at the point  $\infty_{\mathbf{t}}$  on the circle at infinity. In this case, we would say that the ray lands through an **irrational fjord**. What we can actually prove is the following statement.

**LEMMA 7.10.** *There exist countably many dense open sets  $W_n \subset \mathbb{R}/\mathbb{Z}$  such that, for any  $\mathbf{t} \in \bigcap W_n$ , the ray  $\mathcal{R}_{\vartheta_{\mathbf{t}}}$  accumulates at the point  $\infty_{\mathbf{t}}$  on the circle at infinity.*

However, we do not know how to prove that this ray actually lands at  $\infty_{\mathbf{t}}$ . The set of all accumulation points for the ray is necessarily a compact connected subset of  $\mathcal{W}_{\mathbf{t}} \cap \partial\mathcal{H}_0$ , but it could contain more than one point. In that case, all neighboring fjords and tongues would have to undergo very wild oscillations as they approach the circle at infinity.

PROOF OF LEMMA 7.10. Let  $V_n$  be the open set consisting of all internal angles  $\vartheta$  such that the internal ray  $\mathcal{R}_\vartheta$  contains points  $q^2$  with  $|q^2| > n$ . A corresponding open set  $W_n$  of formal rotation numbers can be constructed as follows. For each rational  $r \in \mathbb{R}/\mathbb{Z}$  with odd denominator, choose an open neighborhood which is small enough so that every associated internal angle is contained in  $V_n$ . The union of these open neighborhoods will be the required dense open set  $W_n$ . For any  $\mathbf{t}$  in  $\bigcap W_n$ , the associated internal ray  $\mathcal{R}_{\vartheta_{\mathbf{t}}}$  will come arbitrarily close to the circle at infinity. Arguing as in Corollary 7.7, we see that  $\infty_{\mathbf{t}}$  is the only point of  $\partial\mathbb{C}$  where this ray can accumulate.  $\square$

If the following is true, then we can prove a sharper result. It will be convenient to use the notation  $\mathcal{L}$  for the compact set  $\mathbb{C} \setminus \mathcal{H}_0$ , and the notation  $\mathcal{L}_{\mathbf{t}}$  for the intersection  $\mathcal{L} \cap \mathcal{W}_{\mathbf{t}}$ . Thus  $\mathcal{L}$  is the disjoint union of the compact connected sets  $\mathcal{L}_{\mathbf{t}}$ . (It may be convenient to refer to  $\mathcal{L}_{\mathbf{t}}$  as the **t-limb** of  $\mathcal{L}$ .)

CONJECTURE 7.11. If  $\mathbf{t}$  is rational with odd denominator, then the set  $\mathcal{L}_{\mathbf{t}}$  consists of the single point  $\infty_{\mathbf{t}}$ .

Assuming this statement, we can prove that a generic ray actually lands, as follows. Let  $\overline{\mathbb{D}}_n$  be the disk consisting of all  $q^2 \in \mathbb{C}$  with  $|q^2| \leq n$ , and let  $W'_n \subset \mathbb{R}/\mathbb{Z}$  be the set consisting of all  $\mathbf{t}$  for which  $\mathcal{L}_{\mathbf{t}} \cap \overline{\mathbb{D}}_n = \emptyset$ . The set  $W'_n$  is open for all  $n$ , since  $\mathcal{L}$  is compact. Then  $W'_n$  is dense since it contains all rational numbers with odd denominator. For any  $\mathbf{t} \in \bigcap_n W'_n$ , the set  $\mathcal{L}_{\mathbf{t}}$  evidently consists of the single point  $\infty_{\mathbf{t}}$ , and it follows easily that the associated ray  $\mathcal{R}_{\vartheta_{\mathbf{t}}}$  lands at this point.  $\square$

### Appendix A. CIRCLE MAPS AND ROTATION SETS

This Appendix will first discuss maps of the circle  $\mathbb{R}/\mathbb{Z}$ , and then discuss “rotation sets”, which are compact subsets of  $\mathbb{R}/\mathbb{Z}$  with a well defined rotation number under multiplication by some integer  $d \geq 2$ .

DEFINITION A.1. Any continuous map  $g : \mathbb{R}/\mathbb{Z} \rightarrow \mathbb{R}/\mathbb{Z}$  will be called a **circle map**. For any circle map, there exists a continuous **lift**,  $\widehat{g} : \mathbb{R} \rightarrow \mathbb{R}$ , unique up to addition of an integer constant, such that the square

$$\begin{array}{ccc} \mathbb{R} & \xrightarrow{\widehat{g}} & \mathbb{R} \\ \downarrow & & \downarrow \\ \mathbb{R}/\mathbb{Z} & \xrightarrow{g} & \mathbb{R}/\mathbb{Z} \end{array}$$

is commutative. Here the vertical arrows stand for the natural map from  $\mathbb{R}$  to  $\mathbb{R}/\mathbb{Z}$ . This lift satisfies the identity

$$\widehat{g}(y + 1) = \widehat{g}(y) + d,$$

where  $d$  is an integer constant called the **degree** of  $g$ . We will only consider the case of circle maps of positive degree. The map  $g$  will be called **monotone** if

$$y < y' \implies \widehat{g}(y) \leq \widehat{g}(y').$$

It is not hard to see that  $f$  has degree  $d$  if and only if it is homotopic to the standard map

$$\mathbf{m}_d : \mathbb{R}/\mathbb{Z} \rightarrow \mathbb{R}/\mathbb{Z} \quad \text{defined by} \quad \mathbf{m}_d(x) = dx.$$

DEGREE ONE CIRCLE MAPS.

We first review the classical theory of rotation numbers for monotone degree one circle maps.

It is well known that for any monotone circle map  $g$  of degree  $d = 1$ , we can define a **rotation number**  $\text{rot}(g) \in \mathbb{R}/\mathbb{Z}$ , as follows. Choose some lift  $\widehat{g}$ . We will first prove that the **translation number**

$$\text{transl}(\widehat{g}) = \lim_{n \rightarrow \infty} \frac{\widehat{g}^{\circ n}(x) - x}{n} \in \mathbb{R}$$

is well defined and independent of  $x$ . For any circle map of degree one, setting  $\underline{a}_n = \min_x (\widehat{g}^{\circ n}(x) - x)$ , the inequality  $\underline{a}_{m+n} \geq \underline{a}_m + \underline{a}_n$  is easily verified. It follows that  $\underline{a}_{km+n} \geq k\underline{a}_m + \underline{a}_n$ . Dividing by  $h = km + n$  and passing to the limit as  $k \rightarrow \infty$  for fixed  $m > n$ , it follows that  $\liminf \underline{a}_h/h \geq \underline{a}_m/m$ . Therefore the *lower translation number*

$$\underline{\text{transl}}(\widehat{g}) = \lim_{n \rightarrow \infty} \underline{a}_n/n = \sup_n \underline{a}_n/n$$

is well defined. Similarly, the *upper translation number*

$$\overline{\text{transl}}(\widehat{g}) = \lim_{n \rightarrow \infty} \bar{a}_n/n = \inf_n \bar{a}_n/n$$

is well defined, where  $\bar{a}_n = \max_x (\widehat{g}^{\circ n}(x) - x)$ . Finally, in the monotone case it is not hard to check that  $0 \leq \bar{a}_n - \underline{a}_n \leq 1$ , and hence that these upper and lower translation numbers are equal. By definition, the **rotation number**  $\text{rot}(g)$  is equal to the residue class of  $\text{transl}(\widehat{g})$  modulo  $\mathbb{Z}$ .

REMARK A.2. Note that the rotation number is rational if and only if  $g$  has a periodic orbit. First consider the rotation number zero case. Then the translation number  $\text{transl}(\widehat{g})$  for a lift  $\widehat{g}$  will be an integer. The periodic function  $x \mapsto \widehat{g}(x) - x - \text{transl}(\widehat{g})$  has translation number zero. We claim that it must have a zero. Otherwise, if for example its values were all greater than  $\varepsilon > 0$ , then it would follow easily that the translation number would be greater than or equal to  $\varepsilon$ . The class modulo  $\mathbb{Z}$  of any such zero will be a fixed point of  $g$ , as required.

To prove the corresponding statement when the rotation number is rational with denominator  $n$ , simply apply the same argument to the  $n$ -fold iterate  $g^{\circ n}$ . Each fixed point of  $g^{\circ n}$  will be a periodic point of  $g$ . In addition, the cyclic order of each cycle around the circle is determined by the rotation number. Indeed, if  $\widehat{g} : \mathbb{R} \rightarrow \mathbb{R}$  is a lift with translation number  $m/n \in \mathbb{Q}$ , then the map

$$x \mapsto \frac{1}{n} \sum_{k=0}^{n-1} \left( \widehat{g}^{\circ k}(x) - \frac{km}{n} \right)$$

descends to a monotone degree one map  $\psi : \mathbb{R}/\mathbb{Z} \rightarrow \mathbb{R}/\mathbb{Z}$  which conjugates  $g$  to the rotation of angle  $m/n$  on periodic cycles of  $g$ .

REMARK A.3. In the irrational case, one obtains much sharper control. If  $g$  has irrational rotation number  $\mathbf{t}$ , then there is a unique degree one monotone semiconjugacy  $\psi : \mathbb{R}/\mathbb{Z} \rightarrow \mathbb{R}/\mathbb{Z}$  satisfying

$$\psi(g(x)) = \psi(x) + \mathbf{t}, \quad \text{with} \quad \psi(0) = 0.$$

To see this, note that each forward image  $x_j = g^{\circ j}(0)$  must map to the point  $j\mathbf{t} \in \mathbb{R}/\mathbb{Z}$ . These image points form a countable dense subset of the circle, which we can think of as the

unit interval with endpoints identified. An arbitrary  $x \notin \mathbb{R}/\mathbb{Z} \setminus \{x_j\}$  then corresponds to a “Dedekind cut” in this countable dense set, determining the required unique point  $\psi(x)$ .

Equivalently, there is a uniquely defined  $g$ -invariant probability measure  $\mu$  on the circle which assigns to each interval  $I$  the length of the image interval  $\psi(I)$ . By a Theorem of Hermann Weyl, every orbit  $g : x_1 \mapsto x_2 \mapsto \dots$  is evenly distributed with respect to  $\mu$  in the following sense: For every interval  $I \subset \mathbb{R}/\mathbb{Z}$  the number of orbit points  $x_j \in I$  with  $1 \leq j \leq k$  is asymptotic to  $k \mu(I)$  as  $k \rightarrow \infty$ .

The invariant measure of  $I$  can be computed more explicitly as the asymptotic average of the lengths of the iterated images of  $I$ :

$$\mu(I) = \lim_{k \rightarrow \infty} \frac{1}{k} \sum_{j=0}^{k-1} \text{length}(g^{o j}(I)) . \tag{A.1}$$

To see this, let  $\widehat{\psi} : \mathbb{R} \rightarrow \mathbb{R}$  be the lifted semiconjugacy between  $\widehat{g}$  and translation by  $\widehat{\mathbf{t}}$ . Then the inverse  $\widehat{\psi}^{-1}$  is monotone, and well defined except at jump discontinuities. The difference  $\Delta(u) = \widehat{\psi}^{-1}(u) - u$  is almost everywhere well defined, periodic of period one, and has bounded variation as an almost everywhere defined map from  $[0, 1]$  to  $\mathbb{R}$ . Thus the integral  $c = \int_0^1 \Delta(u) du$  is a well defined real constant. Furthermore, for any  $u \in [0, 1]$ , since the orbit under translation by  $\mathbf{t}$  is evenly distributed modulo  $\mathbb{Z}$ , it follows that this constant  $c$  is equal to the limit as  $k \rightarrow \infty$  of the average of the values  $\Delta(u + j\mathbf{t})$  for  $0 \leq j < k$ . Choosing any point  $\widehat{y} \in \mathbb{R}$  and setting  $u = \widehat{\psi}(\widehat{y})$  so that  $u + j\mathbf{t} = \widehat{\psi}(\widehat{g}^{o j}(\widehat{y}))$ , the resulting equation can be written as

$$c = \lim_{k \rightarrow \infty} \frac{1}{k} \sum_{j=0}^{k-1} \left( \widehat{g}^{o j}(\widehat{y}) - (\widehat{\psi}(\widehat{y}) + j\widehat{\mathbf{t}}) \right) .$$

Subtracting the corresponding equation for another point  $\widehat{y}'$  and canceling the  $j\widehat{\mathbf{t}}$  terms, we obtain

$$\lim_{k \rightarrow \infty} \frac{1}{k} \sum_{j=0}^{k-1} \left( \widehat{g}^{o j}(\widehat{y}) - \widehat{g}^{o j}(\widehat{y}') \right) = \widehat{\psi}(\widehat{y}) - \widehat{\psi}(\widehat{y}') .$$

Now projecting from  $\mathbb{R}$  to  $\mathbb{R}/\mathbb{Z}$ , we obtain the required equation (A.1).

**DEFINITION A.4 (Rotation Sets <sup>†</sup>).** Fixing some integer  $d \geq 2$ , let  $X \subset \mathbb{R}/\mathbb{Z}$  be a non-empty compact subset which is invariant under multiplication by  $d$  in the sense that  $\mathbf{m}_d(X) \subset X$ , where

$$\mathbf{m}_d : \mathbb{R}/\mathbb{Z} \rightarrow \mathbb{R}/\mathbb{Z} \quad \text{is the map} \quad \mathbf{m}_d(x) = dx .$$

Then  $X$  will be called a **rotation set** if the map  $\mathbf{m}_d$  restricted to  $X$  extends to a continuous monotone map  $g_X : \mathbb{R}/\mathbb{Z} \rightarrow \mathbb{R}/\mathbb{Z}$  of degree 1. The **rotation number** of  $X$  is then defined to be the rotation number of this extension  $g_X$ . It is easy to check that this rotation number does not depend on the choice of  $g_X$  since the lifts of two extensions to  $\mathbb{R}$  may always be chosen to coincide over  $X$ .

Here is a simple characterization of rotation sets.

**THEOREM A.5.** *A non-empty compact set  $X \subset \mathbb{R}/\mathbb{Z}$  is a rotation set if and only if the complement  $(\mathbb{R}/\mathbb{Z}) \setminus X$  contains  $d - 1$  disjoint open intervals of length  $1/d$ .*

---

<sup>†</sup> We are indebted to discussions with Saeed Zakeri on this material. (Compare [23].)



The proof will depend on a definition and two lemmas.

DEFINITION A.6. If  $I \subset \mathbb{R}/\mathbb{Z}$  is an open set, we define

$$X_d(I) = \{x \in \mathbb{R}/\mathbb{Z} ; \mathbf{m}_d^{on}(x) \notin I \text{ for all } n \geq 0\}$$

to be the compact set consisting of all orbits which avoid  $I$ .

LEMMA A.7. Let  $I \subset \mathbb{R}/\mathbb{Z}$  be an open set which is the union of disjoint open subintervals  $I_1, I_2, \dots, I_{d-1}$ , each of length precisely  $1/d$ . Then  $X_d(I)$  is a rotation set for  $\mathbf{m}_d$ . Hence the rotation number of  $X_d(I)$  is well defined.

PROOF. The required monotone degree one map  $g = g_I$  will coincide with  $\mathbf{m}_d$  outside of  $I$ , and will map each subinterval  $I_j$  to a single point: namely the image under  $\mathbf{m}_d$  of its two endpoints. The resulting map  $g_I$  is clearly monotone and continuous, and has degree one since the complement  $(\mathbb{R}/\mathbb{Z}) \setminus I$  has length exactly  $1/d$ . It follows easily from Remark A.2 that the set  $X_d(I)$  is non-empty. In fact, if  $g_I$  has an attracting periodic orbit, then it must also have a repelling one, which will be contained in  $X_d(I)$ ; while if there is no periodic orbit, then the rotation number is irrational, and there will be uncountably many orbits in  $X_d(I)$ .  $\square$

REMARK A.8. If the rotation number is non-zero, then each of the  $d - 1$  intervals  $I_j$  must contain exactly one of the  $d - 1$  fixed points of  $\mathbf{m}_d$ . In fact the distance between consecutive fixed points is  $1/(d - 1)$ , so no interval of length  $1/d$  can contain two of them. But if any of the  $d - 1$  fixed points is not in  $I_1 \cup \dots \cup I_{d-1}$ , then the rotation number must be zero.

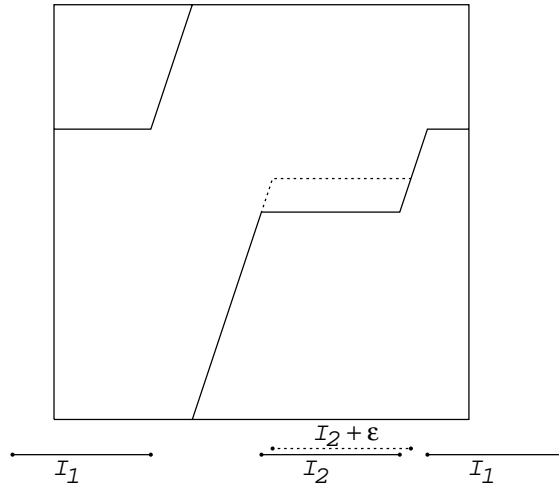


FIGURE A.1. A typical graph for  $g_I$  in the case  $d = 3$ .

REMARK A.9. If we move one or more of the intervals  $I_i$  to the right by a small distance  $\epsilon$ , as illustrated in Figure A.1, then it is not hard to check that for each  $x \in \mathbb{R}/\mathbb{Z}$  the image

$g(x)$  increases by at most  $\varepsilon d$ . Hence the rotation number  $\text{rot}(X_d(I))$  also increases by a number in the interval  $[0, \varepsilon d]$ .

By a **gap**  $G$  in  $X$  will be meant any connected component of the complement  $(\mathbb{R}/\mathbb{Z}) \setminus X$ . (Compare §4.) The notation  $0 < \ell(G) \leq 1$  will be used for the length of a gap. The **multiplicity of a gap**  $G$  is defined as the integer part of the product  $d\ell(G)$ :

$$\mathbf{multiplicity}(G) = \mathbf{floor}(d\ell(G)).$$

If this multiplicity is non-zero, that is if  $\ell(G) \geq 1/d$ , then  $G$  will be called a **major gap**.

LEMMA A.10. *Suppose that  $X \supset \mathbf{m}_d(X)$  is a non-empty compact set. Then  $X$  is a rotation set if and only if it has exactly  $d - 1$  major gaps, counted with multiplicity.* †

PROOF. First note that every rotation set must have measure zero. This follows from the fact that the map  $m_d$  is ergodic, so that almost every orbit is everywhere dense. Let  $\{\ell_i\}$  be the (finite or countably infinite) sequence of lengths of the various gaps. Thus  $\sum \ell_i = 1$ . The  $i$ -th gap must map under  $g_X$  either to a point (if the product  $d\ell_i$  is an integer), or to an interval of length equal to the fraction part

$$\mathbf{frac}(d\ell_i) = d\ell_i - \mathbf{floor}(d\ell_i).$$

It follows easily that  $\sum \mathbf{frac}(d\ell_i) = 1$ . Therefore

$$\sum \ell_i = 1 = \sum (d\ell_i) - \sum \mathbf{floor}(d\ell_i),$$

which implies that  $\sum \mathbf{floor}(d\ell_i) = d - 1$ . This proves Lemma A.10; and Theorem A.5 follows easily.  $\square$

DEFINITION A.11 (**Reduced Rotation Sets**). A rotation set  $X$  will be called **reduced** if there are no wandering points in  $X$  that is, no points with a neighborhood  $U$  such that  $U \cap X$  is disjoint from all of its iterated forward images under  $\mathbf{m}_d$ .

For any rotation set  $X$ , the subset  $X_{\text{red}} \subset X$  consisting of all non-wandering points in  $X$ , forms a reduced rotation set with the same rotation number. (In particular,  $X_{\text{red}}$  is always compact and non-vacuous.) Here is an example: If we take  $d = 2$  and  $I = (1/2, 1)$  in Lemma A.7, then the rotation set  $X = X_2(I)$  has infinitely many points

$$X = \{1/2, 1/4, 1/8, 1/16, \dots, 0\}.$$

The associated reduced rotation set is just the single point  $X_{\text{red}} = \{0\}$ .

LEMMA A.12. *For any rotation set  $X$  with rational rotation number, every point of  $X$  is eventually periodic under  $\mathbf{m}_d$ , and the associated reduced set  $X_{\text{red}}$  is a finite union of periodic orbits. In the irrational case,  $X_{\text{red}}$  is a Cantor set, and is minimal in the sense that every orbit is dense in  $X_{\text{red}}$ .*

PROOF. First consider the case of zero rotation number. Then  $X$  necessarily contains a fixed point, which we may take to be zero. (Compare the proof of Lemma A.7.) Then the associated monotone circle map  $g_X$  can be thought of as a monotone map from the

---

† Compare [6]

interval  $[0, 1]$  onto itself. Suppose that  $X$  contained a point  $x_0$  which does not eventually map to a fixed point, and suppose, for example, that  $x_0 < x_1 = \mathbf{m}_d(x_0)$ . Then the orbit must consist of points  $0 < x_0 < x_1 < \dots < 1$  with  $dx_j \equiv x_{j+1} \pmod{\mathbb{Z}}$ . But this is impossible. The successive differences  $\Delta_j = x_{j+1} - x_j > 0$  would have to have sum  $\sum \Delta_j < 1$ . But since  $d\Delta_j \equiv \Delta_{j+1} \pmod{\mathbb{Z}}$ , one can check easily that  $\Delta_j > 1/d$  for infinitely many values of  $j$ , so that the sum cannot even be finite. Since this is impossible, every point of  $X$  must eventually map to a fixed point, and the reduced set  $X_{\text{red}}$  must consist only of fixed points. Furthermore  $X_{\text{red}}$  is finite since  $\mathbf{m}_d$  has only  $d - 1$  fixed points. The proof when  $x_0 > x_1$  is completely analogous. The corresponding statement when the rotation number of  $X$  has denominator  $n > 1$  now follows easily, since  $X$  can also be considered as a rotation set with rotation number zero under multiplication by  $d^n$ . Thus the only non-wandering points of  $X$  under  $\mathbf{m}_d$  are periodic points, and  $X_{\text{red}}$  is a finite union of periodic orbits.

Now suppose that the rotation number  $\mathbf{t}$  is irrational, and that  $X = X_{\text{red}}$  is reduced. Then  $X$  can have no isolated points, since an isolated point would necessarily be wandering. Hence it must be a Cantor set. Now form a topological circle  $X/\simeq$  by setting  $x \simeq y$  if and only if  $x$  and  $y$  are the endpoints of some gap. Then the map  $\mathbf{m}_d|_X$  gives rise to a degree one circle homeomorphism  $g : X/\simeq \rightarrow X/\simeq$  with the same irrational rotation number. As in Remark A.3, there is a monotone degree one semiconjugacy  $h : X/\simeq \rightarrow \mathbb{R}/\mathbb{Z}$  satisfying  $h(g(x)) = h(x) + \mathbf{t}$ . In fact  $h$  must be a homeomorphism. For if some open interval  $I \subset X/\simeq$  maps to a point, then all of the points in  $I$  would be wandering points for  $g$ , and hence all of the associated points of  $X$  would also be wandering points. Thus every orbit in  $X/\simeq$  is dense, and it follows easily that every orbit in  $X$  is dense.  $\square$

**REMARK A.13 (Rotation Sets under Doubling).** This construction is particularly transparent in the case  $d = 2$ . In fact, let  $I_c$  be the interval  $(c, c + 1/2)$  in  $\mathbb{R}/\mathbb{Z}$ . According to Remark A.9, the correspondence

$$c \mapsto \text{rot}(X_2(I_c)) \in \mathbb{R}/\mathbb{Z}$$

can itself be considered as a monotone circle map of degree one. Hence for each  $\mathbf{t} \in \mathbb{R}/\mathbb{Z}$  the collection of  $c$  with  $\text{rot}(X_2(I_c)) = \mathbf{t}$  is non-vacuous: either a point or a closed interval. Let  $X$  be a reduced rotation set with rotation number  $\mathbf{t}$ . If  $\mathbf{t}$  is rational with denominator  $n$ , then each gap in  $X$  must have period  $n$  under the associated monotone map  $g_X$ . Since there is only one major gap there can be only one cycle of gaps, hence  $X$  must consist of a single orbit of period  $n$ . If  $\ell_0$  is the shortest gap length, then the sum of the gap lengths is

$$1 = \ell_0(1 + 2 + 2^2 + \dots + 2^{n-1}) = (2^n - 1)\ell_0.$$

It follows that the shortest gap has length  $\ell_0 = 1/(2^n - 1)$ ; hence the longest gap has length  $2^{n-1}/(2^n - 1)$ .

For each rational  $\mathbf{t} \in \mathbb{R}/\mathbb{Z}$  there is one and only one periodic orbit  $X = X_{\mathbf{t}}$  which has rotation number  $\mathbf{t}$  under doubling. In fact we can compute  $X_{\mathbf{t}}$  explicitly as follows. Evidently each point  $x \in X_{\mathbf{t}}$  is equal to the sum of the gap lengths between  $x$  and  $2x$ . But we have computed all of the gap lengths, and their cyclic order around the circle is determined by the rotation number  $\mathbf{t}$ .

Note that an interval  $I_c$  of length  $1/2$  has rotation number  $\mathbf{t}$  if and only if it is contained in the longest gap for  $X_{\mathbf{t}}$  which has length  $2^{n-1}/(2^n - 1) > 1/2$ , where  $n$  is the denominator of  $\mathbf{t}$ . Thus the interval of allowed  $c$ -values has length equal to

$$\ell_{\mathbf{t}} = \frac{2^{n-1}}{2^n - 1} - \frac{1}{2} = \frac{1}{2(2^n - 1)}. \tag{A.2}$$

One can check <sup>†</sup> that the sum of this quantity  $\ell_{\mathbf{t}}$  over all rational numbers  $0 \leq \mathbf{t} = k/n < 1$  in lowest terms is precisely equal to one. It follows that the set of  $c$  for which  $\text{rot}(X_2(I_c))$  is irrational has measure zero.

Since the function  $c \mapsto \text{rot}(X_2(I_c))$  is monotone, it follows that for each irrational  $\mathbf{t}$  there is exactly one corresponding  $c$ -value. In particular, there is just one corresponding rotation set  $X_{\mathbf{t}}$ . In the irrational case, it is not difficult to check that  $X_{\mathbf{t}}$  has exactly one gap of length  $1/2^i$  for each  $i \geq 1$ .

**REMARK A.14 (Classifying Reduced Rotation Sets).** Goldberg [7] has given a complete classification of reduced rotation sets with rational rotation number, and Goldberg and Tresser [9] have given a similar classification in the irrational case. For our purposes, the following partial description of these results will suffice. First let  $X$  be a reduced rotation set under multiplication by  $d$  with rational rotation number (so that  $X$  is a finite union of periodic orbits). Divide the circle  $\mathbb{R}/\mathbb{Z}$  into  $d - 1$  half-open intervals  $\left[ \frac{j}{d-1}, \frac{j+1}{d-1} \right)$ , where the endpoints of these intervals are the  $d - 1$  fixed points of  $\mathbf{m}_d$ . Define the **deployment sequence** <sup>†</sup> of  $X$  to be the  $(d - 1)$ -tuple  $(n_0, n_1, \dots, n_{d-2})$ , where  $n_j \geq 0$  is the number of points in  $X \cap \left[ \frac{j}{d-1}, \frac{j+1}{d-1} \right)$ .

**THEOREM A.15 (Goldberg).** *A reduced rotation set  $X$  with rational rotation number is uniquely determined by its deployment sequence and rotation number. Furthermore, for rotation sets consisting of a single periodic orbit of period  $n$ , every one of the  $\frac{(n + d - 2)!}{n!(d - 2)!}$  possible deployment sequences with  $n_j \geq 0$  and  $\sum_j n_j = n$  actually occurs.*

Note that a finite union of periodic orbits  $\mathcal{O}_1 \cup \dots \cup \mathcal{O}_k$ , all with the same rotation number, is a rotation set if and only if the  $\mathcal{O}_j$  are pairwise **compatible**, in the sense that any gap in one of these orbits contains exactly one point of each of the other orbits. **Caution:** Compatibility is not an equivalence relation. <sup>‡</sup> For example, the orbit  $\{1/4, 3/4\}$  under tripling is compatible with both  $\{1/8, 3/8\}$  and  $\{5/8, 7/8\}$ , but the last two are not compatible with each other.

In fact, Goldberg gives a complete classification of such rational rotation sets with more than one periodic orbit. In particular, she shows that at most  $d - 1$  periodic orbits can be pairwise compatible.

In the case of irrational rotation number  $\mathbf{t}$ , a slightly modified definition is necessary. Note that any irrational rotation set  $X$  has a unique invariant probability measure. The semi-conjugacy

$$h : X \rightarrow \mathbb{R}/\mathbb{Z} \quad \text{satisfying} \quad h(\mathbf{m}_d(x)) = h(x) + \mathbf{t},$$

of Remark A.3 is one-to-one except on the countable subset consisting of endpoints of gaps. (Compare the proof of Lemma A.12.) Therefore Lebesgue measure on  $\mathbb{R}/\mathbb{Z}$  can be pulled back

<sup>†</sup> Note that  $2\ell_{\mathbf{t}} = 1/2^n + 1/2^{2n} + 1/2^{3n} + \dots$ , where  $n$  is the denominator of  $\mathbf{t}$ . In other words, we can write  $2\ell_{\mathbf{t}}$  as the sum of  $1/2^k$  over all integers  $k > 0$  for which the product  $j = kt$  is an integer. Therefore  $2\sum_{0 \leq \mathbf{t} < 1} \ell_{\mathbf{t}} = \sum_{k > 0} \sum_{0 \leq j < k} 1/2^k = \sum_{k > 0} k/2^k$ . But this last expression can be computed by differentiating the identity  $\sum_{k \geq 0} x^k = 1/(1 - x)$  to obtain  $\sum kx^{k-1} = 1/(1 - x)^2$ , then multiplying by  $x$ , and setting  $x$  equal to  $1/2$ .

<sup>†</sup> This is a mild modification of Goldberg's definition, which counts the number of points in  $[0, j/(d - 1))$ .

<sup>‡</sup> Similarly, compatibility between humans is clearly not an equivalence relation.

to a measure on  $X$  which is invariant under  $\mathbf{m}_d|_X$ . The deployment sequence can now be defined as  $(p_0, p_1, \dots, p_{d-2})$ , where  $p_j \geq 0$  is the measure of  $X \cap [j/(d-1), (j+1)/(d-1))$ .

**THEOREM A.16 (Goldberg and Tresser).** *A reduced irrational rotation set is uniquely determined by its rotation number and deployment sequence. Furthermore, for any irrational rotation number, any  $(p_0, \dots, p_{d-2})$  with  $p_j \geq 0$  and  $\sum p_j = 1$  can actually occur.*

## SEMICONJUGACIES

By a **semiconjugacy** from a circle map  $g$  to a circle map  $f$  we will always mean a monotone degree one map  $h$  satisfying  $f \circ h(x) = h \circ g(x)$  for all  $x$ . Whenever such a semiconjugacy exists, it follows that  $f$  and  $g$  have the same degree. As an example, if  $g$  is any monotone circle map of degree  $d > 1$ , and if  $x_0$  is a fixed point of  $g$ , then it is not hard to show that there is a unique semiconjugacy from  $g$  to  $\mathbf{m}_D$  which maps  $x_0$  to zero: the monotone degree one map induced by

$$\widehat{h} = \lim_{n \rightarrow +\infty} \widehat{h}_n \quad \text{with} \quad \widehat{h}_n(x) = \frac{1}{d^n} \widehat{g}^{\circ n}(x),$$

where  $\widehat{g}: \mathbb{R} \rightarrow \mathbb{R}$  is a lift of  $g: \mathbb{R}/\mathbb{Z} \rightarrow \mathbb{R}/\mathbb{Z}$  fixing a point above  $x_0$ .

Lemmas A.7 and A.10 have precise analogs in the study of semiconjugacy. For example, if  $I$  is a disjoint union of  $\delta$  disjoint open intervals of length exactly  $1/d$ , then there is a unique circle map  $g_I$  of degree  $d - \delta$  which agrees with  $\mathbf{m}_d$  outside of  $I$  but maps each component of  $I$  to a point. Hence, as noted above, there exists a semiconjugacy from the map  $g_I$  to  $\mathbf{m}_{d-\delta}$ , unique up to  $d - 1$  choices.

Similarly, let  $X \subset \mathbb{R}/\mathbb{Z}$  be any nonempty compact  $\mathbf{m}_d$ -invariant set. Then there exists a monotone continuous map  $g_X: \mathbb{R}/\mathbb{Z} \rightarrow \mathbb{R}/\mathbb{Z}$  of lowest possible degree which satisfies  $g_X(x) = \mathbf{m}_d(x)$  whenever  $x \in X$ . Thus any gap in  $X$  of length  $\ell$  must map to an interval (or point) of length equal to the fractional part of  $d\ell$ . If  $\delta$  is the number of gaps, counted with multiplicity as in Lemma A.10, then it is not hard to see that  $g_X$  has degree  $d - \delta$ .

## References

1. L.V. AHLFORS, *Conformal invariants: topics in geometric function theory* (New York: McGraw-Hill Book Co. 1973.)
2. A. BONIFANT, X. BUFF AND J. MILNOR, ‘Antipode preserving cubic maps: tongues and the Herman ring locus’, Manuscript 2016.
3. K. BORSUK, ‘Drei Sätze über die  $n$ -dimensionale euklidische Sphäre’, *Fund. Math.* **20** (1933) 177–190.
4. B. BRANNER, ‘Turning around the connectedness locus’, *Topological methods in modern mathematics*. (Houston, Publish or Perish), (1993) 391–427.
5. B. BRANNER AND J. HUBBARD, ‘The iteration of cubic polynomials. Part I: the global topology of parameter space’, *Acta Math.* **160** (1988) 143–206.
6. A. BLOKH, J. MALAUGH, J. MAYER, L. OVERSTEEGEN, AND D. PARRIS, ‘Rotational subsets of the circle under  $z^d$ ’, *Topology and Appl.* **153** (2006) 1540–1570.
7. L. GOLDBERG, ‘Fixed points of polynomial maps. Part I: rotation subsets of the circle’, *Ann. Sci. École Norm. Sup. (4)* **25** (1992) 679–685.
8. L. GOLDBERG AND J. MILNOR, ‘Fixed points of polynomial maps. Part II: fixed point portraits’, *Ann. Sci. École Norm. Sup. (4)* **26** (1993) 51–98. (Also available in: *Collected Papers of John Milnor VI: Dynamical Systems 1953 – 2000*, Amer. Math. Soc., Providence RI, (2012) 473–520.)
9. L. GOLDBERG AND C. TRESSER, ‘Rotation orbits and the Farey tree’, *Erg. Th. and Dyn. Sys.* **16** (1996) 1011–1029.
10. S. GOODMAN AND J. HAWKINS, ‘Julia sets on  $\mathbb{R}\mathbb{P}^2$  and dianalytic dynamics’, *Conform. Geom. Dyn.* **18** (2014) 85–109.

11. H. INOU AND S. MUKHERJEE, ‘Non-landing parameter rays of the multicorns’, *Inventiones Mathematicae* **204** (2016) 869–893.
12. D. MEYER AND C.L. PETERSEN, ‘On the notions of mating’, *Ann. Fac. Sci. Toulouse Math.* **21** (2012) 839–876.
13. J. MILNOR, ‘Rational maps with two critical points’, *Experimental Math.* **9** (2000) 481–522. (Also available in: *Collected Papers of John Milnor VII: Dynamical Systems* 1984 – 2012, Amer. Math. Soc., Providence, RI, (2014) 103–170.)
14. J. MILNOR, *Dynamics in one complex variable, Third Edition*, (Annals of Mathematics Studies **160**, Princeton U. Press, Princeton and Oxford, 2006).
15. J. MILNOR, ‘Cubic polynomial maps with periodic critical orbit  $I'$ ’, *Complex dynamics, families and friends*, (ed.) D. Schleicher, (A.K. Peters) (2009) 333–411. (Also available in: *Collected Papers of John Milnor VII: Dynamical Systems* 1984 – 2012, Amer. Math. Soc., Providence, RI, (2014) 409–476.)
16. J. MILNOR, ‘Hyperbolic components, with an Appendix by A. Poirier’, *Conformal dynamics and hyperbolic geometry, in honor of Linda Keen, Contemporary Math.* **573** (2012) 183–232. (Also available in: *Collected Papers of John Milnor VII: Dynamical Systems* 1984 – 2012, Amer. Math. Soc., Providence, RI, (2014) 527–576.)
17. J. MILNOR, ‘Pasting together Julia sets: a worked out example of mating’, *Experiment. Math.* **13** (2004) 55–92. (Also available in: *Collected Papers of John Milnor VII: Dynamical Systems* 1984 – 2012, Amer. Math. Soc., Providence, RI, (2014) 231–292.)
18. C. PETERSEN AND G. RYD, ‘Convergence of rational rays in parameter spaces’, *The Mandelbrot set, theme and variations, London Math. Soc. Lecture Note Ser.* **274**, (Cambridge Univ. Press) (2000) 161–172.
19. T. SHARLAND, ‘Mating of cubic polynomials with a fixed critical point’, Manuscript 2016. (Preliminary report is at ‘Thurston obstructions for cubic branched coverings with two fixed critical points’, arXiv:1502.00070.)
20. M. SHISHIKURA AND TAN LEI, ‘A family of cubic rational maps and matings of cubic polynomials’, *Experiment. Math.* **9** (2000) 29–53.
21. TAN LEI, ‘Stretching rays and their accumulations, following Pia Willumsen’, *Dynamics on the Riemann sphere* (Euro. Math. Soc.) (2006) 183–208.
22. TAN, LEI AND YIN, YONGCHENG, ‘Local connectivity of the Julia set for geometrically finite rational maps’, *Science in China (Series A)* **39** (1996) 39–47.
23. S. ZAKERI, ‘Rotation sets and complex dynamics’, Manuscript to appear.

Araceli Bonifant  
 Mathematics Department,  
 University of Rhode Island  
 5 Lippitt Road, Room 200  
 Kingston RI 02881  
 US  
 bonifant@uri.edu

Xavier Buff  
 Université Paul Sabatier  
 Institut de Mathématiques de Toulouse  
 118, route de Narbonne  
 31062 Toulouse Cedex  
 France  
 xavier.buff@math.univ-toulouse.fr

John Milnor  
 Institute for Mathematical Sciences  
 Stony Brook University  
 Stony Brook, NY 11794-3660  
 US  
 jack@math.sunysb.edu